

# Enhancing the diagnostic security of periprosthetic joint infections by using Dithiotreitol, Next-Generation- Sequencing and C9 as a new biomarker

Thesis  
For the degree of

**doctor rerum naturalium (Dr. rer. nat.)**

Approved by the Faculty of Natural Sciences of Otto von Guericke University Magdeburg

by: Master of Science Ann-Kathrin Meinshausen  
born on: 10.04.1992 in Einbeck

Examiner: Prof. Dr. Jessica Bertrand  
Prof. Dr. med. Dipl.-Ing. Rainer Bader

Submitted on: 17.11.2021

Defended on: 12.05.2022

## Abstract

One of the most common reasons for revision surgery in orthopedics is the periprosthetic joint infection (PJI). Based on the MSIS criteria, one major factor is finding at least two positive cultures of the same organism. The presence of a biofilm can reduce the diagnostic security and can lead to culture-negative PJIs. Dithiothreitol (DTT) can destabilize a biofilm by reducing the disulfide bonds between the polysaccharides and proteins. As the bacteria survive the DTT treatment, the bacteria-containing solution can be used to cultivate and identify the pathogens. Next-Generation-Sequencing has been proposed to be a useful adjunct technique in diagnosing infection and identifying pathogens. Therefore, in the first part of my thesis, I used possible alternative techniques to facilitate the identification of PJIs in more detail. I compared the DTT-treated explant cultures for bacteria identification with the standard (std.) routine microbiological diagnostic using tissue cultures. Furthermore, I compared the NGS from DTT-solution bacteria cultures with std. routine microbiological tissue culturing. The results of the DTT culturing indicated in 8% of the aseptic cohort possible CN-PJIs. Using NGS, more polymicrobial bacteria were identified as compared to the other techniques, which can be attributed to the high sensitivity of NGS. In summary, it has been shown that the DTT pretreated bacteria culturing and the NGS from DTT treated explants were not superior to the std. microbiological diagnostic using tissue cultures for the identification of a pathogen.

Therefore, establishing a new and more reliable methodology to facilitate the detection of PJIs is essential. Using a specific indicator for a more secure PJI analysis could help to improve the treatment of PJI patients. Therefore, a biomarker for PJI identification would be helpful for questionable cases. One of the most promising biomarkers so far is the detection of  $\alpha$ -defensin in synovial fluid samples. As the detection of  $\alpha$ -defensin showed cross-reactivity with certain crystallopathies and metallosis and is additionally very costly, the need for an alternative biomarker is required. Therefore, in the second part of my thesis, I have been analysed possible novel biomarkers by using immunohistochemical stainings of periprosthetic tissue. I analyzed  $\alpha$ -defensin, CD68 as a marker for macrophages, CD66b as a marker for neutrophils, and different proteins of the terminal complement pathway (C3, C5, and C9). With the ROC (receiver operating characteristics) curve, I identified C9 (AUC; area under the curve; of 0.94, sensitivity of 100% and specificity of 89%) as a new possible biomarker for detecting PJIs. To validate C9 as a biomarker for PJI, I used a cohort of 98 patients undergoing hip and knee revisions. The statistical analysis showed a significant difference ( $p < 0.0001$ ) between the septic and aseptic cohorts. The AUC of 0.84 confirmed that C9 immunohistological staining serves as an excellent biomarker for identifying PJI. The sensitivity of 89% and the specificity of 75% were slightly lower than the  $\alpha$ -

defensin detection in synovial fluid. By comparing different parameters e.g., type of pathogen, serum CRP level, and implantation time, I showed that the C9 biomarker works independently from these factors. Furthermore, I have analyzed if other typical inflammatory joint conditions such as chondrocalcinosis (CC), Rheumatoid Arthritis (RA), and abrasion particles can influence the sensitivity and specificity of C9 detection for PJI identification. I found that the C9 biomarker could be used in the presence of CC and RA to identify PJIs.

With this Ph.D. thesis, I provide the basis for developing a novel biomarker for more accurate detection of PJI to decrease the number of CN-PJIs in the future. Due to the high sensitivity and specificity of C9 immunostaining, I propose using this biomarker in the unclear diagnosis of PJI to secure the treatment suggestion.

## Zusammenfassung

Einer der häufigsten Gründe für eine Revisionsoperation in der Orthopädie ist die periprothetische Gelenksinfektion (PGI). Nach den MSIS-Kriterien ist ein wichtiger Faktor der Nachweis von mindestens zwei positiven Gewebekulturen desselben Organismus. Allerdings kann das Vorhandensein eines Biofilms die diagnostische Sicherheit verringern und zu kulturnegativen PGIs führen. Es konnte gezeigt werden, dass Dithiothreitol (DTT) einen Biofilm destabilisieren kann indem es die Disulfidbindungen zwischen den Polysacchariden und Proteinen reduziert. Da die Bakterien die DTT-Behandlung überleben, kann die bakterienhaltige Lösung zur Kultivierung und Identifizierung der Erreger verwendet werden. Next-Generation-Sequenzierung wurde wiederum als nützliche Zusatztechnik für die Diagnose von Infektionen und die Identifizierung von Krankheitserregern vorgeschlagen. Daher habe ich im ersten Teil meiner Doktorarbeit mögliche alternative Techniken untersucht, um die Identifikation von PGI zu verbessern. Ich verglich die DTT-behandelten Explantatkulturen zur Bakterienidentifizierung mit der standardmäßigen mikrobiologischen Routinediagnostik durch Gewebekulturen. Darüber hinaus verglich ich die NGS Ergebnisse der DTT-behandelten Explantatlösung mit der standardmäßigen mikrobiologischen Routine-Gewebekultivierung. Die Ergebnisse der DTT-Kulturen zeigten bei 8% der aseptischen Kohorte mögliche Kulturnegative-PGIs an. Mit NGS wurden im Vergleich zu den anderen Techniken mehr polymikrobielle Bakterien diagnostiziert, was auf die hohe Empfindlichkeit von NGS zurückzuführen ist. Zusammenfassend wurde gezeigt, dass die DTT-vorbehandelte Bakterienkultur und die Lösung für NGS aus DTT-behandelten Explantaten der herkömmlichen mikrobiologischen Diagnostik mit Gewebekulturen zur Identifizierung eines Erregers nicht überlegen war.

Daher ist die Entwicklung einer neuen und zuverlässigeren Methodik zur Erleichterung des Nachweises von PGI unerlässlich. Die Verwendung eines spezifischen Indikators für eine sicherere PGI-Analyse könnte dazu beitragen, die Behandlung von PGI-Patienten zu verbessern. Deshalb wäre ein Biomarker für die Identifizierung von PGI in zweifelhaften Fällen nützlich. Einer der bisher vielversprechendsten Biomarker ist der Nachweis von  $\alpha$ -Defensin in Synovialflüssigkeitsproben. Da der Nachweis von  $\alpha$ -Defensin eine Kreuzreaktivität mit bestimmten Kristallopathien und Metallosen aufweist und zudem sehr kostspielig ist, besteht Bedarf an einem alternativen Biomarker. Daher habe ich im zweiten Teil meiner Arbeit mögliche neue Biomarker anhand von immunhistochemischen Färbungen von periprothetischem Gewebe untersucht. Ich analysierte  $\alpha$ -Defensin, CD68 als Marker für Makrophagen, CD66b als Marker für Neutrophile und verschiedene Proteine des terminalen Komplementwegs (C3, C5 und C9). Anhand der ROC-Kurve habe ich C9 (AUC (*area under the curve*) von 0,94, Sensitivität von 100 % und Spezifität

von 89 %) als neuen möglichen Biomarker für die Erkennung von PGI identifiziert. Für die Validierung von C9 als Biomarker für PGI verwendete ich eine Kohorte von 98 Patienten, die sich einer Hüft- und Knierevision unterzogen hatte. Die statistische Analyse zeigte einen signifikanten Unterschied ( $p < 0,0001$ ) zwischen der septischen und der aseptischen Kohorte. Der AUC von 0,84 bestätigte, dass die immunhistologische C9-Färbung ein hervorragender Biomarker für die Identifizierung von PGI ist. Die Sensitivität von 89 % und die Spezifität von 75 % waren jedoch im Vergleich zum  $\alpha$ -Defensin-Nachweis in der Synovialflüssigkeit etwas geringer. Durch den Vergleich verschiedener Parameter, z. B. Art des Erregers, Serum-CRP-Spiegel und Implantationszeit, konnte ich zeigen, dass der C9-Biomarker unabhängig von diesen Faktoren funktioniert. Außerdem habe ich untersucht, ob andere typische entzündliche Gelenkerkrankungen wie Chondrokalzinose (CC), rheumatoide Arthritis (RA) und Metall-Abriebpartikel die Sensitivität und Spezifität des C9-Nachweises bei der Identifizierung von PGI beeinflussen können. Ich habe herausgefunden, dass der C9-Biomarker bei Vorliegen von CC und RA für die Identifizierung von PGI verwendet werden kann.

Mit dieser Doktorarbeit habe ich die Grundlage für die Entwicklung eines neuen Biomarkers für eine genauere Erkennung von PGI geschaffen, um hoffentlich die Zahl der KN-PGIs in der Zukunft zu verringern. Aufgrund der hohen Sensitivität und Spezifität der C9-Immunfärbung schlage ich den Einsatz dieses Biomarkers bei der unklaren Diagnose von PGI vor.

# Table of Contents

<b>ABSTRACT</b> .....	<b>2</b>
<b>ZUSAMMENFASSUNG</b> .....	<b>4</b>
<b>TABLE OF CONTENTS</b> .....	<b>6</b>
<b>1. INTRODUCTION</b> .....	<b>9</b>
<b>1.1 Periprosthetic Joint Infections</b> .....	<b>10</b>
1.1.1 Medical Definition of a PJI .....	10
1.1.2 Identification of PJI by MSIS criteria .....	11
1.1.3 Definition of PJI-Grade .....	14
<b>1.2 Pathogens</b> .....	<b>15</b>
1.2.1 Biofilms .....	16
<b>1.3 Alternative techniques to identify a PJI</b> .....	<b>17</b>
1.3.1 Next-Generation-Sequencing .....	17
1.3.2 Biofilm-destabilizing techniques to improve diagnostics .....	18
<b>1.4 Immune response to PJI</b> .....	<b>19</b>
1.4.1 Biomarkers .....	20
1.4.2 The complement pathway .....	22
<b>1.5 AIM OF THE STUDY</b> .....	<b>25</b>
<b>2. MATERIAL AND METHODS</b> .....	<b>26</b>
<b>2.1 Materials</b> .....	<b>26</b>
2.1.1 Reagents .....	26
2.1.2 Consumables .....	27
2.1.3 Equipment .....	28
2.1.4 Primer .....	30
2.1.5 Antibodies .....	34
2.1.6 Buffer and media .....	35
<b>2.2 Methods</b> .....	<b>36</b>

2.2.1 Sample Collection and preservation .....	36
2.2.1.1 Tissue collection and preservation .....	36
2.2.1.2 MicroDTTect handling and preservation .....	36
2.2.2 Molecular biological methods .....	37
2.2.2.1 DNA Isolation from microDTTect solution .....	37
2.2.2.2 16s DNA gene preparation and NGS sequencing.....	38
2.2.2.3 Agarose gel electrophoresis .....	40
2.2.3 Microbiological routine diagnostic testing.....	40
2.2.4 Histological methods .....	40
2.2.4.1 Paraffin sections .....	40
2.2.4.2 Immunohistochemically staining.....	41
2.2.4.3 Fluorescence microscopy .....	41
2.2.5 Statistical analysis.....	42
2.2.5.1 Bioinformatic analysis .....	42
<b>3 RESULTS.....</b>	<b>43</b>
<b>3.1. Demographic data of the patient cohort .....</b>	<b>43</b>
3.1.1 Pathogen Spectrum of PJI .....	45
3.1.2 Serum inflammatory markers in PJI.....	47
<b>3.2 Comparison of different analytical techniques to improve the diagnostic security for PJI .....</b>	<b>48</b>
<b>3.3 Tissue biomarkers for PJI diagnosis .....</b>	<b>54</b>
<b>3.4 Validation of C9 as possible Biomarker for the improved diagnosis of PJI .....</b>	<b>62</b>
<b>4. DISCUSSION.....</b>	<b>70</b>
<b>4.1 The demographic data of the cohorts.....</b>	<b>70</b>
<b>4.2 Serum inflammatory markers are not indicative of the presence of PJI .....</b>	<b>73</b>
<b>4.3 Dithiothreitol and Next Generation Sequencing showed Similar Diagnostic Security as Periprosthetic Tissue Cultures to Diagnose a PJI .....</b>	<b>74</b>
<b>4.4 Parts of the terminal complement pathway can be used as a biomarker for the diagnosis of PJI .....</b>	<b>76</b>
<b>4.5 Validation of C9 as a novel biomarker for the identification of PJIs .....</b>	<b>80</b>
<b>5. CONCLUSION AND FUTURE WORK.....</b>	<b>84</b>

**6. SUPPLEMENT .....86**

**ABBREVIATIONS.....87**

**LIST OF FIGURES.....90**

**LIST OF TABLES .....91**

**7. REFERENCES.....92**

**LEBENS LAUF ..... FEHLER! TEXTMARKE NICHT DEFINIERT.**

**PUBLIKATIONEN..... FEHLER! TEXTMARKE NICHT DEFINIERT.**

**DANKSAGUNG ..... FEHLER! TEXTMARKE NICHT DEFINIERT.**

**EHRENERKLÄRUNG.....110**

## 1. Introduction

Especially with increasing age, many people experience chronic joint pain, and the joints' mobility becomes severely limited. When non-surgical measures are no longer effective, the affected person can undergo a joint replacement. Due to the extended lifespan of humans, the need for joint replacements in orthopedic surgery is growing [1]. On the one hand, this is due to the demographic change of the society and, on the other hand, due to the demand for improving life quality and mobility, which is severely limited by the progression of osteoarthritis [2, 3]. Nowadays, multiple joints can be replaced, for example, knee, hip, and shoulder joint. In 2020, approximately 315,000 cases of hip and knee joint replacements were performed in Germany, while the number of shoulder prostheses is lower at around 25,000. [4]. These numbers are expected to increase over the next two decades [1]. An endoprosthetic replacement consists of different components, mainly made from metals such as cobalt-chromium or titanium alloys, ceramics, or polyethylene polymers [5]. The standard materials used for orthopedic prostheses are cobalt- and titanium-based metal alloys, polymers, alumina ceramics, and ultrahigh molecular weight polyethylene (UHMWPE) [6, 7]. An orthopedic implant should be biocompatible, have a high fracture resistance, and wear and corrosion resistance [8]. Orthopedic implants are inevitably recognized as foreign by the human body, whereby the immune system is activated when a prosthesis is implanted [9]. In this context, the nature of the foreign body reaction depends on various factors. One reaction is depending on the composition or surface properties of the prosthesis. *In vivo* was shown that the implant surface tissue interface is one of the most critical aspects of biomaterials [9, 10]. In this regard, the biocompatibility of an implant depends on various factors such as polarity, roughness/smoothness, hydrophobicity /-philicity and thereby the surface charge. Taken together, biocompatibility depends mainly on the physical properties of the implant surface and is only secondary to its chemical composition [11].

A typical hip implant consists of a femoral stem, femoral head, acetabular cup, and an inlay (fig. 1A). The stem is anchored in the femur during the operation. The acetabulum is anchored in the pelvis. In between is the femoral head, which is located between the inlay of the acetabulum and is placed on the stem. While a hip prosthesis consists of at least four parts, a knee endoprosthesis usually consists of three components (fig. 1B). A femoral component installed in the femur and a tibia component anchored in the tibia bone on the tibia component is a plastic inlay. It serves as a sliding surface for the femoral component [5]. A shoulder endoprosthesis also consists of three essential components. A humeral stem is attached to the humerus; on top of is a humeral cap that is connected to the glenoid sphere (fig. 1C). [12].

The lifetime of orthopedic implants is limited for various reasons that lead to premature implant failure, resulting in an unplanned earlier need for revision surgery. The most common reasons for revision surgery are aseptic loosening (75%), dislocation of the implant (6%), fractures (5%), and infections (7%) [13].

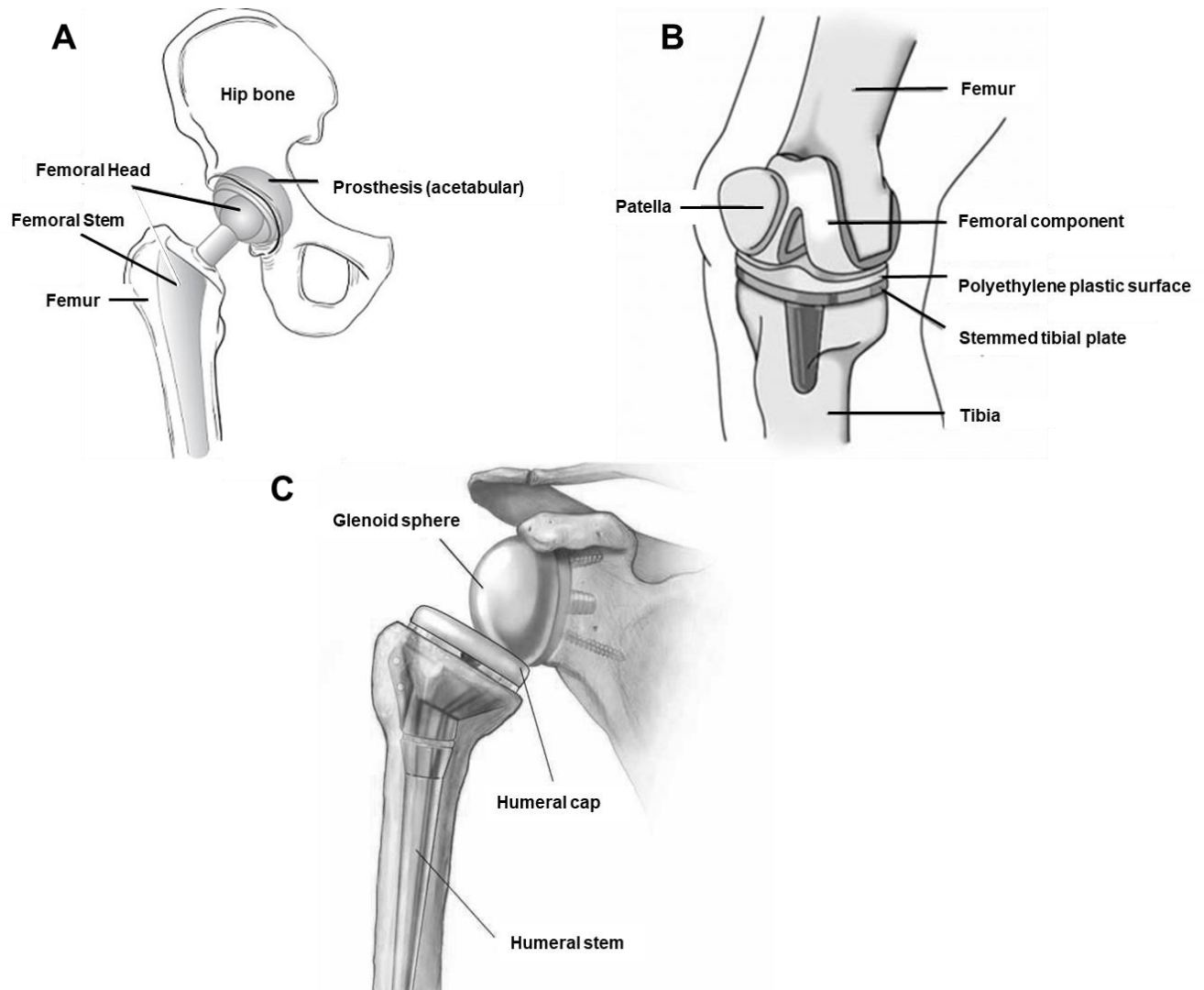


**Figure 1 Structure of a hip and knee endoprosthesis**

(A) Diagram of a hip implant (modified from the American Academy of Orthopaedic Surgeons <https://www.seitelman.com/wp-content/uploads/2016/10/hip1.jpg> 21.06.2021 14:05) (B) Diagram of a knee implant (modified from Sivarasu et al. 2008; 21.06.2021 14:05) (C) Diagram of the shoulder implant (modified from <https://www.drcarofino.com/blog/how-long-do-shoulder-replacements-last> 18.08.2021 11:26)

## 1.1 Periprosthetic Joint Infections

### 1.1.1 Medical Definition of a PJI

Periprosthetic joint infections (PJIs) bear a high economic and patient burden, with increased numbers of surgeries, pain, and prolonged mobility restrictions [14, 15].

The incidence rate of a PJI varies depending on different factors. A study by Zimmerli et al. in 2008 describes the risk of hip endoprosthesis PJI to be about 1% during the first two years after implantation, while the risk for a PJI of knee and shoulder implants is about 2% [16]. Furthermore, the risk of PJI increases up to 7% with each revision surgery and reinfection [17]. However, revision surgeries pose a higher risk for a PJI, and different comorbidities are determining factors. In particular, heart failure, diabetes, depression, anemia, chronic lung disease, obesity, rheumatologic diseases, renal disease, pulmonary circulatory disorders and history of osteomyelitis or septic arthritis are listed as typical risk factors for a PJI [18, 19]. Moreover, the sex and age of the patient also play an important role. Patients over 65 years are more prone to develop a PJI, and men are more likely to develop a PJI than women [20, 21]. It is not fully understood how gender influences the risk of acquiring an infection. The influence of other comorbidities on the development of a PJI is better characterized. For example, obesity increases the time of surgery during the implantation of an implant [22], which increases the risk of infection. Other comorbidities such as diabetes mellitus and rheumatoid arthritis are associated with a higher risk for PJI [23]. An *in vitro* study showed that biofilm formation on endoprosthesis is enhanced in the presence of elevated glucose concentrations, representing glucose levels in blood vessels of patients suffering from diabetes [24]. In addition, patients who have rheumatoid arthritis were shown to have an up to 2.3% higher increased risk for PJI due to immunosuppressive therapy [25]. Also, the implant material can increase the risk of a PJI, as the literature describes that metal-on-metal knee arthroplasties are more frequently infected than metal-on-plastic arthroplasties [26].

### 1.1.2 Identification of PJI by MSIS criteria

For the better identification of a PJI, the Musculoskeletal Infection Society (MSIS) has proposed some criteria defined by Parvizi et al. [27]. However, the identification of PJI according to the MSIS criteria is time-consuming and complex; therefore the use of these criteria in daily orthopedic practice is controversial [28-31]. According to the MSIS criteria, a PJI is diagnosed when the patient has at least one of the major criteria or a score over six from the minor criteria (fig. 2). To distinguish acute from chronic infections, a cut-off of 90-days after the operation is used. During a revision operation, three to six intraoperative specimens are taken from the synovial and interface membrane. The tissue and synovial fluid are sent to the microbiological diagnostic laboratory for bacteria culturing. The periprosthetic tissue samples are minced, mechanically homogenized and the fluids are inoculated on different agar under aerobic and anaerobic conditions. In addition, the samples are inoculated in broth for up to 14 days under aerobic and anaerobic conditions. The identification of the germs is performed by matrix-assisted laser desorption-ionization time-of light mass spectrometry (MALDI TOF MS) [32, 33]. Optimal culture sensitivity and specificity are

achieved when at least two cultures are positive with a pathogen, as a single positive culture can occur because of sample contamination [34]. This contamination can be caused by improper specimen collection, transportation, and processing [35]. Also, the incubation time of the cultures can increase the number of contaminations [23]. However, a single positive culture can be an important clue if the same organism is also found in another sample type, such as the synovial fluid [23].

In addition, typical inflammatory mediators in the blood are evaluated as identification of PJI. In fig. 2, the representative inflammatory serum markers like the C-reactive protein (CRP) or the white blood cell (WBC) count are minor factors for the identification of a PJI [36].

The CRP is an acute-phase protein produced in the liver, and the expression is induced upon inflammatory stimuli such as interleukin-6 (Il-6) [37, 38]. CRP can bind to gram-positive and gram-negative bacteria and stimulate leukocytes' adhesion and phagocytosis [39]. It is also involved in the activation of the complement cascade [40]. In PJI diagnostics, the CRP value is used as a blood marker to detect infection-related inflammation. However, the CRP value is not working as a specific parameter for the diagnosis of PJI, as the CRP can also be increased under inflammatory conditions and in autoimmune diseases such as rheumatoid arthritis, after a trauma, or even after a surgery [39]. As the CRP value is increased with inflammation, infection, as well as tissue damage, it cannot be used as a stand-alone technique for the diagnosis of a PJI and needs always to be interpreted in conjunction with other clinical and pathologic parameters [41]. The CRP value in a healthy patient is less than 5 mg/l, while the WBC count is less than 10 Gpt/l. It is shown that the CRP level is usually above 10 mg/l during an infection; the value correlates with the number of positive cultures [42]. However, as mentioned before, the CRP level alone is not a reliable indicator for PJI and can be within the physiological range in biofilm mediated or low-grade PJIs [43].

Another minor criterion for identifying a PJI is the use of histopathology (fig. 2) to determine the presence of infections and their extent [44, 45]. The histopathological evaluation is particularly useful when microbiological diagnostics cannot investigate tissue cultures because the pathogen is too difficult to culture due to the culturing conditions or too slow-growing [46, 47]. Similar to the serum markers, CRP and WBC, histopathology is an additional tool to the conventional methods. However, it can mainly support the microbiological diagnostics, as the microbiology diagnostic cannot distinguish between the colonization and true tissue invasion [47]. The inflammatory tissue response is different for bacterial, viral or, fungi infections [48]. In the case of a bacterial infection, there is an increased proportion of granulocytes, megakaryocytes and erythrocytes. Neutrophils, monocytes, macrophages, eosinophils, basophils, and mast cells are formed from granulocytes. Especially, neutrophils are found in cases of bacterial infections, as they are involved in the

elimination of bacteria on the one hand and the repair of tissues on the other hand [49, 50]. The histopathological diagnosis of a PJI is based on the number of neutrophils per high-power field [51]. Neutrophils also express the antimicrobial peptide  $\alpha$ -defensin [52, 53]. Alpha-defensin interacts with the cell membrane of the pathogen inducing its destruction. Therefore, the detection of  $\alpha$ -defensin in the synovial fluid has been proposed as a minor criterion for PJI diagnostic (fig. 2) [29].

However, as described before, the histopathological diagnosis is an additional tool to the conventional methods [47] as some staining methods can lead to artifacts. For example, gram staining can cause deposition fine dye crystals reminiscent of the bacterial-looking rods [47]. The interpretation of the histopathological results can also be complicated by the fact that especially in revision cases, the patients already suffered from a slight trauma due to the loosening of the implant caused by a PJI or because of abrasion material that can also cause inflammatory reactions in the tissue [54, 55] [56, 57]. Therefore, it is important to use histopathology always in conjunction with other criteria to diagnose a PJI.

Regardless of the major and minor criteria, the patient's health status is always considered in the diagnosis of PJI, as well as the five typical signs of inflammation as a local reaction at the respective joint.

Major criteria (at least one of the following)				Decision
Two positive cultures of the same organism				Infected
Sinus tract with evidence of communication to the joint or visualization of the prosthesis				
Minor criteria			Score	Decision
Preoperative diagnosis	Serum	Elevated CRP or D-Dimer	2	≥6 Infected
		Elevated ESR	1	
	Synovial	Elevated Synovial WBC or LE	3	2-5 Possibly Infected <sup>a</sup>
		Positive $\alpha$ -Defensin	3	
		Elevated Synovial PMN (%)	2	
		Elevated synovial CRP	1	
Intraoperative diagnosis <sup>a</sup>	Positive Histology <sup>c</sup>		3	≥6 Infected
	Positive Purulence		3	
	Single positive Culture		2	
				4-5 Possibly Infected <sup>b</sup>
				≤3 Not infected

**Figure 2** The updated 2018 definition for PJI from the Musculoskeletal Infection Society (MSIS).

The figure shows the criteria defined by MSIS for determining whether a PJI exists. Marked in white are the relevant criteria for this work to determine whether it is a PJI. Criteria in gray, such as positive  $\alpha$ -defensin, were not considered because they were not performed at the University of Magdeburg or were not relevant for this work.

<sup>a</sup>Operational criteria can also be used when the minor criteria are ambiguous. <sup>b</sup>Other molecular diagnostics should be considered e.g. Next-Generation Sequencing. <sup>c</sup>If there are more than 5 neutrophils per high-power field, histology is considered positive (x400) (modified from [58]).

### 1.1.3 Definition of PJI-Grade

In case of an acute infection of the joint, the five typical signs of inflammation are apparent at the respective joint. The joint is warm, the skin is red, and the joint is swollen. The patient has a fever, pain, and the ability to move the joint is reduced [59]. Using the major and minor MSIS criteria (fig. 2), a PJI can be easily identified. However, in particular infections, some of these criteria may not be present. Therefore, another critical PJI identification factor is based on the time until the immediate onset of the symptoms [23]. In general, PJI can be classified into early, delayed, and late PJI. The early PJI occurs less than three months after the last surgery at the respective joint. High-virulent pathogens predominantly cause these kinds of infections, for example, *Staphylococcus aureus*, *Streptococcus* spp., or *Enterococcus* spp. [60]. Moreover, they occur mainly due to intraoperative contamination. Therefore, mostly high-grade PJIs (HG-PJI) are classified as early PJIs. These are manifest with the typical signs of systemic inflammation, and local inflammatory reactions at the respective joint. Usually, two or more signs of inflammation (e.g., swelling, warmth, redness) are present [61].

Delayed PJIs usually occur between three and twelve months after surgery, while late-onset PJIs occur up to 12 months after the surgery [62]. These types of PJIs are often associated with low-grade infections (LG-PJI) and biofilm-related implant malfunctions (BIM). Delayed and late PJIs are often associated with unexplained pain, swelling of the joint, and stiffness. In some cases, a sinus tract is associated with the PJI and other systemic signs of inflammation, such as an increased serum CRP level [63]. These infections, in general, show a more subtle appearance which appears as rather unspecific symptoms making the diagnosis more complex [64] and hard to distinguish from aseptic failure [62]. LG-PJIs are often associated with low-virulent infections [62, 63] or slow-growing [65] bacteria like coagulase-negative *Staphylococcus* (e.g., *S. epidermidis*) or *Cutibacterium acnes*.

BIM is very similar to LG-PJI; however, the difference is that a LG-PJI shows the cardinal signs of infection in histopathology, whereas BIM shows no such signs [66]. In addition, the samples taken from BIM for microbiological diagnosis are usually only positive after prolonged cultivation time. In some cases, the patients show moderate functional limitations as well as pain. Due to a lack of typical inflammation signs, the infection may be falsely declared as aseptic loosening, and no septic revision surgery is performed [65]. Overall, LG-PJI and BIM occur more frequently (about 5 – 10%) than high-grade infections (0.5 – 2 %) [67].

LG-PJI or BIM are sometimes falsely diagnosed as culture-negative PJIs (CN-PJI), which occur with an incidence of up to 7% [68]. CN-PJIs are characterized by some typical inflammation factors, but no pathogens are detected in the microbiological cultures. This is often due to the pre-administration of antibiotics or the presence of biofilms. In addition, pathogens from BIM often do not form colonies when cultured on agar plates. [69]. Especially in cases of a low-grade infection that *Cutibacterium* or *Myobacterium* causes the diagnosis is difficult due to the ambitious culturing conditions of these pathogens. In such cases, aseptic loosening is usually assumed, and these patients suffer from re-occurring prosthesis loosening events and pain in the respective joint [69, 70]. The typically applied screening methods like tissue culturing [71] are not sensitive enough, or the bacteria have low virulence factors or specific culturing conditions (e.g., slow-growing or aerobic pathogens) [43]. In particular, a CN-PJI highlights the importance of making a precise diagnosis and considering other markers to take an entire clinical history.

## 1.2 Pathogens

Various bacteria are capable of causing a PJI. However, the most frequently found pathogens in a PJI belong to the *Staphylococcus* genus, particularly *S. aureus* and *S. epidermidis* [72]. *S. aureus* is one of the most common bacteria in early infections [60]. In particular, *S. aureus* is associated with an increased risk of infection in patients with rheumatoid arthritis, diabetes, hemodialysis and nasal colonization with the respective bacterium [73, 74]. *S. epidermidis* frequently causes BIM of the implant due to its ability to adhere to endoprosthetic materials and form a biofilm [75, 76]. However, similar to *S. aureus*, *S. epidermidis* can be identified during early-, delayed- and late-PJIs [23]. Bacteria that can cause a PJI can either occur monomicrobial or polymicrobial [77]. Usually, *Staphylococcus* spp. occurs as monomicrobial infections. In contrast, other bacteria such as *Enterococcus* spp. or anaerobic bacteria are often associated with polymicrobial infections.

Bacteria such as *Streptococcus* spp. or *Enterococcus* spp. occur less frequently compared to *Staphylococcus*, with approximately 10% of all PJIs [72]. It is described that *Streptococcus* spp. is mainly found on the skin and mucous membranes in humans, while *Enterococcus* spp. is present in the gastrointestinal tract and the urogenital tract. *Enterococcus* spp. rarely occur monomicrobial, but frequently associated with other bacteria (polymicrobial infection) [78, 79].

Anaerobic bacteria can also occur during a PJI but are less familiar with approximately 3 – 6 % of PJIs [23, 80]. One of the most common anaerobic bacteria, which can be found, is *Cutibacterium acnes*, which is part of the normal skin microbiota. Interestingly, *C. acnes* is the most frequently found bacteria in shoulder arthroplasty infections [81]. This infection with *C. acnes* seems to result

from direct contamination during the surgery [82]. Other germs such as *Bacteroides* spp. occur more rarely, and here *Bacteroides fragilis* can be described as the most common rare pathogens. Presumably, the infection occurs hematogenously [80] and occurs in association with polymicrobial infections (except for *C. acnes*) [77].

It has been described that polymicrobial infections can occur in up to 6% to 37% of all PJIs [83-85]. The pathogen spectrum of polymicrobial infection includes the presence of *S. aureus*, and more virulent bacteria such as gram-negative bacilli, methicillin-resistant *S. aureus* (MRSA), *Enterococcus* species, and anaerobic bacteria [77]. Typical risk factors of polymicrobial infections are the presence of various comorbidities [86], age above 65 years [77], rheumatoid arthritis [85], and wound drainage after the surgery [77]. The problem of polymicrobial PJIs is that the bacteria can work together and form more efficient biofilms that increase the tolerance towards antimicrobial agents [87, 88]. For example, the literature describes that some bacteria are less susceptible to antibiotics in biofilm than free-floating cells [89, 90].

### 1.2.1 Biofilms

Biofilms are referred to as microbial communities that can attach to abiotic or biotic surfaces [91]. Biofilms can be found on solid components as well as liquid surfaces [92, 93]. Consequently, biofilms have been found on medical devices such as catheters or implants [94]. The formation of a biofilm is an efficient way for pathogens to protect themselves from mechanical influences, antibiotics, and the host's immune system [95, 96]. Due to the limited diffusion of antimicrobial agents through the biofilm, the pathogens in deeper layers are protected against antibiotic reagents [97, 98].

The bacteria can adhere to hydrophobic surfaces such as plastics, latex, or silicone, and powerfully charged, hydrophobic surfaces such as glass or various metal alloys. Colonized materials can be differentiated into rough, structured, and smooth surfaces [92]. In general, it has been shown that rougher, hydrophobic materials are more attractive for pathogen attachment and biofilm formation [92, 99, 100].

The biofilm formation can be divided into five stages. The first stage is the initial and reversible attachment (1) of planktonic bacteria to the surface. This step is followed by an irreversible attachment of the bacteria to the surface and the formation of an extracellular matrix (2), the bacteria embedded in the extracellular matrix form microcolonies that result in bacteria multilayers. Within these microcolonies, the bacteria proliferate (proliferation phase) (3). The fourth stage is the biofilm maturation and growth; in this phase, the typical biofilm matrix is formed, consisting of exopolysaccharides, proteins, and DNA [101]. In the last phase (dispersion stage; 5), bacteria are released from the biofilm as planktonic cells [91], spreading and colonizing new sites. Thus, a new

cycle of biofilm formation is initiated [102]. The problem is that bacterial biofilms can make it challenging to analyze the bacteria within this film using the classical diagnostic methods (see chapter 1.1.2 Identification of PJI by MSIS criteria). As a result, typical signs of infection may be present in the patient, but no germ can be detected by microbiological diagnostic [66]. To improve the identification rate of infection, different methods are suggested that support microbial diagnostics, including molecular sequencing techniques such as next-generation sequencing (NGS) [103, 104] but also biofilm destabilization for better isolation of bacteria [105].

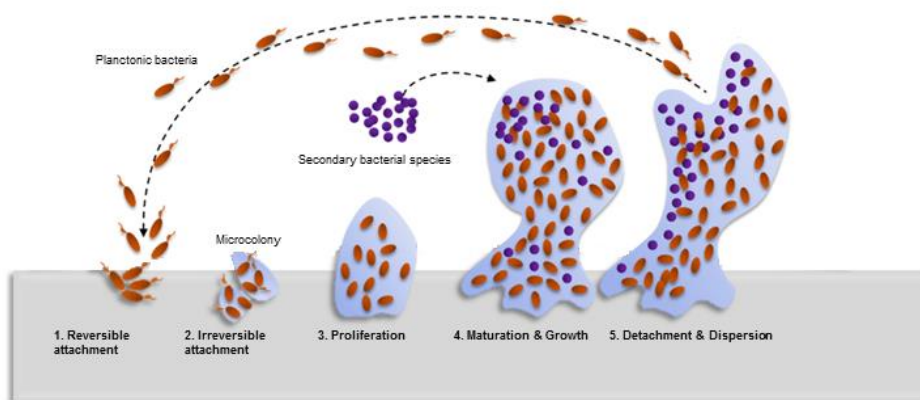


**Figure 3 The five steps leading to the biofilm formation**

The biofilm formation can be divided into five stages, reversible (1), the irreversible (2) attachment, the proliferation phase (3), the maturation and growth phase (4), and the detachment and dispersion of bacteria to colonize new areas (modified from Pinto et al. 2020 [106]).

## 1.3 Alternative techniques to identify a PJI

### 1.3.1 Next-Generation-Sequencing

Next-Generation Sequencing (NGS) has been proposed to be a proper adjunct technique in diagnosing infection and identifying pathogens [103, 104]. NGS is a method for sequencing DNA and RNA. The technique can characterize the entire microbial DNA to provide a complete microbial profile of a clinical sample. In addition to the microbial database, viruses, yeasts, fungi, and parasites can be sequenced and identified [107]. Two methodological approaches utilizing NGS have been described in the literature: (1) 16S amplicon-targeted NGS and (2) shotgun metagenome sequencing [108]. Employing the 16S amplicon technique, the 16S ribosomal RNA (rRNA) genomic region is amplified and sequenced using primers [109], recognizing the highly conserved region of these genes [110]. The 16S rRNA is chosen for various reasons: (1) the 16S rRNA gene is present in almost all bacteria; (2) at 1,500 bp, it is large enough for sequencing; (3) the gene is evolutionary conserved, which means it has not changed over the time [111]. Commonly the 16S rRNA is not sequenced completely, and only single variable regions are

analyzed. In total, there are nine of these variable regions in 16S rRNA (V1 - V9). In particular, MiSeq sequencing of Illumina has been used to examine the bacterial 16S rRNA V1-V2 gene region, which has up to 300 bp and overlaps completely [112]. The disadvantage of sequencing the 16S rRNA method is that the identification is based on the annotation of the 16S rRNA gene with taxa defined as an operational taxonomic unit (OTU). Overall, sequencing at the species level is less precise than the phyla or the genus level [113, 114]. The second methodological approach used by NGS is the whole-genome shotgun sequencing (WGS) [108]. Using WGS the bacterial genome is sheared into small fragments sequenced using random primers, and subsequently, overlapping regions are computationally assembled to reconstruct the original sequence. In contrast to the 16S amplicon method, whole-genome sequencing allows more precise identification at the species level. However, major disadvantages of WGS are its high cost and the requirement for more extensive data analysis [115].

Nowadays, there are approaches to use NGS as a new diagnostic tool for identifying PJIs [116]. The use of synovial fluid to identify pathogens by NGS and mass spectrometry has a sensitivity of 81% and a specificity of 95%. In recent years, it has been shown that this method could detect microorganisms in the synovial fluid of patients diagnosed with aseptic loosening [117], indicating a possible CN-PJI. While NGS for identifying bacteria in the synovial fluid has a relatively high specificity and sensitivity, it is slightly lower for tissue cultures (overall sensitivity of 50% - 86%) [60]. Sonication of explants and subsequent bacteria cultures in combination with NGS can further increase the sensitivity. This has been shown mainly in cases of CN-PJIs, biofilms, and in patients who have previously received antibiotic therapy [42, 117]. Another way to improve microbial diagnostics is to use biofilm-destabilizing techniques.

### **1.3.2 Biofilm-destabilizing techniques to improve diagnostics**

Sonication has been described as a successful method to destabilize biofilms from prostheses to isolate the bacteria subsequently [105]. However, sonication carries a relatively high risk of contamination. Damage or inaccurate sealing of the sample can lead to contamination from the sonication water [118]. This can lead to false-positive results in the std. microbiological diagnostic. Furthermore, sonication can damage sensitive bacteria; therefore, they cannot be identified by culturing later. This leads to false-negative results [105, 119, 120]. Dithiothreitol (DTT) has been tested as an alternative technique to sonication. DTT should destabilize the biofilm more efficiently by reducing disulfide bonds in the biofilm and breaking up the biofilm's extracellular matrix; this method is more cost-effective in comparison to sonication [121] [122]. The idea is that especially BIM or LG-PJIs can be detected more efficiently by using DTT. Thus, due to its low toxicity and easy use, the DTT reagent would be a good alternative to sonication [121].

A study from 2013 [121] investigated whether the use of DTT could provide better diagnostic results than sonication. It was shown that the bacteria survived the DTT treatment and could be cultured afterward. *S. epidermidis* was identified with higher sensitivity by the DTT method compared to sonication. Overall, it was recommended that DTT treatment be used as a substitute for sonication due to its easy use [121]. However, further studies need to be performed as only a limited number of patients were tested in the current study [121].

Another study showed that DTT and sonication are approximately equally sensitive [123]. In turn, a study from 2021 indicated that DTT provides worse overall sensitivity than sonication or conventional tissue culture. This was explained because of a possible low pH of DTT [124]. This inconsistency in the results does not indicate whether DTT would be suitable as a possible diagnostic method. In addition, whether the use of DTT positively influences the sensitivity of NGS has not yet been investigated. Possibly the interaction of two different techniques could additionally support or improve the std. tissue cultivation for PJI identification.

Microbiological identification of pathogens is the key factor for detecting PJI, but secondary factors like CRP, WBC, or histopathology also help secure the diagnosis [27]. Especially, persister cells can be a major problem in this context, as they are too inactive to be identified by cultivation.

Persister cells are found in the deeper layers of the biofilm; their growth rate is extremely slow or close to zero. Persister cells makeup 1% of the total cell population [125] and downregulate biosynthesis genes. As soon as the antibiotic wears off or the immune response of the body starts to get weaker. At this time point, these cells can reactivate and divide again [126].

Therefore, there is a need for alternative diagnostic features, which could recently concentrate on the immune response for PJI.

#### **1.4 Immune response to PJI**

The standard defense reaction against infections in the human body is inflammation, which is essential for tissue healing [127]. After a pathogen overcomes the host's physical barriers, such as skin or mucosa, various chemical and enzymatic processes get activated at the infection site. The cellular host defense includes the recruitment of macrophages and granulocytes to the infected area, followed by the activation of relatively slow defense mechanisms like B- and T-cell response [50]. The acute inflammatory response induces healing processes. The damaged regions are infiltrated by leukocytes, which are supposed to inhibit or eliminate bacteria and repair the tissue [128, 129].

During inflammation, the innate and adaptive immune systems are activated. As described before, the activation of the immune system results in the immigration of different immune cell types into

the inflamed tissue. Granulocytes differentiate into neutrophils, monocytes, eosinophils, basophils, mast cells, and macrophages [49, 50]. However, aseptic loosening is also characterized by macrophage infiltration [130]. Low-grade inflammation triggered by wear particles from the prosthesis results in chronic inflammation and activation of macrophages [131, 132]. These cells secrete cytokines and chemokines that attract further macrophages. This cycle leads to the suppression of osteoblast formation and function and promotes osteoclast formation, which resorbs the periprosthetic bone and results in aseptic implant loosening [133, 134]. In routine histology, CD68 is used as a marker for macrophages [135]. CD68 expression in macrophages is triggered as an inflammatory response to the presence of bacterial lipopolysaccharide (LPS) and the inflammatory cytokine interferon- $\gamma$  (IFN-  $\gamma$ ) [136]. CD68 positive neutrophils could also be detected in inflamed tissue [137]. However, if CD68 could serve as a marker for PJI has not yet been investigated in detail until now.

Neutrophils are among the most crucial granulocyte cells and get recruited to the site of infection in high numbers [138]. Neutrophils contribute to bacterial elimination through phagocytosis and release cytokines, proteases, and reactive oxygen species [49, 50]. An increased presence of CD66b – a marker for neutrophils - can be detected in PJI patients [139]. CD66b is a glycoprotein located in the specific granules, is expressed by granulocytes, and helps in the aggregation of neutrophils [140, 141]. As previously described, the numbers of neutrophils are increased in bacterial inflammation; therefore they are the main criterion in determining infection in the histopathological diagnostic [49, 50] [51]. However, wear particles generated from the implants can also induce neutrophil immigration. One study showed that a sterile inflammatory response to implants in mice resulted in the recruitment of active neutrophils [56]. Likewise, neutrophils bind to sterile implant surfaces after implantation and release extracellular DNA structures [57].

Both macrophages and neutrophils have been described to be used in histology to detect infections in tissues [135] [51]. However, both can be present in aseptic loosening, too. More specific markers for the detection of PJI are therefore urgently needed.

### 1.4.1 Biomarkers

Biomarkers are an essential analytical tool for the evaluation of biological parameters. These can be used to detect and quantify specific indicators which are increased during infection [142]. Biomarkers include laboratory tests, physiological tests, and imaging techniques [143]. For the detection of infections, a biomarker is defined as a biological molecule that can be analyzed in blood, body fluids, or tissues. The biomarkers provide information on whether an inflammatory process is taking place in the body [144]. Before a biomarker can be used as a diagnostic tool, it must be validated in four main phases defined by the Food and Drug Administration (FDA) [145].

These consist of the discovery of a potential biomarker (1) and the analytical validation (2); here, the sensitivity and specificity of the biomarker are crucial. It is followed by a clinical validation (3), which focuses on how well the biomarker can detect processes. Monitored by the final phase, which determines how well the biomarker confirms a diagnosis (4) [145]. To analyze the predictive value of a Biomarker, the sensitivity is plotted against the specificity (100 %-specificity). Using the respective area values for each sample, the receiver operating characteristic (ROC) curve showed the area under the curve (AUC). Based on the AUC classification of Turabieh et al. 2018, the biomarker can be evaluated (fig. 4) [146].

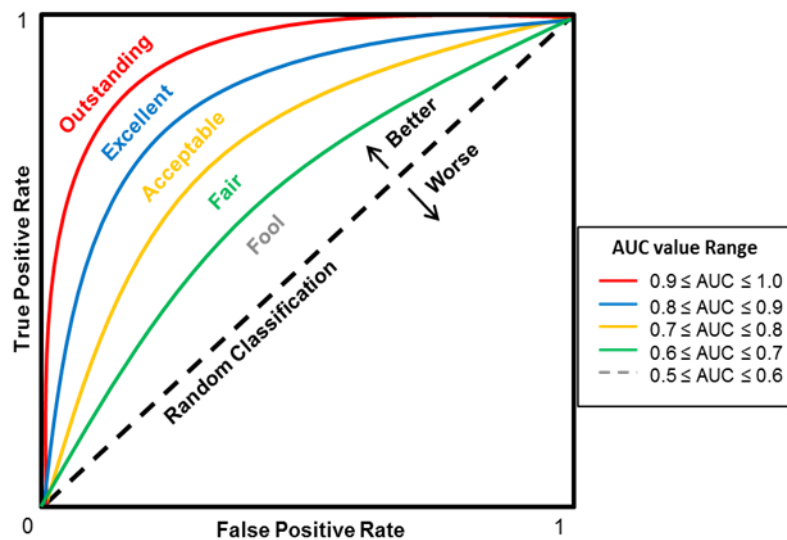


**Figure 4 Biomarker classification based on the AUC value**

The receiver operating curve is used to calculate the sensitivity and specificity for each possible parameter value. The area under the curve defines the range of values between the ROC curve and the x-axis. The biomarker classification can be used to evaluate the biomarker (modified after [146]).

Biomarkers are already widely used in laboratory diagnostics. The detection of WBC or CRP is already a secondary criterion for detecting PJI [27]. Using serum biomarkers such as CRP and WBC, reasonable diagnostic indications for PJI were achieved. However, these are not specific enough for PJI identification as both serum markers can be increased upon other inflammation-related processes, as described before (1.1.2 Identification of PJI by MSIS criteria) [147]. Therefore, other serum biomarkers such as IL-6, interferon- $\gamma$  (IFN- $\gamma$ ), and TNF- $\alpha$  have been tested in different studies. Similar to CRP and the erythrocyte sedimentation rate (ESR), they were not specific enough but showed a higher sensitivity [147, 148].

One of the most promising biomarkers so far is  $\alpha$ -defensin [147, 148]. During the phagocytosis process of pathogens, neutrophils secrete  $\alpha$ -defensin [53] while it induces bacterial cell death by permeabilizing the bacterial cell membrane [149] and disrupting the chemo-osmotic gradient [150, 151]. The detection of  $\alpha$ -defensin in synovial fluid of PJI patients by an ELISA showed the highest

accuracy for the diagnosis of PJI to date. The test has a sensitivity of 100% and a specificity of 95% [29, 152-154]. In a study from 2014 [28], the results of the  $\alpha$ -defensin test were compared with other criteria for detecting PJI based on the MSIS criteria (seen 1.1.2 Identification of PJI by MSIS criteria) [27]. These criteria consider mainly the serum CRP, ESR, and synovial fluid cell count. No statistical significance was observed for these values, and the sensitivity and specificity of  $\alpha$ -defensin exceeded those compared to other clinical detections [28]. In another study, it was shown that  $\alpha$ -defensin is activated independently of the pathogen. Neither species, virulence, or Gram-type affected the secretion of  $\alpha$ -defensin [155]. The  $\alpha$ -defensin lateral flow (ADLF) test is another technique to evaluate  $\alpha$ -defensin in the synovial fluid of patients; the test is provided by Synovasure, Zimmer, Warsaw, IN. The diluted synovial fluid is applied to the Synovasure PJI test cassette. In contrast to the ELISA, the test result is already available after 10 minutes [156]. The sensitivity of the ADLF test is 92.1%, and the specificity is 100% [157]. The ADLF test has a lower sensitivity than the  $\alpha$ -defensin ELISA. Therefore, it is not recommended as a screening method but rather for confirming a potential PJI diagnosis [158]. However, the tests do not work in the presence of massive metallic wear debris in the tissue (metallosis), in which case the tests lead to false-positive results [159]. Also, the presence of crystal deposits in the periarticular tissue (e.g., in gout or pseudogout patients) affects the test to the extent that false-positive results are obtained [160]. Nevertheless, the  $\alpha$ -defensin is listed among the MSIS ancillary criteria for the practical identification of PJI [27].

In contrast, a study from 2020 announced not to use the  $\alpha$ -defensin test in the routine analysis of a PJI. This study suggests using the  $\alpha$ -defensin test for cases in which PJI was not diagnosed upfront, which was nevertheless suspected to be septic [31]. Because the test can influence the treatment decision making [31] on the one hand, and on the other hand is the test costly [31, 147]. The  $\alpha$ -defensin test costs US\$524.79 per application, and in conjunction with additional tests, the price may increase up to US\$874.20 [31]. Therefore, the  $\alpha$ -defensin biomarker should only be used as a supplementary method [108] in unclear cases [31]. The use of alternative biomarkers to identify PJI should be further explored. Since CRP already provides preliminary information on whether an infection is present, the idea was to explore different complement system factors as a possible biomarker for PJI, as the CRP is involved in the activation of the complement cascade [40].

#### 1.4.2 The complement pathway

The complement system is an essential component of the innate immune system activated during inflammation and is organized through a cascade (fig. 5). The most important tasks are the labeling of pathogens for phagocytosis and lysis (opsonization), the formation of proinflammatory

mediators (anaphylatoxin), and the lysis of pathogens by the membrane attack complex (MAC), the latter being activated by the terminal complement pathway [161]. The activation of the complement pathway occurs via three pathways: the classical, the lectin, and the alternative pathway [161, 162].

The binding of C1q that binds on IgG or IgM activates the classical pathway. The mannose-binding lectin pathway is activated by binding mannose-lectin, a serum protein expressed upon infection with viruses or bacteria. The third possibility is the alternative pathway initiated by the decomposition of C3 into C3a and C3b [161, 163, 164]. All three pathways lead to the activation of the C3 convertase, a protease protein, with the subsequent cleavage of C5 [165, 166] (fig. 4).

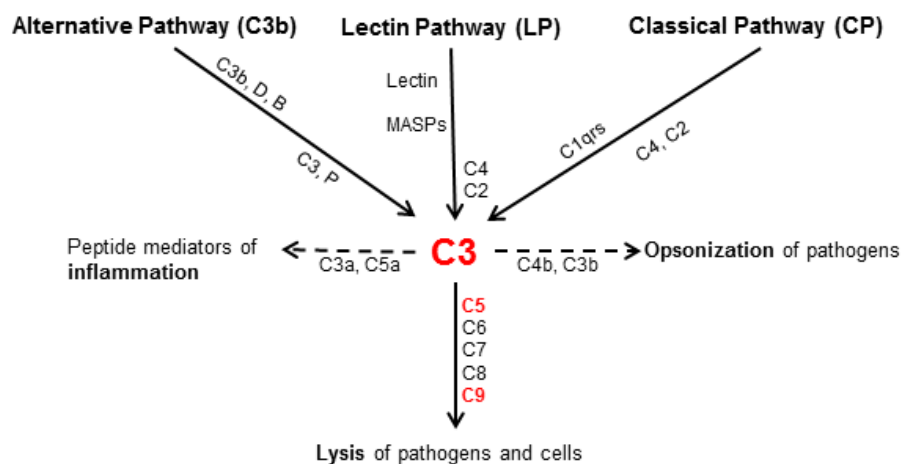


**Figure 5 A scheme of the complement system.**

The complement system has three major functions (1) lysis of infectious organisms, (2) activation of inflammation, and (3) opsonization of pathogens. The complement pathway gets activated by three pathways that lead to homologous variants of the protease C3 (red). The terminal complement pathway is initiated with C5 (red) and starts to form the membrane attack complex (C6, C7, C8 and C9 (red)) (Modified from IDF Patient & Family Handbook for Primary Immunodeficiency Diseases FIFTH EDITION, 2013 by Immune Deficiency Foundation, USA; [https://primaryimmune.org/wp-content/uploads/2011/05/complement\\_figure\\_1.gif](https://primaryimmune.org/wp-content/uploads/2011/05/complement_figure_1.gif) 23.06.2021 11.10)

One of the main tasks of the complement system is the elimination of pathogens by pore formation in the bacterial cell membrane. This is achieved by the terminal complement pathway and is initiated by the cleavage of C5 [162]. C3b initiates the assembly of the following complement components in the cell membrane. C5b binds to molecule C6 and forms the C5b,6-complex, which can bind the C7 molecule. These binding results in a conformational change where exposed a hydrophobic site on C7 that inserts into the lipid bilayer of the pathogen. Once C8 and C9 bind to the complex, they expose a hydrophobic site. In this process, C8 induces the polymerization of multiple copies of C9, which convert into a pore-like structure, referred to as the membrane attack complex (MAC) [167]. MAC forms a hydrophilic channel in the lipid bilayer of pathogens, resulting in the loss of cellular homeostasis, disruption of the proton gradient, and enzymes can enter the

bacteria, which ultimately leads to the destruction of the pathogen [167, 168]. By labeling the cells (opsonization) using complement receptors, the MAC complex can recognize which pathogens need to be destroyed, while other cells are attracted to the site by proinflammatory mediators [162-164].

The complement system is an essential factor in the destruction of pathogens. However, only a few studies investigated whether proteins of the complement pathway could be used as potential biomarkers to identify PJI. Furthermore, the literature describes that the complement pathway can be activated in patients with rheumatoid arthritis and after knee injuries. However, only C3 and C4 have been studied in more detail in the context of PJI [169, 170]. Activation of the complement system has also been demonstrated after primary hip arthroplasties [171]. Here the classical and the alternative pathway were investigated three days after surgery. As the CRP activation the activation of the complement cascade [40] and the CRP value is increased directly after an arthroplasty, the usefulness of this study is questionable [172]. Therefore, it is unknown whether the complement system would also be active during aseptic loosening.

To investigate possible new biomarkers, the utility of single synovial complement factors to distinguish LG-PJI from aseptic revisions has already been investigated [173]. C3b/iC3b, C4b, C5, and C5a showed increased levels in LG-PJI. These proteins are crucial for the subsequent formation of the membrane attack complex. In turn, an increased concentration of C5a was also measured in the presence of *Staphylococcus epidermidis* [174]. Identifying new biomarkers for the detection of LG-PJI and aseptic revision focused more on the complement system in the synovial fluid[173]; whether there might be higher activation of the complement system in the tissue was not investigated.

Until now, no study has investigated whether specifically C3, C5, and C9 as potential biomarkers for the detection of PJI, as they are involved in the direct destruction of pathogens.

## 1.5 Aim of the study

315,000 hip and knee revisions and up to 25,000 shoulder revisions were performed in 2020, with up to 7% of all cases attributable to infection. However, possible CN-PJIs are not included in the statistics because they are often declared as an aseptic revision. Due to the lack of inflammatory signs or a missing pathogen in diagnostic culture. By using alternative diagnostic tools such as NGS and biofilm destabilizing techniques, the idea is to reduce the number of CN-PJIs by identifying LG- and BIM-PJIs more easily.

Therefore, in the first part of this thesis, possible alternative techniques to facilitate the identification of PJIs were investigated using dithiothreitol (DTT). The aim was to compare the diagnostic results of the commercially available microDTTect device with routine PJI diagnostics and next-generation sequencing from DTT-treated samples.

Therefore, the following specific questions should be answered in this work:

- ❖ Can the use of DTT improve the standard microbiological diagnostic?
- ❖ Can the std. microbiological diagnostic be supported by the combined use of DTT and NGS?

For identifying a PJI, the  $\alpha$ -defensin biomarker has been proposed in the literature as an additional effective diagnostic tool. However, this biomarker is very expensive and shows false-positive results in patients suffering from metallosis and crystallopathies. The identification of alternative biomarkers to identify PJIs was further explored. Therefore, in the second part of this work, the aim was to investigate possible promising biomarkers such as CD68, CD66b, C3, C5 and C9 by immunohistochemically staining in periprosthetic tissue. The best candidate for a new biomarker should then be validated in a control cohort of PJI.

The aim was to answer the following questions:

- ❖ Can CD68, CD66b, C3, C5, and C9 proteins in periprosthetic tissue identify PJI better than  $\alpha$ -defensin by immunohistochemically staining?
- ❖ What is the sensitivity and specificity of each protein when comparing septic and aseptic revisions?
- ❖ How reliable is the possible new biomarker?
- ❖ Can potential comorbidities influence the biomarker?

## 2. Material and Methods

### 2.1 Materials

#### 2.1.1 Reagents

All biochemicals and chemical reagents which have been used during the experiments were obtained from these companies; AppliChem (Darmstadt), Merk (Darmstadt), Roche (Mannheim), Roth (Karlsruhe), Sigma Aldrich (München). If other reagents or chemicals were used from different companies, it will be stated. All reagents which have been used in this thesis can be seen in table 1.

Table 1: Biochemical and chemical reagents

Reagents	Manufacturer
100 bp DNA Ladder	HZI Braunschweig
37% HCl	Carl Roth
2-Propanol	Carl Roth
100% and 70% absolute undenatured alcohol	Carl Roth
Acetic acid, 100%	Carl Roth
Acetone	Carl Roth
Bovine Serum Albumin Fraction V	Sigma-Aldrich
BSA A1391,0250 Albumin Fraction V (pH 7.0)	AppliChem
Chloramphenicol (12.5 mg/mL in EtOH)	Carl Roth
Citratbuffer pH 6, pH 9	Dako
Dako Pen	Dako
Dako Waschpuffer	Dako
dNTP Mix 10 mM, PCR grade	Qiagen
Dulbeccos Phosphate Buffered Saline	Gilbco
Ethanol	Carl Roth
Ethanol absolute, denatured	Fischar
Fetal Calf Serum	Biochrom
Formaldehyde (4%)	Fischar,
Gen Ruler 100 bp Plus DNA Lader	NCBI
Immersion oil 518F	Zeiss, O
Incidin Foam Spray Head	Apotheke UK OVGU
Incidin Foam, Spray	Apotheke UK OVGU
QIAzol Lysis Reagent	Qiagen
Random Hexamer Primer	Fermentas
Rnase away Spray	Carl Roth

Reagents	Manufacturer
RNAse inhibitor	Thermo Scientific
Roti-Mount Fluorcare Dapi	Carl Roth
SDS ultra-pure	Carl Roth
Sodium chloride	Carl Roth
sodium deoxycholate	Sigma-Aldrich
Trichlormethan/Chloroform	Carl Roth
Tris Puffer	Carl Roth
Triton x	Carl Roth
Trizol Reagent	Invitrogen
Trypsin (0.5%)/EDTA (0.2%) Solution (10x) in PBS	Biochrom
Trypsin/EDTA Lösung (10x) (L2153)	Biochrom
Water, DEPC treated	Carl Roth

### 2.1.2 Consumables

All consumables which have been used in this thesis can be seen in table 2.

Table 2: Consumables

Material	Manufacturer
Cover glasses (24 x 50 mm)	Thermo Scientific
Cone cotton plug (12 x 17 x 37 mm)	neoLab Migge
Culture tubes (14 ml)	Corning Falcon
Culture dishes (60/15 mm)	Greiner Bio-one
Pipette tips (0.1 – 10 µl, 2 – 200 µl, 50 – 1000 µl)	Eppendorf
Reaction vessels (15 ml, 50 ml)	Greiner Bio-one
Reaction vessels (1.5 ml, 2 ml, 5 ml)	Eppendorf
Stripettes (1 ml, 5 ml, 10 ml, 25 ml, 50 ml)	Corning Costar
Well plate (24-well)	Greiner Bio-one
Filter pipette tips (0.1 - 2.5 µl, 2-200 µl, 100-10000 µl)	Biosphere
Microtome blades	Pfm medical
Scalpel blades	Schreiber Instrumente
Sterile filter (0.4 µM)	TPP
Tissue homogenization CK Mix (Ceramic Beat in 1.4 und 2.8 mm Diameter in 2 ml Tubes)	Bertin
MicroDTTect Device	4i for infection, Monza, NCS Lab Srl, Carpi, Italy

## 2.1.3 Equipment

All Equipment that have been used to conduct the experiments were listed below (see table 3).

Table 3: Equipment

Equipment	Manufacturer
Agarose electrophoresis voltage source	Bio-Rad
Analytical balance analytic A120 S	Sartorius
Automatic drainage TP1020	Leica Biosystems
Biological Safety Cabinets KS 18	Thermo Scientific
Biological Safety Cabinets S2020 1.5	Thermo Scientific
Centrifuge Heraeus, Fresco 17	Thermo Scientific
Centrifuge Heraeus, Megafuge 16R	Thermo Scientific
Centrifuge Miko 200R	Hettich
CrosLab 870 fume cupboard table	Medis Weber
Diode LED 405 nm	Strato
DNA/RNA UV Cleaner	Kisker Biotech
Embedding Center Shandon Histo Centre2	GMI
Gel documentation station	Bio-Rad
Histocentre2	Thermo Shandon
Homogenisator, Precelly ® 24	Bertin
Hyrax M55 Mikrotom	Zeiss
Incubator B6030	Heraeus
Incubator CD150	Binder Labortechnik GmbH
Incubator Orbital Shaker	VWR
Inverse microscope ABX51	Olympus
Inverse microscope Axio Observer.ZI	Zeiss
Inverse microscope Eclipse TS100	Nikon
Leica CM1850	Leica Biosystems
Light Cyclor 480	Roche
Magnetic stirrer C-MAG HS7	IKA
Megafuge 16R	Thermo Scientific
Microscope	Zeiss
Microscope Axio Observer, Camera: Axiocam 702 mono, Lampe HXP 120 V	Zeiss
Microtome Hyrax M55	Zeiss
Microtome Hyrax M55	Zeiss

Equipment	Manufacturer
Microscope BX50	Olympus
Minicentrifuge	Biozym
Multiple Dispenser Handy Step Electronic	Brand
Perfect Spin plate Spinner C1000-PEQ,230EU	PeqLab
Photometer GeneQuant1300	Biochrom
Pipette BioHit	Sartorius
Pipette Research (plus)	Eppendorf
Pipetting aid Accu-jet pro	Brand
Platform rocker SSL4	Stuart
Precelly@24 Homogenisator	Bertin Instruments
Precision scale EWB	Kern
QuantStudio 6 Flex	Applied Biosystems
Real Time-PCR Detector	Applied Biosystems
Roll-Mixer RM 5.40	Hecht Assistant
Roll-Mixer RS-TR05	Phoenix Instruments
Rotor Fa-45-30-11	Eppendorf
Rotor, F-35-6-30	Eppendorf
Scale A120S	Sartorius
Scale ALC-810.2	Sartorius
Scale core EWB 620-2M	Sartorius
Scanning electron microscope XL30-FEG/ESEM	FEI
Shaker MTS2	IKA
Shaking Incubator Thermo Mixer C	Eppendorf
Sputter Coater K550	Emitech
Standard Power Pack 25	Biometra
Steril bench S2020 1.5	Thermo Scientific
Sterile bench Herasafe KS18	Thermo Scientific
Sterile bench KS18	Thermo Scientific
T100 Thermo Cyclor	Bio-Rad Laboratories
T100 Thermal Cyclor for PCR	Bio-Rad Laboratories
Thermal shaker Themomixer compact	Eppendorf
Thermocycler iCycler thermal cyclor	Bio-Rad Laboratories
Thermocycler iCycler thermal cyclor	Eppendorf
Thermoincubator	Binder Labortechnik GmbH
Tilt and roll mixer rs-TR05	Phoenix Instruments
Tissue processor TP1020	Leica Biosystems

Equipment	Manufacturer
Tube Revolver/Rotator	Thermo Scientific
Ultrasonic cleaner USC1200D	VWR
Vortex Genie 2 Mixer	Scientific Industries
Vortexer	Phoenix Instruments
Warming cabinet large	Heraeus
Warming cabinet small	Heraeus
Water bath Thermolab type 1070	GFL
Zentrifuge Heraeus , Megafuge 16R	Thermo Scientific
Zentrifuge Heraeus Megafuge 16R	Thermo Scientific

### 2.1.4 Primer

The Primer which have been used for the first and second nested PCR as well as the Illumina Next-Generation Sequencing were listed below (table 4; table 5) and were bought by metabolism. The Concentration of the Stock solution was 1 pmol/µl in water. For the PCR the Stock solution was diluted at 1:10.

Table 4: Primer for the first and second nested PCR

Description	Sequence
Fw_16s_bif2	AGRGTTTGATYMTGGCTCAG
338R	TGCTGCCTCCCGTAGGAGT
16SFw_BK	ACGACGCTCTTCCGATCTAGRGTTTGATYMTGGCTCAG
16SR_BK	GACGTGTGCTCTTCCGATCTTGCTGCCTCCCGTAGGAGT

Table 5 Primer for the Illumina-Next-Generation Sequencing

Forward and Reversed Primer for Illumina Next-Generation Sequencing	
I_A501	AATGATACGGCGACCACCGAGA TCTACACTGAACCTTTCTTTCCCTACACGACGCT CTTCCGATCT
I_A502	AATGATACGGCGACCACCGAGA TCTACACTGTTCTTTCTTTCCCTACACGACGCT CTTCCGATCT
I_A503	AATGATACGGCGACCACCGAGA TCTACACTAAGACACTTTTCCCTACACGACGCT CTTCCGATCT
I_A504	AATGATACGGCGACCACCGAGA TCTACACCTAA TCGATCTTTCCCTACACGACGCT CTTCCGATCT

Forward and Reversed Primer for Illumina Next-Generation Sequencing	
I_A505	AATGATACGGCGACCACCGAGA TCTACA CCTA GAACA TCTTTCCCTACACGACGCT CTTCCGATCT
I_A506	AATGATACGGCGACCACCGAGA TCTACA CTAAGTTCTCTTTCCCTACACGACGCT CTTCCGATCT
I_A507	AATGATACGGCGACCACCGAGA TCTACA CTAGACCTA TCTTTCCCTACACGACGCT CTTCCGATCT
I_D501	AATGATACGGCGACCACCGAGA TCTACA CTA TAGCCTTCTTTCCCTACACGACGCT CTTCCGATCT
I_D502	AATGATACGGCGACCACCGAGA TCTACA CA TAGAGGCTCTTTCCCTACACGACGCT CTTCCGATCT
I_D503	AATGATACGGCGACCACCGAGA TCTACA CCCTA TCCTTCTTTCCCTACACGACGCT CTTCCGATCT
I_D504	AATGATACGGCGACCACCGAGA TCTACA CCGGCTCTGATCTTTCCCTACACGACGCT CTTCCGATCT
I_D505	AATGATACGGCGACCACCGAGA TCTACA CAGGCGAAGTCTTTCCCTACACGACGCT CTTCCGATCT
I_D506	AATGATACGGCGACCACCGAGA TCTACA CTAATCTTA TCTTTCCCTACACGACGCTC TTCCGATCT
I_D507	AATGATACGGCGACCACCGAGA TCTACA CCAGGACGTTCTTTCCCTACACGACGCT CTTCCGATCT
I_D508	AATGATACGGCGACCACCGAGA TCTACA CGTACTGACTCTTTCCCTACACGACGCT CTTCCGATCT
I_N502	AATGATACGGCGACCACCGAGA TCTACA CCTCTCTATTCTTTCCCTACACGACGCT CTTCCGATCT
I_N504	AATGATACGGCGACCACCGAGA TCTACA CAGAGTAGA TCTTTCCCTACACGACGCT CTTCCGATCT
I_N505	AATGATACGGCGACCACCGAGA TCTACA CGTAAGGAGTCTTTCCCTACACGACGCT CTTCCGATCT

Forward and Reversed Primer for Illumina Next-Generation Sequencing	
I_N506	AATGATACGGCGACCACCGAGA TCTACA CACTGCA TA TCTTTCCCTACACGACGCT CTTCCGATCT
>I_N507	AATGATACGGCGACCACCGAGA TCTACA CAAGGAG TA TCTTTCCCTACACGACGCT CTTCCGATCT
>I_N508	AATGATACGGCGACCACCGAGA TCTACA CCTAAGCCTTCTTTCCCTACACGACGCT CTTCCGATCT
>I_N509	AATGATACGGCGACCACCGAGA TCTACA CGCGTAAGA TCTTTCCCTACACGACGCT CTTCCGATCT
>I_S510	AATGATACGGCGACCACCGAGA TCTACA CCGTCTAA TTCTTTCCCTACACGACGCT CTTCCGATCT
>I_S511	AATGATACGGCGACCACCGAGA TCTACA CTCTCTCCGTCTTTCCCTACACGACGCT CTTCCGATCT
>I_S512	AATGATACGGCGACCACCGAGA TCTACA CTGACTAGTCTTTCCCTACACGACGCT CTTCCGATCT
I_A701	CAAGCAGAAGACGGCATA C GAGATA TCACGACGTGACTGGAGTTCAGACGTGTGC TCTTCCGATCT
I_A702	CAAGCAGAAGACGGCATA C GAGATA CAGTGGTGTGACTGGAGTTCAGACGTGTGC TCTTCCGATCT
I_A703	CAAGCAGAAGACGGCATA C GAGATCCA GTGACTGGAGTTCAGACGTGTGC TCTTCCGATCT
I_A704	CAAGCAGAAGACGGCATA C GAGATA CAAACGGGTGACTGGAGTTCAGACGTGTGC TCTTCCGATCT
I_A705	CAAGCAGAAGACGGCATA C GAGATACCAGCAGTACTGGAGTTCAGACGTGTGC TCTTCCGATCT
I_A706	CAAGCAGAAGACGGCATA C GAGATA ACCCTCGTACTGGAGTTCAGACGTGTGC TCTTCCGATCT
I_A707	CAAGCAGAAGACGGCATA C GAGATCCCAACCTGTACTGGAGTTCAGACGTGTGC TCTTCCGATCT

Forward and Reversed Primer for Illumina Next-Generation Sequencing	
I_A708	CAAGCAGAAGACGGCATAACGAGATCACCACACGTGACTGGAGTTCAGACGTGTGC TCTTCCGATCT
I_A709	CAAGCAGAAGACGGCATAACGAGATGAAACCCAGTGACTGGAGTTCAGACGTGTGC TCTTCCGATCT
I_A710	CAAGCAGAAGACGGCATAACGAGATTGTGACCAAGTGACTGGAGTTCAGACGTGTGC TCTTCCGATCT
I_A711	CAAGCAGAAGACGGCATAACGAGATAGGGTCAAGTGACTGGAGTTCAGACGTGTGC TCTTCCGATCT
I_A712	CAAGCAGAAGACGGCATAACGAGATAGGAGTGGGTGACTGGAGTTCAGACGTGTGC TCTTCCGATCT
I_D701	CAAGCAGAAGACGGCATAACGAGATATTAICTCGGTGACTGGAGTTCAGACGTGTGCT CTTCCGATCT
I_D702	CAAGCAGAAGACGGCATAACGAGATTCGGAGAGTGACTGGAGTTCAGACGTGTGC TCTTCCGATCT
I_D703	CAAGCAGAAGACGGCATAACGAGATCGCTCAATTGTGACTGGAGTTCAGACGTGTGC TCTTCCGATCT
I_D704	CAAGCAGAAGACGGCATAACGAGATGAGATTCCGTGACTGGAGTTCAGACGTGTGC TCTTCCGATCT
I_D705	CAAGCAGAAGACGGCATAACGAGATATTCAGAAAGTGACTGGAGTTCAGACGTGTGCT CTTCCGATCT
I_D706	CAAGCAGAAGACGGCATAACGAGATGAATTCGTGTGACTGGAGTTCAGACGTGTGC TCTTCCGATCT
I_D707	CAAGCAGAAGACGGCATAACGAGATCTGAAGCTGTGACTGGAGTTCAGACGTGTGC TCTTCCGATCT
I_D708	CAAGCAGAAGACGGCATAACGAGATTAATGCGCGTGACTGGAGTTCAGACGTGTGC TCTTCCGATCT
I_D709	CAAGCAGAAGACGGCATAACGAGATCGGCTATGGTGACTGGAGTTCAGACGTGTGC TCTTCCGATCT

Forward and Reversed Primer for Illumina Next-Generation Sequencing	
I_D711	CAAGCAGAAGACGGCATAACGAGATTCTCGCGCGTGACTGGAGTTCAGACGTGTGC TCTTCCGATCT
I_D712	CAAGCAGAAGACGGCATAACGAGATAGCGATA GGTGACTGGAGTTCAGACGTGTGC TCTTCCGATCT
I_N701	CAAGCAGAAGACGGCATAACGAGATTTCGCCTTAGTGACTGGAGTTCAGACGTGTGC TCTTCCGATCT

### 2.1.5 Antibodies

All used primary antibodies, IgG control, and secondary antibodies which have been used in this thesis were listed below in table 6, table 7 and table 8.

Table 6: Antibodies

Antibody	IgG	Stock Concentration	Dilution	Demasking	Manufacturer
C3	Rabbit	0,16 mg/ml	1:100	Pepsin	Invitrogen - PA5-12349
C5	Rabbit	1 mg/ml	1:200	Pepsin	Invitrogen - PA5-22183
C9	Rabbit	1 mg/ml	1:500	Pepsin	Abcam - ab71330
$\alpha$ -Defensin	Goat	0.5 $\mu$ g/ml	1:100	Citrate-buffer pH 6	Acris - AP23709
CD68	Mouse	200 $\mu$ g/ml	1:500	Citrat-Buffer pH 6	Santa Cruz - sc59104
CD66b	Rabbit	0.8 mg/ml	1:200	Citrat-Buffer pH 6	Abcam - ab197678

The antibodies listed in table 7 were used as controls. The stock concentration was diluted to match the respective antibody in table 6.

Table 7: IgG Control

Antibody	Stock Concentration	Manufacturer
Rabbit IgG	5 mg/ml	Thermo Fischer - 02-6202
Mouse IgG	2.5 mg/ml	Thermo Fischer - 02-6502
Goat IgG	5 mg/ml	Thermo Fischer - 02-6202

Table 8: Secondary Fluorescence Antibodies

Antibody	Typ	Stock Concentration	Dilution	Manufacturer
Alexa Fluor® 555	Anti-Rabbit	2 mg/ml	1:200	Abcam - ab150130
Alexa Fluor® 555	Anti-Mouse	2 mg/ml	1:200	Thermo Fischer - A-21202
Alexa Fluor® 488	Anti-Mouse	2 mg/ml	1:200	Thermo Fischer - A-31570
Alexa Fluor® 555	Anti-Goat	2 mg/ml	1:200	Abcam - ab150129

### 2.1.6 Buffer and media

Buffer and media which have been used were listed the table below (table 9).

Table 9: Buffer and media

Buffer	Reagents	Concentration/Amount
50x Electrophoresis Buffer TAE	EDTA disodium salt	50 mM
	Tris	2 M
	Glacial/acetic acid	1 M
Extraction buffer	Urea	6 M
	Tris	10 mM
	PiC	
PBS in ddH <sub>2</sub> O, pH 7.4	NaCl	140 mM
	KCl	2.7 mM
	Na <sub>2</sub> HPO <sub>4</sub>	8 mM
	KH <sub>2</sub> PO <sub>4</sub>	1.8 mM
Wash buffer	dH <sub>2</sub> O	900 ml
	Wash buffer (Dako)	100 ml

**2.2 Methods****2.2.1 Sample Collection and preservation**

Patients who underwent a revision THA, TKA, and TSA were included in this dissertation after they were informed and consent. IRB approval for this study was provided by the Institutional Review Board of the Medical School, Otto-von-Guericke University, Magdeburg (No 150/12, 207/17, and No 57/18).

All surgeries were performed in the Department of Orthopedic Surgery at the University Hospital in Magdeburg. The revisions were classified as aseptic or septic based on the MSIS criteria [27].

**2.2.1.1 Tissue collection and preservation**

The specimens from the synovial membrane and synovial fluid were taken during surgery. The tissue was incubated with RNA-later for two days at 4 C and stored at -80°C. Also, samples were preserved in formaldehyde for paraffin sections and were frozen without adding any solution for protein isolation. The synovial fluid was aliquoted and stored at -80°C until use.

**2.2.1.2 MicroDTTect handling and preservation**

The microDTTect bag was handled according to the manufacture's protocol (4i for infection, Monza, NCS Lab Srl, Carpi, Italy). The explants were placed in the microDTTect bag under sterile conditions during the surgery. In the laboratory, 150 ml of the DTT solution supplied with the bags were added to the explant within the device. The microDTTect bag was shaken using Rocker SSL4, Biocore continuously at RT; the solution was taken off and transferred to three 50 ml falcons and centrifuged at 3.200 rpm, for 10 min at RT. Afterward, the supernatant was discarded except for 2 ml DTT solution. These were used to dissolve the pellet; 2 ml was sent to the routine microbiological diagnostic for culturing and specification of possible bacterial infection. The other 2x2 ml were subjected to DNA isolation which was used for NGS sequencing. The experimental setup can be seen in fig. 6.

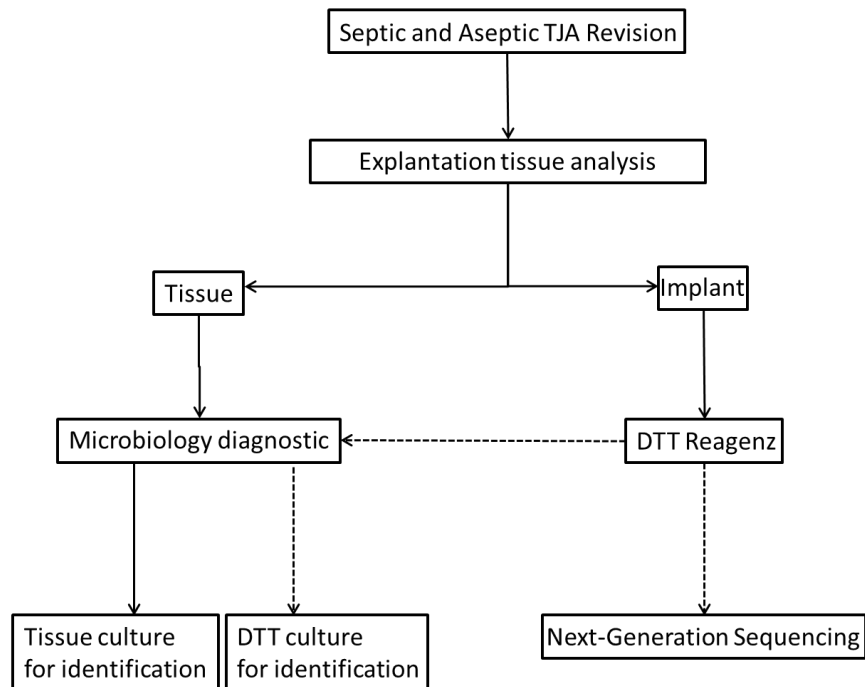


**Figure 6 The analytical process in a flow-chart**

During surgery, the respective joint implant was explanted, and adjacent tissue samples were collected. Left branch: The tissue samples were sent to the microbiological department for homogenization and tissue culturing, identifying a pathogen. Right branch: After revision of the prostheses, the implant was placed into the microDTTect bag for treatment with DTT. One part of the solution was sent to the microbiological diagnostic department for DTT culturing. In contrast, the other part of the solution was used for DNA isolation and Next-generation sequencing (NGS).

## 2.2.2 Molecular biological methods

### 2.2.2.1 DNA Isolation from microDTTect solution

The DNA was isolated following the manufacturer's protocol from the FastDNA Spin Kit for Soil (MP Biomedicals™); all steps were done at RT. This kit provided the reagents.

The tissue specimens from the synovial membrane were put into Precellys Lysing Kit (P000918-LysKO-A, Berting, Montigny-le-Bretonneux, France) tubes with 878 µl Sodium Phosphate Buffer and 122 µl MT solution; the solution begins to solubilize membrane proteins with detergents as well as extracellular proteins and contaminants. Using Precellys® 24 homogenizer (Bertin, Montigny-le-Bretonneux, France), the swabs and the tissue were disrupted at 5.5 Hz for 60 seconds. The tubes were centrifuged at 14,000x g for 5 min to remove cell debris, extracellular matrix, or other impurities. The supernatant was transferred into a new 2 ml tube, and 250 µl PPS (Protein precipitation solution) was added and mixed vigorously; this separates the solubilized nucleic acids from the cellular debris and lyses the matrix. Again, the solutions were centrifuged for 5 min at 14,000 g to pellet the precipitates. The supernatant was transferred to a clean 15 ml microcentrifuge tube. The supernatant was added to the binding matrix and inverted by hand for 2 min to allow DNA binding to the silica matrix. Afterward, the samples rested for at least 15 min

to ensure the complete settling of the silica matrix. The binding matrix was gently resuspended by repeatedly pipetting the solution up and down; 600 µl of the solution was transferred to a SPIN™ filter and centrifuge at 14,000 g for 1 min. The collection tube was emptied, and the remaining mixture was added to the SPIN™ Filter. Before using the SEWS-M solution, 100 ml of 100 % ethanol was added. For washing the silica matrix, 500 µl of SEWS-M was added and resuspended. The samples were again centrifuged for 1 min at 14,000 g, and the collection tubes were emptied again. For the drying of the filter, the collection tube was centrifuged without any liquid for 2 min at 14,000x g. The collection tube was discarded, and the filter was put into a new, clean collection tube. Removing residual ethanol, the spin filters were air-dried for 5 min at RT. Before using the DES- (DNase/Pyrogen-free) water was incubated for 5 min at 55°C on a heat block that helps to increase the yields. 30 µl of DES was added to the filter. The purified nucleic acids elute from the silica-matrix on the filter, as the cation bridges collapse because low salt elution solution rehydrates both the silica the DNA. Again, the tubes were centrifuged at 14,000x g for 1 min to elute the DNA into the clean collection tube. The DNA can be stored at -20°C for extended periods or 4°C until use.

### 2.2.2.2 16s DNA gene preparation and NGS sequencing

To amplify the bacterial-specific V1V2 region of the 16S rDNA gene, a 3-step-PCR (nested-PCR) was approached. The DNA samples were prepared from the DTT solution of chapter 2.2.1.2 MicroDTTect handling and preservation. To obtain the DNA, the procedure described in 2.2.2.1 DNA Isolation from microDTTect solution was used. The Primer Fw\_16s\_bif2 and 338R for 20 cycles were used to enrich the target sequences for the first PCR. For amplification, the forward (Fw\_16s\_bif2) and reverse (338R) primers bind to the bacterial-specific V1V2 region of the 16S rDNA gene. For the second amplification, the resulting PCR product was used, and here 16SFW\_BK was used as the forward primer and 16SR-BK as the reverse primer; these have a larger overhang than the primers in the first PCR. A total of 15 cycles were used for the second PCR. For the first and the second PCR following reaction mix was used (table 11 and table 12).

Table 10: Reagents for the first and second reaction mix of the nested PCR

Reagent	Amount for 1 sample [µl]
Buffer (5x)	4
dNTPs	1.6
Forward Primer	0.5
Reverse Primer	0.5
Takara Enzym	0.2

Reagent	Amount for 1 sample [ $\mu$ l]
DNA-Sample	2
RNase free water	11.2
total	20

The PCR protocol is displayed in table 12.

*Table 11: Protocol first and second reverse transcription using Takara*

Step	Temperature [ $^{\circ}$ C]	Time [min]
Initial denaturation	95 $^{\circ}$ C	3 min
Denaturation	98 $^{\circ}$ C	10 s
Annealing	55 $^{\circ}$ C	10 s
Elongation	72 $^{\circ}$ C	10 s
Dissociation stage	72 $^{\circ}$ C	2 min
Resting	4 $^{\circ}$ C	$\infty$

After the second PCR, an agarose gel electrophoresis [175] was performed to verify which samples showed products in the V1V2 region. Samples that failed to give a PCR product were not further analyzed and defined as “no PCR product”, the absence of DNA may be due to the presentation of an aseptic revision. The samples with a positive PCR product seen at 350 bp [176] in the electrophoresis gel were prepared for the third amplification. For the third amplification, the Illumina adapters [177] as primers (Primer Sequence IA\_501 – I\_S512) were added to the reaction mix (table 13). The third PCR protocol can be seen in table 15 and was used for 10 cycles. Obtained products were pooled in equimolar ratios and sequenced on Illumina MiSeq (2x300 bases, San Diego, USA).

*Table 12: Reaction mix for the third amplification*

Reagent	Amount for 1 sample [ $\mu$ l]
Buffer (5x)	10
dNTPs	4
Forward Primer	1.25
Reverse Primer	1.25
Takara Enzym	0.5
DNA-Sample	1
RNase free water	32
total	50

To analyze the purity of the PCR products after the third amplification, gel electrophoresis was performed. Subsequently, the PCR products were shipped to the Institute of Genome Analytics at the Helmholtz Centre for Infection Research (HZI), Braunschweig, and processed by Illumina-NGS.

### **2.2.2.3 Agarose gel electrophoresis**

A 2 % agarose gel was used to analyze the quality of the DNA samples after the second and third amplification method with RT-PCR. Therefore, 2 g of agarose was melted in 1 x TAE buffer, per 100 ml 2 µl of Ethidiumbromid were added. The mixture was poured into a casting chamber. After polymerization, the gel was transferred into the electrophoresis chamber and overlaid with 1 x TAE buffer. The samples were mixed with 1:10 10x Gel loading dye, and 2 – 3 µl of the sample was applied to the gel. To determine the size of the separated DNA fragments, a 100 bp DNA loading Dye was also applied to the gel. For the documentary of the agarose gel via UV light, a documentation system from Bio-Rad, Netherlands, was used.

### **2.2.3 Microbiological routine diagnostic testing**

Microbiological analysis of tissue samples was performed by the Institute of Medical Microbiology and Hospital Hygiene; the contact person was Dr. Jaqueline Färber. 3 to 6 tissue samples were collected and subsequently processed by standard microbiology routine during the revision surgery. Upon arrival, the periprosthetic tissue samples were cut into pieces and mechanically homogenized by the Ultra-Turrax Drive control disperser (IKA®-Werke GmbH & Co. KG, Germany) at 6000 rpm for 2 min with interval direction change. The homogenized samples were then inoculated onto agar plates. The following plates were used: Columbia agar with 5 % sheep blood (Becton Dickinson, Heidelberg, Germany), chocolate agar, and Schaedler agar (Oxoid, Munich, Germany) under aerobic conditions with 5% CO<sub>2</sub> and aerobically at 35 ± 1°C. In addition, samples were inoculated in thioglycolate- and Schaedler-Boullion (bioMérieux, Marcy L'Etoile, France) at 35 ± 1°C for 14 days. The identification of the pathogens was performed by MALDI-TOF MS (Vitek ®, bioMérieux, Marcy L'Etoile, France).

### **2.2.4 Histological methods**

#### **2.2.4.1 Paraffin sections**

Soft tissues were fixed in 4 % formaldehyde (27279, Fischer, Zurich, Switzerland) for a minimum of 24 h. For dehydration of the samples, a tissue processor (Leica TP1020, Leica) was used;

afterward, they were embedded in paraffin. The paraffin samples were cut into 4 µm thick sections with a microtome (Hyrax M55, Zeiss) for the immunohistological and histological staining. They were placed on microscope slides and dried overnight at 37°C.

#### **2.2.4.2 Immunohistochemically staining**

For staining with immunohistological antibodies, the section had to be deparaffinized and rehydrated. For deparaffination, the samples were treated with xylene twice for 10 min each. The sections were treated using a descending alcohol series (100 %, 96 %, 70 %, and 50 %) for 5 min each for rehydration. Finally, the samples were treated two times with water for 5 minutes. During the storage in formaldehyde, cross-links between proteins were formed, which can be dissolved by unmasking the slides, thus restoring the antigenicity of the proteins. The demasking can be performed enzymatically using trypsin or pepsin or by heat using citrate buffer with pH 9 or 6. Which type of unmasking needed to be used was previously tested with various antibodies and samples. The slides stained with antibodies of the complement system (anti-C3, anti-C5, and anti-C9; Quidel, San Diego, CA, USA) were demasked enzymatically. Therefore specimens were incubated with 0.02 % HCl solution at RT for 15 min, following pepsin (0.25 mg/ml in PBS) for 45 min at 37°C. Slides that were stained with α-Defensin (Acris, OriGene Technologies, Rockville, MD, USA), CD68 (Santa Cruz Biotechnology, Santa, CA, USA), and CD66b (Abcam, Cambridge, England) needed to be treated with citrate buffer (pH6) for 25 min at 95°C, followed by a cooling period in the buffer solution for another 25 min at RT. After demasking, the slides were washed with wash buffer three times for 5 min and blocked with 4 % BSA for 1 h at RT to block free epitopes. The antibodies and the isotype control (IgG control of the species) were diluted in 4 % BSA according to the protocol (table 6 and table 7), and specimens were incubated overnight at 4°C with the primary antibodies. To remove unbound antibodies from the slides, they were washed three times with wash buffer for 5 min and incubated with the fluorescent-labeled secondary antibody (Alexa 488 or Alexa555) (table 8) for 1 h in the dark at RT. Again, the slides were washed three times with wash buffer for 5 min and then coverslipped using Roti®-Mount FlouresCare DAPI (Roth) and stored at 4°C in the dark until use.

#### **2.2.4.3 Fluorescence microscopy**

For fluorescence microscopy, the Zeiss fluorescence microscope Axio Observer.Z1 was used. The slides were microscope in the dark while the fluorescence intensity and the exposure time were adapted to the isotype control. Therefore, exposure time and THY Lamp intensity were selected to minimize the isotype control's fluorescence staining (Alexa 488 or Alexa 555). For the quantification, the percentage of the fluorescence-positive area of the antibody-treated sample

and the isotype control were analysed, respectively. For every sample, three representative images were taken. For the analysis, the percentage of fluorescence per area of the isotype control was subtracted from the fluorescence per area of the antibody-treated sample. To determine the number of the average percent of fluorescence positive area per sample, the mean of all three images was taken. The selected magnification was indicated in the respective figure legends.

### **2.2.5 Statistical analysis**

All statistical analyses were performed using GraphPad Prism (version 9.01; GraphPad Software, San Diego, CA, USA). Results were presented as scatter plots, bar graphs, or dot plots. The chosen method of presentation can be found in the respective figure legends, and the presentation of the mean  $\pm$  SEM, mean  $\pm$  SD, or median  $\pm$  SEM. The statistical analysis used was also indicated in the corresponding figure legend.

#### **2.2.5.1 Bioinformatic analysis**

The bioinformatics analysis was performed as described in Camarinha-Silva et al. [178]. The raw data from the Illumina-NGS performed by the Helmholtz Institute for Infection research were merged with the Ribosomal Database Project (RDP) assembler [179]. For the virtualization of the network, Cytoscape was used (version 3.7.2) [180]. The analysis showed three independent groups of phylotypes showing co-occurrences differentiating from ultrapure water system contaminants[181] and contaminants in the DNA extraction kit and various other probable contaminants[182].

Co-occurrences were documented as contaminants and were deleted from the total abundance matrix. Also, phylotypes from the same taxa but not included in the correlation matrix due to their low abundance were deleted. Sequence data can be found under the following reference number: PRJNA656723.

## 3 Results

### 3.1. Demographic data of the patient cohort

To investigate whether the pathogen profile of PJIs might be influenced by different factors e.g., age, site, of infection or sex, 178 patients were analyzed that were hospitalized for revision surgery at the hip (THA), knee (TKA), and shoulder (TSA) joint. The reasons for revision were either due to a septic condition (93) or implant loosening under aseptic conditions (85) (table 13). According to the MSIS criteria, 57 males and 38 females with an average age of  $73 \pm 9$  were included in the septic cohort. According to the aseptic cohort, 42 males and 39 females with an average age of  $70 \pm 12$  were included in the MSIS criteria. Therefore, the average age of the patients in the septic and aseptic cohort was similar. An influence of the patients' age on the other parameters can therefore be excluded. More male patients than female patients were present in the septic cohort. However, the number of women was almost identical in both cohorts. Because both septic and aseptic loosening occurred in males and females, both genders were studied for the subsequent subprojects of this work.

The septic cohort includes the revisions of the following implants, 42% (40/95) THA, 39% (37/95) TKA, and 19% (18/95) TSA, while the following implant revisions were included in the aseptic cohort 36% (29/81) THA, 41% (33/81) TKA and 23% (19/81) TSA (table 14). In this cohort, we included more infected THA (40/95) than the TKA (37/95) or the TSA (18/95). While in the aseptic group, more aseptic failure of TKA (33/81) than of THA (29/81) or TSA (19/81) were included. In this cohort, more septic hip than aseptic hip revisions were done.

The implantation time differed according to the prosthesis type. However, in the septic THA cohort, the implantation time was 2.4 times less ( $45 \pm 72$  months) than in the aseptic cohort ( $108 \pm 109$  months). In the septic TKA cohort, implantation time ( $37 \pm 35$  months) was twice as short as in the aseptic cohort ( $76 \pm 65$  months). A reduced implantation time of  $24 \pm 29$  months could also be calculated in the septic TSA cohort; this was almost halved compared to the aseptic cohort ( $44 \pm 59$  months).

A risk factor for acquiring a PJI are various comorbidities. Potential influencing comorbidities were analyzed in the two cohorts and are summarized in table 14. Patients in the septic cohort exhibited more frequent comorbidities such as diabetes (25/95), renal (16/95) and heart insufficiency (12/95), COPD (9/95), osteoporosis (4/95), and asthma (3/95) compared to the aseptic cohort. In the aseptic, cohort the number of diabetes (21/81) was equal to the septic cohort. In contrast, the number of renal (4/81) and heart (1/81) insufficiency was lower in the aseptic cohort. COPD (1/81), osteoporosis (2/81), and asthma (2/81) were also analyzed less often in the aseptic cohort in comparison to the septic cohort. Not all patients indicated their comorbidities during hospital

admission, and some patients did not exhibit any comorbidities. Overall, in the septic cohort, a higher incidence rate of renal and heart insufficiency was observed. In turn, the other comorbidities showed a similar trend in comparison to each cohort.

Table 13 Demographic data

Cohort	Number	Age [yr]	Sex	Location	Implantation time [m]
Septic	95	73 ± 9	♂ 57	THA: 42%	45 ± 72
			♀ 38	TKA: 39%	37 ± 35
				TSA: 19%	24 ± 29
Aseptic	81	70 ± 12	♂ 42	THA: 36%	108 ± 109
			♀ 39	TKA: 41%	76 ± 65
				TSA: 23%	44 ± 59

Table 14 Comorbidities

	Septic (95)	Aseptic (81)
Diabetes	25	21
Osteoporosis	4	2
renal insufficiency	16	4
COPD	9	1
Heart insufficiency	12	1
Asthma	3	2
Other	17	16

To investigate at which age septic and aseptic PJI occurs, the patient age was plotted for each patient in black (septic) and grey (aseptic) and both cohorts (red) (fig. 7A). I observed a Gaussian distribution of age within both cohorts. The peak of patients coming for aseptic or septic revision surgery was observed at around 75 years.

In this thesis, also more male (57/95) than female (38/95) patients underwent septic revision surgeries (fig. 7B). In the aseptic cohort, 42 men and 39 women received aseptic revisions; here, the distribution between the genders was approximately similar.

I found more late PJIs (48/83) where the infection occurred 12 months after implantation in my PJI cohort (fig. 7C). In comparison, I observed less frequent infections occurring between 3 to 12 months after implantation (delayed) (20/83) and even less PJI belonging to the early infection group (3 months after implantation) (15/83). However, the implantation time was not available for all patients (12/83). Therefore, it is difficult to say whether there were more late infections in the septic cohort. Interestingly, the occurrence of late PJIs (12 months after joint implantation) was

more frequent than early PJIs (up to 3 months after implantation). Since anaerobia and slow-growing bacteria mainly cause these infections, these are expected to occur more frequently in the pathological spectrum.

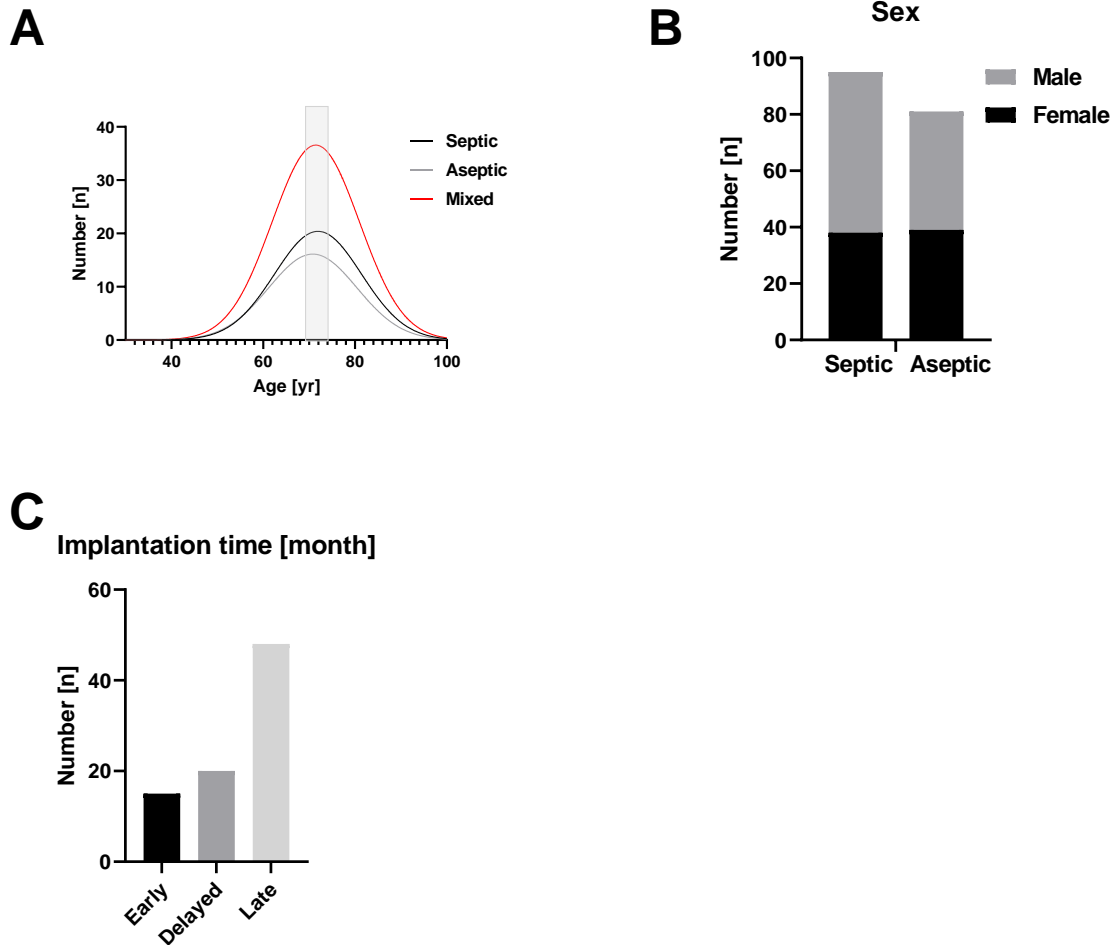


**Figure 7 Demographic data of the patients in the septic and aseptic revision cohort**

(A) Gaussian distribution of the age based on the septic (black), aseptic (gray), and mixed (red) revision cohorts was presented. The gray box indicates the range (70 – 75) at which age the most frequent revision surgeries were performed. (B) The bar chart shows the septic (left) and aseptic (right) cohort divided into female (black) and male (light grey). More males (57/95) had a septic TJA revision than females (38/95) in the septic cohort. (C) The bar charts showed the implantation time divided into three categories. Early describes infections that occur >3 months after the last implantation of the revised prosthesis, delayed describes infections that occur between 3 to 12 months after implantation, and late describes the infections that occur <12 months after implantation. Here, more patients with late PJIs were observed.

### 3.1.1 Pathogen Spectrum of PJI

To observe the pathogen spectrum of the cohorts, the spectrum was analyzed using a pie chart for the septic cohort and the various implant types (fig. 8). For the analysis of the pathogen spectrum, the bacteria analyzed by the institute of microbiology using tissue cultures were used. *Staphylococcus* spp caused most PJIs in this cohort (58%) and polymicrobial infections (16%).

Anaerobia (11%) was found a bit more frequently than *Streptococcus* spp. (8%), and were more prevalent in total than *Enterococcus* spp. (5%). Subdivision of the pathogen spectrum according to the infected joint showed in THA (fig. 8B), TKA (fig. 8C), and TSA (fig. 8D) *Staphylococcus* spp. (THA: 58%; TKA: 68%; TSA: 39%) being the most prominent pathogen. The pathogen profile of the shoulder showed the least variance. However, the number of patients in the shoulder cohort was lower than the hip and knee cohorts, making an accurate assessment difficult. Nonetheless, more anaerobia were identified in the shoulder cohort (22%) than in the THA (10%) and TKA (5%) group. Polymicrobial infections occurred in all revision groups but were more common in the shoulder and hip than in the knee. In the hip and knee, the pathogen diversity was very similar. *Staphylococcus* spp. and polymicrobial infections are the most common pathogens found in the septic cohort and individual implant groups.

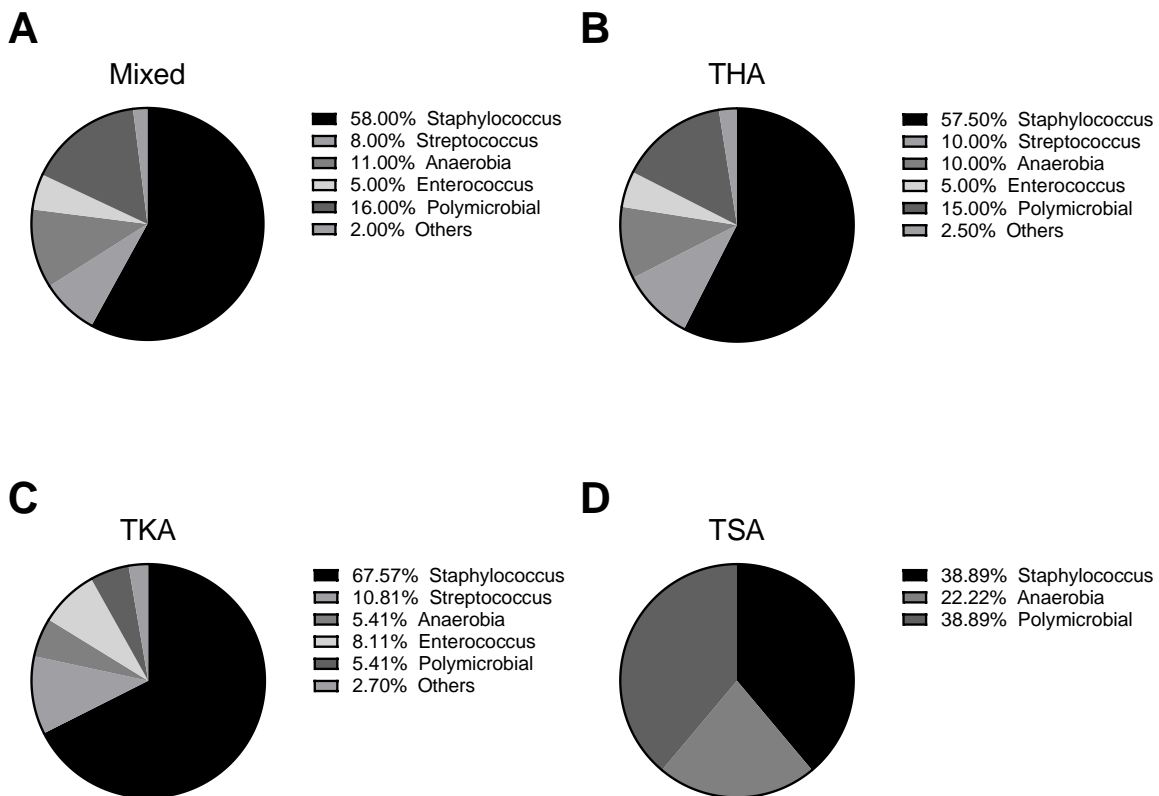


**Figure 8 Pathogen spectrum of the patients from the septic cohort**

(A) Pie chart of the identified pathogen spectrum, including all joints calculated in percent. *Staphylococcus* spp. (black) was the major pathogen analysed by the diagnostic. Other bacteria were less frequently detected. (B) Pie chart of the identified pathogen spectrum analysed in the septic-THA group calculated in percent. Again more *Staphylococcus* spp. (black) were found followed by polymicrobial (dark grey) infections. (C) Pie chart of the identified pathogen spectrum analysed in the septic-TKA group calculated in percent. *Staphylococcus* spp. (black) was found most frequently, closely followed by *Streptococcus* spp. and *Enterococcus* spp. (D) Pie chart of the identified pathogen spectrum analysed in the septic-TSA group calculated in percent. The pathogen spectrum was not as variable as in the TKA and THA group; *Staphylococcus* spp. (black), anaerobia (grey) and polymicrobial infections (dark grey) were found in this group.

### 3.1.2 Serum inflammatory markers in PJI

As the WBC and the CRP values are used as a blood serum marker to identify PJIs (fig. 2), these markers were compared between the septic and aseptic cohort and were presented as scatter dot plot (fig. 9).

The statistical analysis using the Mann-Whitney-U-Test showed no significant ( $p = 0.3470$ ) difference between the septic (mean with SEM:  $10 \pm 1$ ) and the aseptic (mean with SEM:  $8 \pm 0.4$ ) group for the WBC count. (fig. 9A). The threshold of WBC is 10 Gpt/l (black dashed line); because elevated WBC may indicate infection, it was expected that more patients would have elevated WBC. However, in 91 patients, only 30% (27/91) had an elevated WBC above 10 Gpt/l. The remaining 70% (64/91) had a WBC below 10 Gpt/l. The data for four patients were missing. In the aseptic cohort, again, 17% (13/78) patients had an elevated WBC level. In contrast, 83% (65/78) of patients had a WBC level below 10 Gpt/l, which aligns with the expectations. For three patients, no information was provided.

As the CRP value is a systemic inflammation parameter [39], the serum CRP value of the septic (mean with SEM:  $65.65 \pm 8.68$  mg/l) cohort was compared to the aseptic (mean with SEM:  $15.68 \pm 2.99$  mg/l) cohort (fig. 9B), and statistically analyzed using the Mann-Whitney-U-test. The difference in the mean value was significantly ( $p < 0.0001$ ) increased in the septic cohort. Overall, I observed that 7% (6/91) of patients in the septic cohort had a serum CRP level below the pathologic threshold of 5 mg/l (black dashed line). The expectation was that more patients in the aseptic cohort would have a CRP below 5 mg/ml. However, the mean value in the group already showed a value of  $15.68 \pm 2.99$  mg/l, and overall even 58% (44/76) of the aseptic cohort exhibited an elevated CRP value.

Therefore, the CRP value alone is not indicative of the presence of an infection. Accordingly, I investigated how accurate the standard microbiological diagnostic identifies a pathogen from PJI tissue cultures and whether other techniques may improve the diagnostic security.

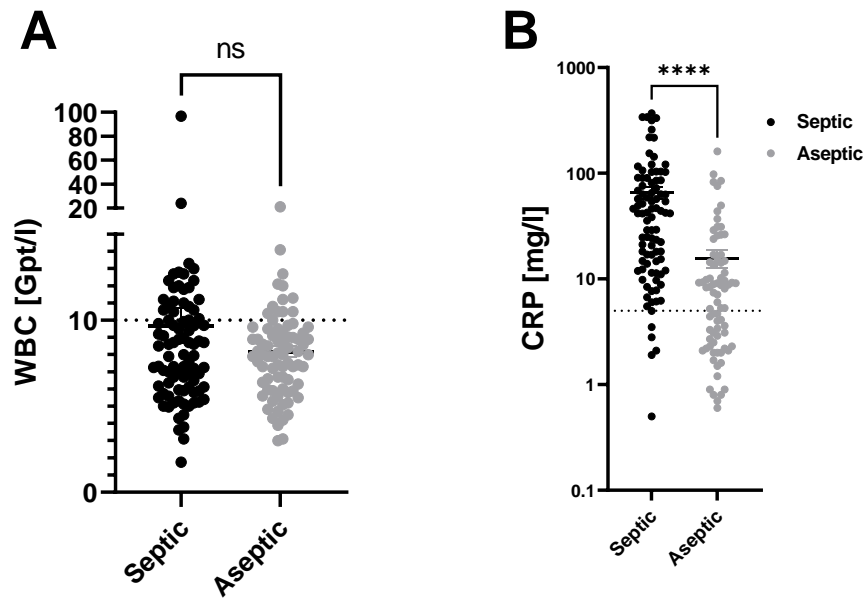


**Figure 9 WBC- und CRP-values of the patients in the septic and aseptic revision cohort**

(A) The WBC (Gpt/l) of the septic (black) and aseptic (light grey) cohort can be seen present as a scatter dot plot. The pathologic threshold is 10 Gpt/l and was indicated as a black dashed line. There was no significant ( $p = 0.3470$ ) difference between the septic (mean with SEM:  $10 \pm 1$  Gpt/l) and the aseptic (mean with SEM:  $8 \pm 0.4$  Gpt/l) cohort. (B) CRP values (mg/l) in the septic (black) (mean with SEM:  $65.65 \pm 8.68$  mg/l) and aseptic (light grey) (mean with SEM:  $15.68 \pm 2.99$  mg/l) cohort can be seen as a scatter dot plot, for a better representation the logarithmic illustration was chosen. The CRP value was significantly ( $p < 0.0001$ ) different between both cohorts. The pathologic threshold is 5 mg/l and was indicated as a black dashed line in the graph.

### 3.2 Comparison of different analytical techniques to improve the diagnostic security for PJI

Bacteria from biofilm mediated infection or low-grade PJIs are often challenging to isolate and culture. The diagnostic problems of the typically applied screening methods, such as tissue culture, are either not sensitive enough or lack the specific culturing conditions (e.g., anaerobic conditions) [183, 184] [71]. Dithiothreitol (DTT) destabilized the extracellular matrix of biofilms on orthopedic implants by reducing the disulfide bonds between polysaccharides and proteins [122]. Therefore, a DTT solution was given in a pouch in a specific device to identify PJI called microDTTect device (NCS Lab Srl, Carpi, Italy). The idea was that upon implant retrieval, the implant was sealed under sterile conditions in the device, the pouch containing DTT was broken, and the DTT solution flowed around the implant to dissolve the adhering biofilm. Two syringes were used to remove the DTT solution from the bag of the device. One syringe was sent to diagnostic microbiology for the cultivation of potential bacteria. Since NGS is also becoming more relevant in diagnosing PJI [103, 104], the other syringe of the DTT solution was used for DNA isolation and subsequent NGS analyses. The tissue cultivation performed by the Institute of [48]

diagnostic microbiology served as a reference. Based on the MSIS criteria [27], a patient was declared septic if at least two positive tissue cultures of the same organism were found (fig. 2).

For the investigation, if DTT solution used for culturing or for NGS can be used as an equivalent tool compared to tissue culturing, I analyzed 66 patients undergoing hip or knee revision surgery (see 3.1). The routine microbiological diagnostic indicated a PJI in 28 patients; 38 patients underwent aseptic revision surgery (table 13). The assignment of patients to the septic cohort or aseptic cohort was based on the clinical decision and microbiology standard diagnostic, serum inflammatory markers, and the macroscopic inspection of the joint and intraoperative appearance during revision surgery. Equal numbers of men and women were included (table 13). The average age of the included patients was 70 years in both cohorts and therefore comparable.

For the analysis, the infection identified in DTT solution cultures was compared with the tissue culture of the std. routine microbiology. Likewise, the NGS data were also compared with the results from the tissue cultivation. To investigate the concordance between the different applied methods for PJI diagnosis and pathogen identification, the results of microbiological diagnostic were matched with the results from the microDTTect solution culture. The results of the different cohorts (septic and aseptic) are summarized in table 15.

Based on the clinical assessment, 28 patients were included in the septic cohort. For the analysis, the results from DTT solution cultures were compared with the std. routine microbiology using tissue culture. In 75% (21/28), a pathogen was detected using the DTT culture solution and the std. diagnostic. In 25% (7/28), the DTT culture solution showed no pathogen, whereas the std. diagnostic found a pathogen. In the aseptic cohort in 92% (35/38), no pathogen was detected using both methods. However, in three cases which were diagnosed as aseptic in the std. diagnostic a bacterium was detected using the DTT culturing method. Suggesting possible false-negative results, but for a precise diagnosis, further research needs to be done.

Table 15 Concordance of standard microbiology diagnostic vs. DTT culturing based identification of infection

	<b>Std. diagnostic vs. DTT culture</b>
<b>Septic</b>	N = 28
<b>Positive (+) in both methods</b>	75% (21/28)
<b>Negative (-) only in DTT</b>	25% (7/28)
<b>Aseptic</b>	N = 38
<b>- in both methods</b>	92% (35/38)
<b>+ only in DTT</b>	8% (3/38)

To use culture-independent pathogen identification, I isolated the DNA from the DTT solution. In preparation for NGS, the V1V2 region of the 16S rDNA gene was amplified by PCR. To check both the quantity and quality of the PCR products, gel electrophoresis was used. If no PCR product could be detected, the samples were not further processed for sequencing and were listed as negative. This means that no bacterial DNA was detected. If a PCR product with 350 bp was detectable [176], it was further processed for Illumina-NGS.

For comparison, the results from microbiological diagnostic were compared with NGS being positive for pathogen DNA in a first step (table 16). In a second step, the specificity for the pathogen detected with both methods was compared.

In 71 % (20/28) of the septic samples, a pathogen was detected using the std. microbiological diagnostic as well as the NGS from DTT solution. In eight cases, no PCR product was detected with NGS.

79% (30/38) no PCR product was detected using NGS from DTT solution and std. microbiological diagnostic in the aseptic cohort. However, in 21% (8/38) of the tested samples, NGS detected bacterial DNA but not the microbiological std. diagnostic. These eight samples could indicate possible CN-PJIs, but further research is needed.

Table 16: Concordance of standard microbiology diagnostic vs. NGS from DTT solution

	Std. diagnostic vs. NGS from DTT
<b>Septic</b>	N = 28
<b>Positive (+) in both methods</b>	71% (20/28)
<b>Negative (-) only in DTT</b>	29% (8/28)
<b>Aseptic</b>	N = 38
<b>- in both methods</b>	79% (30/38)
<b>+ only in DTT</b>	21% (8/38)

The following paragraph discusses the samples in more detail, which gave divergent results using different detection methods.

The std. microbiological diagnostic identified a pathogen in ten cases, not detected using the DTT solution for culturing and NGS (Fig. 10A). In three cases (#18, #71, #78), the DTT culturing indicated a bacterial infection, whereas no pathogenic DNA was detected using NGS from DTT solutions. These patients' increased serum CRP values also indicate an ongoing inflammatory process that might indicate an infection. However, in these cases, NGS from DTT solutions did not identify pathogenic DNA. In one sample (#70), the std. microbiological diagnostic identified a

pathogen that was not detectable using DTT culturing, whereas the NGS from DTT solutions found pathological DNA. This patient exhibited a high CRP value indicating an active inflammation process, suggesting that DTT culturing failed in this case. However, two samples (#5 and #44) were diagnosed as septic exclusively by std. microbiological diagnostic, while the CRP value was under the average threshold (5 mg/l). This observation could indicate that these samples were contaminated during the culturing process in the std. microbiological diagnostic.

Fig. 10B shows three samples that were classified as aseptic using the std. microbiological diagnostic with tissue cultures while a pathogen was identified using the DTT culturing technique. Taking into account the slightly increased CRP values (#48 and #53) suggested a possible ongoing inflammatory process in these patients; this might indicate a low-grade infection. In one case (#94), DTT culturing and NGS from DTT solutions detected a pathogen, while the std. diagnostic microbiology failed for the detection of a pathogen. Also, in this case, the implantation time of 6 months was short; this sample might be a false-negative case that was not identified by the std. microbiological diagnostic.

Fig. 10C shows seven samples, where only NGS from DTT solution detected bacterial DNA, while the std. microbiological diagnostic using tissue cultures and the DTT culturing did not identify a pathogen. Most cases showed a serum CRP level below the pathological threshold. Due to the low CRP and longer implantation time, a possible false-positive result in NGS was considered.

A						C					
ID	Microbiology tissue	Microbiology DTT	DTT NGS	CRP	Implantation time [month]	ID	Microbiology tissue	Microbiology DTT	DTT NGS	CRP	Implantation time [month]
5	+	-	-	2.8	55	2	-	-	+	1.7	19
18	+	+	-	15.4	104	9	-	-	+	2.5	23
27	+	-	-	85.1	0	13	-	-	+	10	140
44	+	-	-	0.5	382	19	-	-	+	0.6	36
56	+	-	-	42.5	1	23	-	-	+	2.7	189
66	+	-	-	18.2	1	42	-	-	+	2.2	253
70	+	-	+	41.7	3	50	-	-	+	3.1	66
71	+	+	-	90.4	10						
78	+	+	-	7.65	16						
89	+	-	-	7.8	1						

B					
ID	Microbiology tissue	Microbiology DTT	DTT NGS	CRP	Implantation time [month]
48	-	+	-	10.1	178
94	-	+	+	-	6
53	-	+	-	23.9	23

**Figure 10** The correlation between the three used methods were in some results distinct.

The row marked in green were diagnosed as aseptic (-) using tissue culturing by the std. microbiology diagnostic, DTT culturing, or NGS from DTT solution. The row marked in red were diagnosed as septic (+) using tissue culturing by the std. microbiology diagnostic, DTT culturing, or NGS from DTT solution. Additionally, the respective serum CRP values in mg/l and the implantation time in months were indicated for each patient. When the CRP value was above the threshold of 5 mg/l, the row was marked in red. (A) Samples were diagnosed as septic using the std. microbiological tissue culturing. (B) Shows the samples diagnosed as septic by using DTT for culturing, and (C) shows samples that were diagnosed as septic using NGS from DTT solutions.

As DTT has a destabilizing effect on the extracellular matrix of the biofilm, I wanted to analyze whether the use of DTT makes the identification of the bacterial strain and especially polymicrobial infections more reliable (fig. 11). I was comparing the std. microbiological diagnostics with DTT bacteria culturing, the same bacteria were identified in 67% (20/30) of the analyzed samples (fig. 11A). In 33% (10/30) of all cases, different bacteria were identified using both techniques.

The identified pathogens for all septic cases are summarized in fig. 11A+B. As expected, *Staphylococcus* spp. was the most prominent pathogen in the septic samples. The detection for *Staphylococcus* spp. was reliable in 14 cases from tissue and DTT culturing samples. However, in 8 cases, *Staphylococcus* could be identified exclusively from tissue cultures (6X) or DTT culturing samples (2X). NGS from the DTT solution indicated the presence of a monomicrobial infection in 15 out of 28 cases. Thirteen cases were polymicrobial. Interestingly, in seven of these samples, both culturing methods identified *Staphylococcus* spp. as a pathogen; NGS confirmed a *Staphylococcus* spp. mono-infection, and in three different cases, it confirmed *Staphylococcus* spp. as a major component of a supposedly polymicrobial infection.

Pathogens other than *Staphylococcus* spp. were detected rarely by culturing, making it difficult to evaluate the reliability of the different techniques. *Enterococcus* spp. was detected twice using the std. microbiological routine and supported by DTT culturing and NGS of DTT samples, whereas conflicting results were observed for the other case.

The detection of anaerobia was highly variable between the applied methods. As a major constituent of the skin microbiota, *C. acnes* was identified using the applied techniques in a few samples. NGS indicated *Cutibacterium* spp. as dominating pathogen in only one case, whereas DTT culturing indicated *C. acnes* in one sample confirmed by the tissue culturing.

Mainly polymicrobial infections were identified by NGS, which can be attributed to the high sensitivity of NGS [185].

For a better and easier comparison of the pathological spectrum, I plotted the identified pathogen profile for each method as a pie chart (fig. 11B). The literature describes that *Staphylococcus* spp. is one of the main pathogens causing a PJI [23]. My results confirm this observation.



**Figure 11 Pathogens identified from microDTTect samples are typically also identified by routine diagnostic.**

(A) The columns represent the ID for each sample, the pathogen found using the std. microbiological diagnostic with tissue culturing, DTT culturing, and NGS from DTT solution. The left column indicates the respective cohort of the patient: septic (marked in red) and aseptic (marked in green). The following three columns on the right hand indicate the identified pathogen via culturing technique or NGS. The identified pathogens were also labelled in different colours (*Staphylococcus* spp.: red, *Streptococcus* spp.: green, *Enterococcus* spp.: yellow, *Anaerobia*: blue, Polymicrobial Infection: light green). (B) The Pie chart of the identified pathogen spectrum represents every technique used. Above: Tissue culturing; Middle: DTT culturing; Below: NGS from DTT solution. *Staphylococcus* spp. (red) was the major pathogen identified using the three various techniques, all other pathogens were less frequently detected.

These data highlighted the importance of the std. microbiological diagnostics from tissue biopsies, but also the downfalls of this technique. Using DTT bacteria culturing and NGS-based DNA identification from DTT solution, a few samples showed different results and might indicate in 8% (3/38) of the aseptic cohort a CN-PJI. Therefore, establishing a new and more reliable methodology to secure the detection of PJIs is essential. Using a specific indicator for a more secure PJI diagnosis could help to improve the treatment of PJI patients. Therefore, a biomarker for PJI identification would be helpful for questionable cases.

### 3.3 Tissue biomarkers for PJI diagnosis

One of the most promising synovial fluid biomarkers for PJI is based on the detection of  $\alpha$ -defensin. As the ELISA-based detection of  $\alpha$ -defensin is costly and the cross-reactivity makes it less reliable [108] [31]., the need for alternative biomarkers to support the detection of PJI is important. CD68 tissue staining indicates the presence of monocytes and macrophages. The presence of the latter can be the first indication of septic complications [186, 187]. During an infection also neutrophils invade the tissue; therefore, the presence of neutrophils in the histological section is associated with an ongoing infection in histopathology. A typical marker for neutrophils is CD66b [188, 189]. The complement pathway is activated very early upon bacterial infection, and the terminal complement pathway leads to the elimination of bacteria using C3, C5, and C9. Therefore, in the following, I investigated whether CD68, CD66b, and parts of the terminal complement pathway (C3, C5, and C9) are suitable biomarkers for detecting a PJI by screening periprosthetic tissue using immunohistological staining.

For this investigation, I analyzed 33 patients undergoing shoulder revisions surgery (see 3.1). The routine microbiological diagnostic indicated a PJI in 16 patients; 17 patients underwent aseptic revision surgery (table 14).

Both cohorts (septic and aseptic) were assessed for the presence of  $\alpha$ -defensin using immunohistological stainings (fig. 12). For the detection of  $\alpha$ -defensin, the periprosthetic tissue was stained with anti- $\alpha$ -defensin (red), and the cell nuclei were stained with Dapi (fig. 12A). For an overview, the tissue was first microscope at 100x magnification (above), and for a more detailed view, the images were taken at 630x magnification (below); the representative pictures show that the  $\alpha$ -defensin (red staining) could be detected in both septic (right) and aseptic (left) tissue. For quantifying the staining (septic: N = 9; aseptic: N = 9) the amount of red fluorescence within the tissue area was calculated and shown as a scatter dot plot (fig. 12B). Using the Mann-Whitney-U-Test the septic (black) cohort (mean  $\pm$  SEM: 1.1 %  $\pm$  0.42 %) showed no significant difference ( $p = 0.2224$ ) compared to the aseptic (light grey) cohort (mean  $\pm$  SEM: 0.29 %  $\pm$  0.16 %). To analyse the predictive value of  $\alpha$ -defensin as a biomarker for PJI, I plotted the percentage of red fluorescence in the septic tissue (sensitivity) against the percent of red fluorescence in the aseptic tissue (100 %-specificity) (fig. 12C). Using the respective fluorescent area values for each sample, the receiver operating characteristic (ROC) curve showed an area under the curve of 0.68, which describes the suitability of the biomarker. The threshold for the sensitivity and specificity (red dashed line) was calculated by using Youden's criteria; the sensitivity was at 55.56 % (95% of CI: 26.67 % to 81.12 %) while the specificity was at 88.89% (95% of CI: 56.50 to 99.43 %).  $\alpha$ -defensin

was not detected in all septic tissues by immunohistochemical staining and partially detected in aseptic tissues, indicating a low predictive value of  $\alpha$ -defensin staining as a biomarker for PJI.

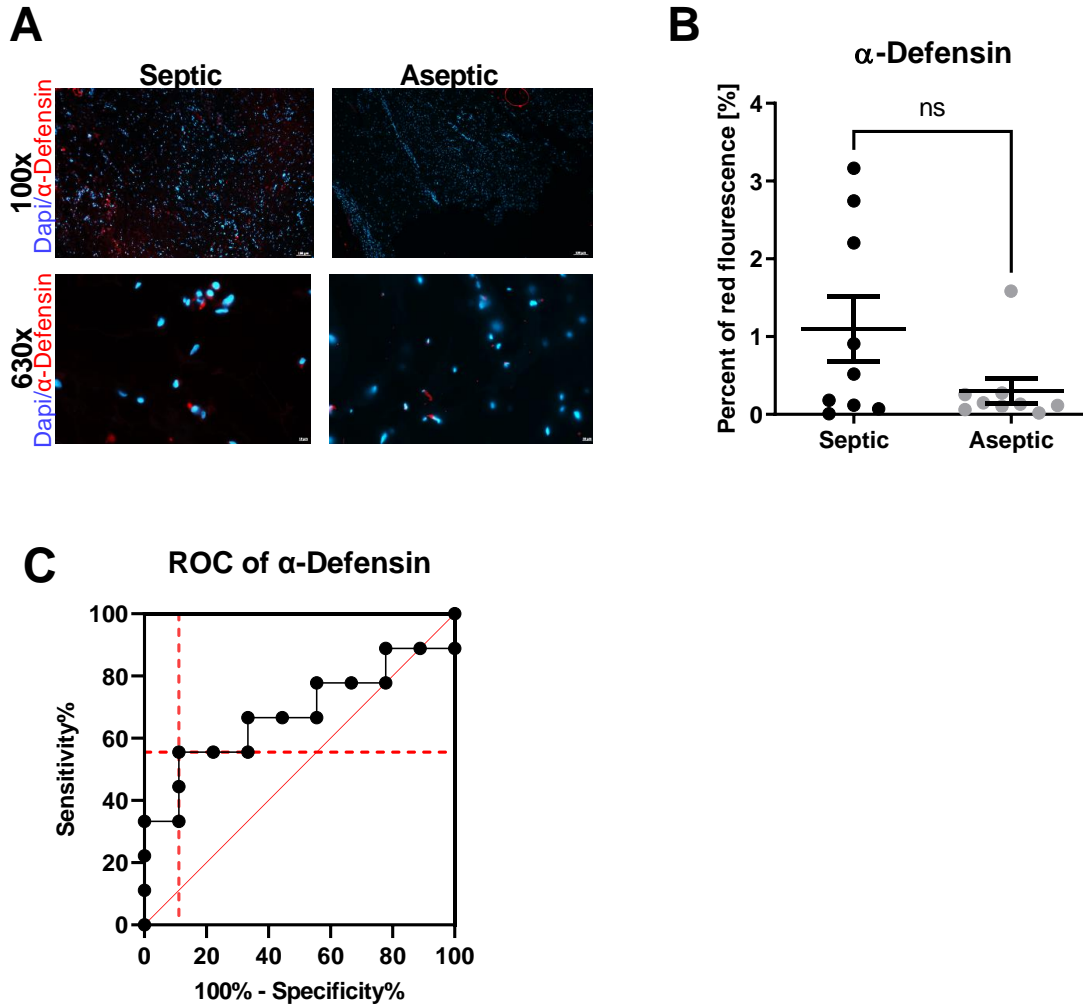


**Figure 12 Immunohistological staining of  $\alpha$ -defensin in periprosthetic tissue shows no significant difference between the septic and the aseptic cohort**

(A) For the detection of  $\alpha$ -defensin in shoulder samples from septic (right) and aseptic (left) samples, periprosthetic tissue was immunohistochemically stained with anti- $\alpha$ -defensin (red), and the cell nuclei were stained with Dapi (blue). Representative immunohistochemical staining of  $\alpha$ -defensin with a magnification of 100x (above; scale bar: 100  $\mu$ m) and 630x (below; scale bar: 2  $\mu$ m) were given. (B) The quantification (septic: N = 9; aseptic N = 9) of the red fluorescence of the tissue area was presented as a scatter dot plot and was given as mean  $\pm$  SEM. The septic cohort was presented in black (1.1 %  $\pm$  0.42 %), and the aseptic cohort was presented in light grey (0.29 %  $\pm$  0.16 %). The statistical analysis using the Mann-Whitney-U-Test showed no significant difference between the groups ( $p = 0.2224$ ). (C) To analyse the predictive value of  $\alpha$ -defensin as a biomarker for PJI using immunohistological staining in periprosthetic tissue, the percent of red fluorescence in the septic tissue (sensitivity) was plotted against the percent of red fluorescence in the aseptic tissue (100%-specificity). Using each sample's respective fluorescent area values, the receiver operating characteristic (ROC) curve calculated an area under the curve (AUC) of 0.68. Using the Youden's criteria, the best ratio of sensitivity to specificity was selected (red dashed line). The sensitivity was 55.56% (95% of CI: 26.67 % to 81.12 %) while the specificity was at 88.89% (95% of CI: 56.50 to 99.43 %).

As macrophages are a good indicator for inflammatory reactions and septic complications, tissue staining for CD68 was used as an indicator for the presence of monocytes and macrophages. Therefore, both cohorts (septic and aseptic) were assessed for the presence of CD68 using immunohistological staining. For the detection of CD68, the periprosthetic tissue was stained with anti-CD68 (red) while the cell nuclei were stained with Dapi (blue) (Fig. 13A).

Again, for an overview, the tissue was first microscope at 100x magnification (above), and for a more detailed view, the images were taken at 630x magnification (below). It can be seen that the red staining was detected in both septic (right) and aseptic (left) tissue; here, the staining was seen around the cell nuclei. For quantifying the staining (septic: N = 9; aseptic: N = 9), the red fluorescence of the tissue area was presented as a scatter dot plot (fig. 13B). The septic cohort was presented in black (mean  $\pm$  SEM: 0.11 %  $\pm$  0.02 %), and the aseptic cohort was given in light grey (mean  $\pm$  SEM: 0.06 %  $\pm$  0.03 %). Using the statistical examination of the Mann-Whitney-U-Test, the septic cohort showed no significant difference ( $p = 0.1135$ ) to the aseptic cohort. Again, for the analysis of the predictive value of CD68 as a biomarker for PJI, the percent of red fluorescence identified in the septic cohort (sensitivity) was plotted against the percent of red fluorescence in the aseptic cohort (100%-specificity) (fig. 13C). Using the respective fluorescent area values, the ROC curve shows an AUC of 0.73. The threshold for the sensitivity and specificity (red dashed line) was analysed using the Youden's criteria; the sensitivity was at 100 % (95% of CI: 70.09% to 100.0%) while the specificity was at 66 % (95% of CI: 35.42% to 87.94%). CD68 was detected in all septic tissues by immunohistochemically staining and partially detected in aseptic tissue. This indicated a low predictive value of CD68 staining as a biomarker for PJI.

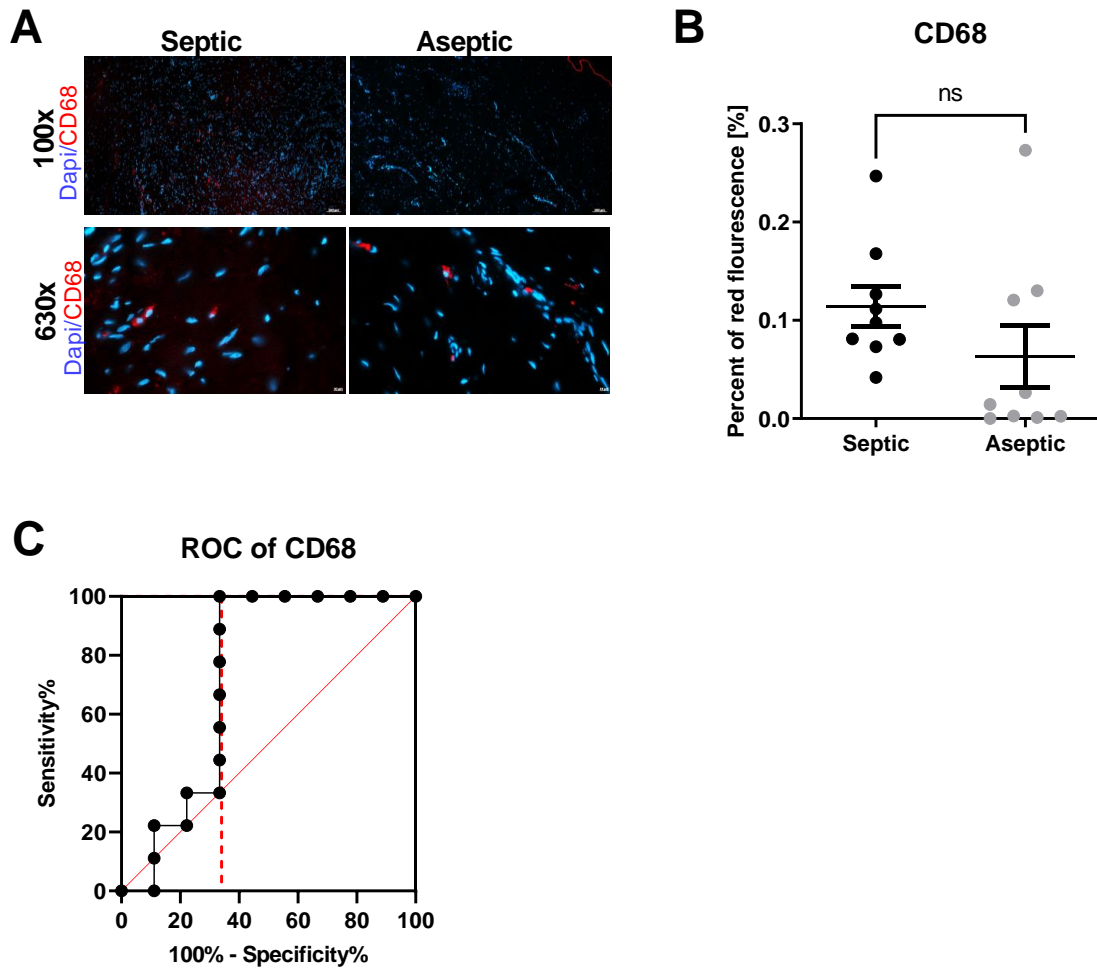


**Figure 13 Immunohistological staining of CD68 in periprosthetic tissue shows no significant difference between the septic and the aseptic cohort**

(A) For the detection of CD68 in shoulder samples from septic (right) and aseptic (left) samples, periprosthetic tissue was immunohistologically stained with anti-CD68 (red), and the cell nuclei were stained with Dapi (blue). Representative immunohistochemical staining of CD68 with a magnification of 100x (above, scale bar: 100  $\mu$ m) and 630x (below; scale bar: 2  $\mu$ m) were given. (B) The quantification (septic: N = 9; aseptic: N = 9) of the red fluorescence of the tissue area were presented as a scatter dot plot and was given as mean  $\pm$  SEM. The septic cohort was presented in black (0.11 %  $\pm$  0.02 %), and the aseptic cohort was presented in light grey (0.06 %  $\pm$  0.03 %). The statistical analysis using the Mann-Whitney-U-Test showed no significant difference between the groups ( $p = 0.1135$ ). (C) To analyze the predictive value of CD68 as a biomarker for PJI using immunohistological staining in periprosthetic tissue, the percent of red fluorescence in the septic tissue (sensitivity) was plotted against the percent of red fluorescence in the aseptic tissue (100%-specificity). Using the respective fluorescent area values for each sample, the ROC curve calculated an AUC of 0.73. Using the Youden's criteria, the best ratio of sensitivity to specificity was selected (red dashed line). The sensitivity was 100% (95% of CI: 70.09% to 100.0%) while the specificity was at 66% (95% of CI: 35.42% to 87.94%).

The presence of neutrophils in tissue indicates an ongoing infection in histopathologic examination and is also given as one marker for infection in the MSIS criteria. To investigate CD66b in periprosthetic tissue, I analyzed 79 patients undergoing hip and knee revision surgery (see 3.1). The routine microbiological diagnostic indicated a PJI in 23; 47 patients who underwent aseptic revision surgery (table 13).

In both cohorts (septic and aseptic), I assessed for the presence of CD66b, using immunohistological staining. For the detection of CD66b the periprosthetic tissue was stained with anti-CD66b (red) while the cell nuclei were stained with Dapi (blue) (fig. 14A). For an overview, the tissue was first microscope at 100x magnification (above). There can be seen that more septic (left) sections showed increased red staining in comparison to aseptic tissue (right). The more detailed magnification at 400x (below) showed this difference even more clearly; more red fluorescence can be observed in the septic tissue than in aseptic tissue. For quantifying the staining (septic: N = 32; aseptic: N = 47), the red fluorescence of the tissue was presented as a scatter dot plot (fig. 14B) for better visibility of the samples were plotted logarithmically. Using the statistical analysis of the Mann-Whitney-U-Test the septic (black) cohort (mean  $\pm$  SEM: 7.5 %  $\pm$  2 %) showed a significant difference ( $p = 0.024$ ) in comparison to the aseptic (light grey) cohort (mean  $\pm$  SEM: 3.4 %  $\pm$  1.1 %). For the analysis of the predictive value of CD66b as a biomarker for PJI, the percent of red fluorescence from the septic cohort (sensitivity) was plotted against the percent of red fluorescence in the aseptic tissue (100 %-specificity) (fig. 14C). Using the respective fluorescent area values for each sample, the ROC curve showed an area under the curve of 0.65. Youden's criteria calculated the best ratio for the sensitivity 63 % (95% of CI: 45.25 % to 77.07 %) and the specificity 72 % (95 % of CI: 58.24 % to 83.06 %) (Red dashed line). CD66b was detected in all septic as well as aseptic tissues by immunohistochemically staining. I was indicating a low predictive value of CD66b staining as a biomarker for PJI.

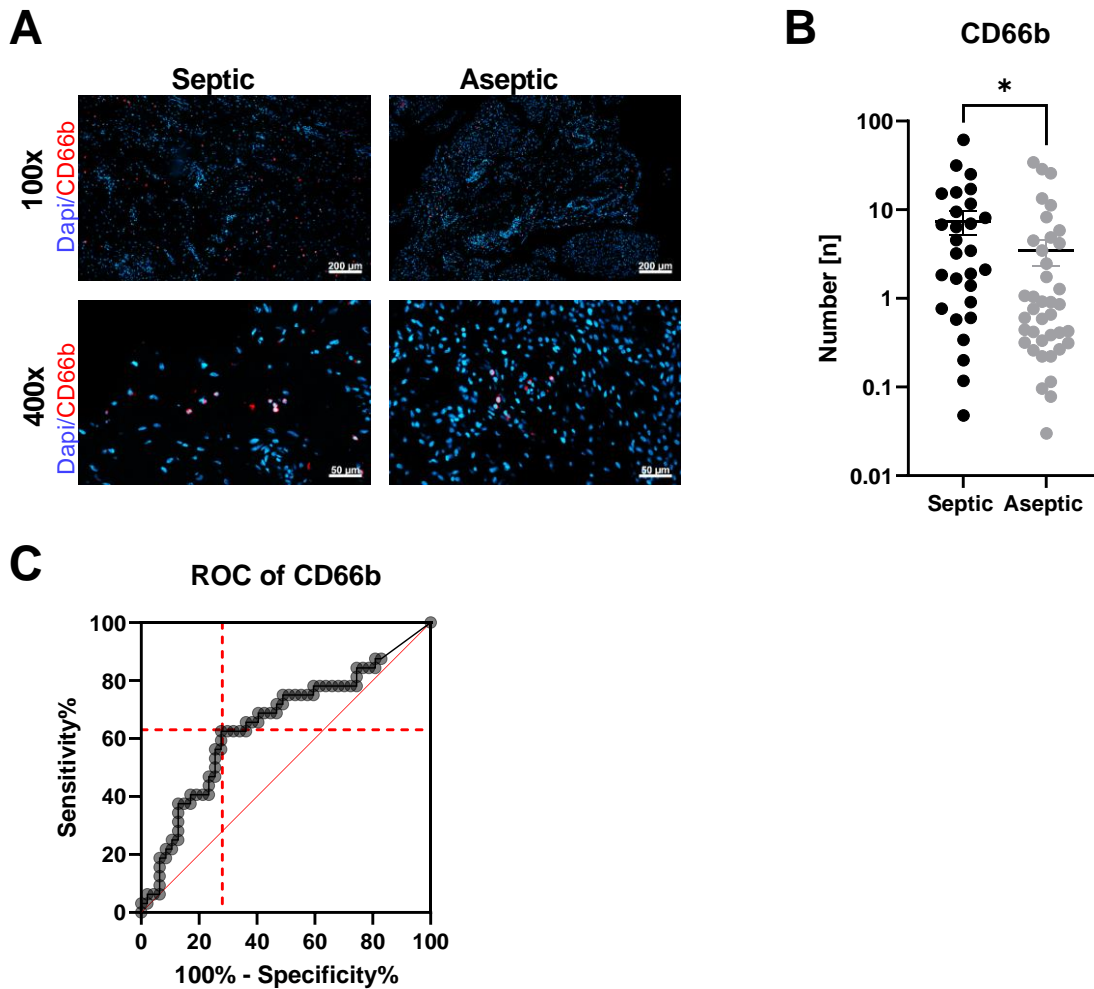


**Figure 14 Immunohistological staining of CD66b in periprosthetic tissue shows a significant difference between the septic and the aseptic cohort**

(A) For the detection of CD66b in THA and TKA samples from septic (right) and aseptic (left) samples, periprosthetic tissue was immunohistologically stained with anti-CD66b (red), and the cell nuclei were stained with Dapi (blue). Representative immunohistochemical staining of CD66b with a magnification of 100x (above, scale bar: 200  $\mu\text{m}$ ) and 400x (below; scale bar: 50  $\mu\text{m}$ ) were given. (B) The quantification (septic: N = 32; aseptic: N = 47) of the red fluorescence of the tissue area was presented as a scatter dot plot and was given as mean  $\pm$  SEM. The septic cohort was presented in black (7.5 %  $\pm$  2 %), and the aseptic cohort was presented in light grey (3.4 %  $\pm$  1.1 %); for better visibility, the samples were plotted logarithmically. The statistical analysis using the Mann-Whitney-U-Test showed a significant difference between the groups ( $p = 0.024$ ). (C) To analyze the predictive value of CD66b as a biomarker for PJI using immunohistological staining in periprosthetic tissue, the percent of red fluorescence in the septic tissue (sensitivity) was plotted against the percent of red fluorescence in the aseptic tissue (100%-specificity). Using the respective fluorescent area values for each sample, the ROC curve calculated an AUC of 0.65. Using the Youden's criteria, the best ratio of sensitivity to specificity was selected (red dashed line). The sensitivity was 63 % (95% of CI: 45.25 % to 77.07 %) while the specificity was at 72 % (95 % of CI: 58.24 % to 83.06 %).

The terminal complement pathway leads to the destruction of bacteria via the key factors C3, C5, and C9. For the detection of these, I analysed 33 patients undergoing shoulder revisions surgery (see 3.1). The routine microbiological diagnostic indicated a PJI in 16 patients; 17 patients underwent aseptic revision surgery (table 14).

Both cohorts (septic and aseptic) were assessed for the presence of C3, C5, and C9 using immunohistological staining. For the detection of the terminal complement pathway, the periprosthetic tissue was stained with anti-C3 (red, fig. 15A), C5 (red; fig. 15D), and C9 (red; fig. 15G). The cell nuclei were stained with Dapi (blue). For an overview, the tissue was first microscope at a magnification of 100x (above). The septic (left) staining showed more red fluorescence than the aseptic (right) side. This became clearer with a magnification of 630x; more red fluorescence was observed in the septic slide than in the aseptic slide. The discrimination between septic and aseptic tissue became clearer the further down the protein marker in the terminal complement pathway's cascade was detected.

For the quantification of the C3 staining (septic: N = 9; aseptic: N = 9), the red fluorescence of the tissue area was presented as a scatter do plot (fig. 15B). The septic (black) cohort (mean  $\pm$  SEM: 0.48 %  $\pm$  0.98 %) and the aseptic (light grey) cohort (mean  $\pm$  SEM: 0.08 %  $\pm$  0.14 %) was examined statistical using the Mann-Whitney-U-test. The septic cohort showed a significant difference ( $p = 0.0315$ ) in comparison to the aseptic cohort. To analyse the predictive value of C3 as a biomarker for PJI, I plotted the percent of red fluorescence in the septic tissue (sensitivity) against the percent of red fluorescence in the aseptic tissue (100 %-specificity) (fig. 15C). Using the respective fluorescent area values for each sample, the ROC curve showed an AUC of 0.80. Using Youden's criteria, the best ratio of sensitivity to specificity was selected (red dashed line). The sensitivity was 56 % (95 % of CI: 26.67 % to 81.12 %) while the specificity was at 100 % (95 % of CI: 70.09 % to 100 %).

For the quantification of the C5 staining (septic: N = 9; aseptic: N = 9), the red fluorescence of the tissue area was presented as a scatter do plot (fig. 15E). The septic cohort was presented in black (mean  $\pm$  SEM: 0.24%  $\pm$  0.08%), and the aseptic cohort was presented in light grey (mean  $\pm$  SEM: 0.04%  $\pm$  0.07%). Using the Mann-Whitney-U-test, the statistical analysis showed a significant difference between both cohorts ( $p = 0.0056$ ). For the analysis of the predictive value of C5 as a biomarker for PJI using immunohistological staining in periprosthetic tissue, the percent of red fluorescence in the septic tissue (sensitivity) was plotted against the percent of red fluorescence in the aseptic tissue (100%-specificity) (fig. 15F). Using the respective fluorescent area values for each sample, the ROC curve calculated an AUC of 0.88. Using Youden's criteria, the best ratio of sensitivity to specificity was selected (red dashed line). The sensitivity was 67 % (95 % of CI: 35.42 % to 87.94 %) while the specificity was at 89 % (95 % of CI: 56.50% to 99.43 %).

For the quantification of the C9 staining (septic: N = 9; aseptic: N = 9), the red fluorescence of the tissue area was presented as a scatter dot plot (fig. 15H). The septic (black) cohort (mean  $\pm$  SEM 0.68 %  $\pm$  0.16 %) was statistically approached using the Mann-Whitney-U-test in comparison to the aseptic (light grey) cohort (mean  $\pm$  SEM: 0.09 %  $\pm$  0.07 %). A statistical difference between

the two cohorts ( $p = 0.0008$ ) was seen. For the analysis of the predictive value of C9 as a biomarker for PJI, I plotted the percent of red fluorescence in the septic tissue (sensitivity) against the percent of red fluorescence in the aseptic tissue (100 %-specificity) (fig. 15). Using the respective fluorescent area values for each sample, the ROC curve showed an AUC of 0.94. Using Youden's criteria, the best ratio of sensitivity to specificity was selected (red dashed line). The sensitivity was 100 % (95 % of CI: 70.09 % to 100 %) while the specificity was at 89 % (95 % of CI: 56.50 % to 99.43 %).

C3, C5, and C9 were detectable in all septic tissues by immunohistochemically staining and partially detected in aseptic tissue. The detection of PJI becomes more certain further down the cascade of the terminal complement pathway. The detection of C3 was already significant, but the distinction becomes more evident with C5. The detection of the protein C9 using anti-C9 by immunohistochemically staining in patient tissues was shown to be a very reliable indicator for infection.

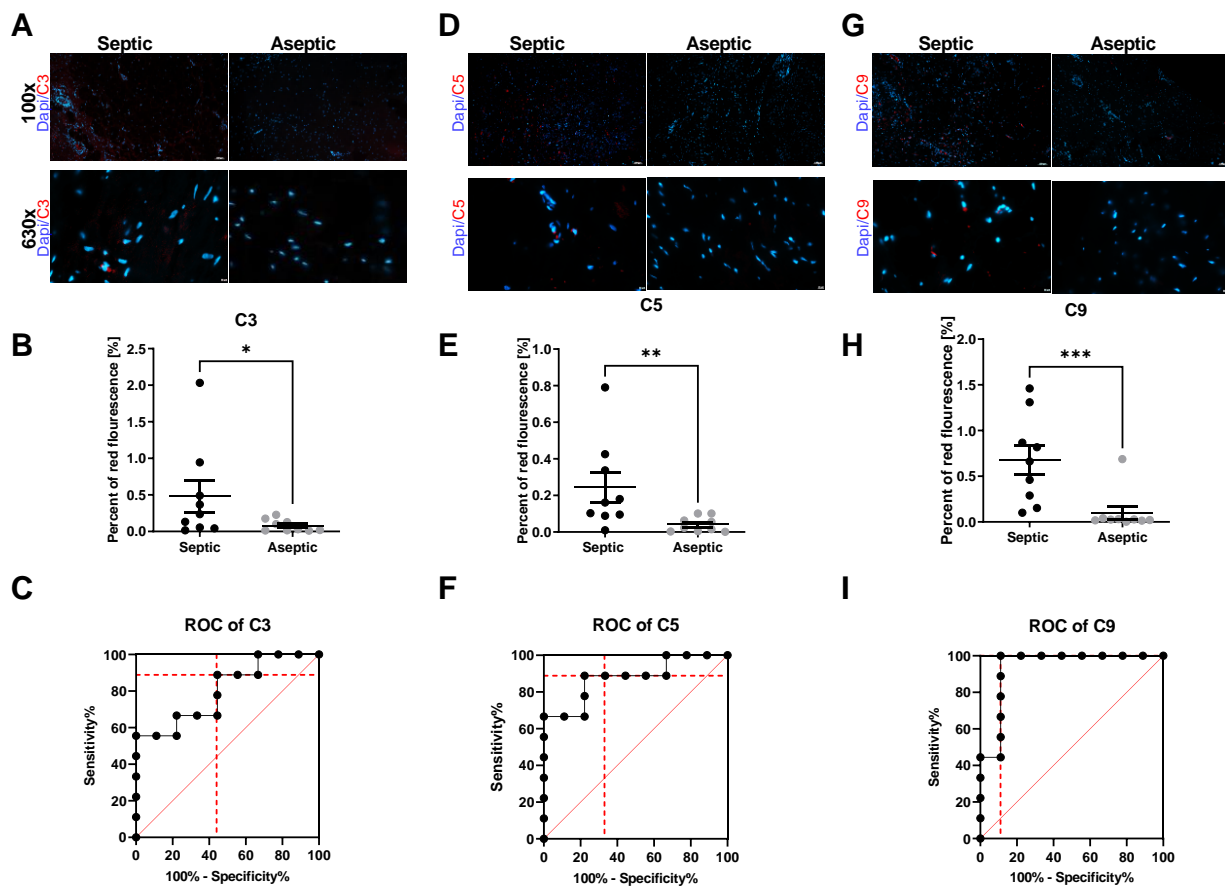


**Figure 15 Immunohistological staining of the terminal complement pathway (C3, C5, C9) in periprosthetic tissue shows a significant difference between the septic and the aseptic cohort.**

For the detection of the terminal complement pathway in shoulder samples from septic (right) and aseptic (left) samples, periprosthetic tissue was immunohistologically stained with anti-C3, anti-C5, and anti-C9 (red), and the cell nuclei were stained with Dapi (blue). (A) Representative immunohistochemical staining of C3 with a magnification of 100x (above,

scale bar: 100  $\mu\text{m}$ ) and 630x (below; scale bar: 2  $\mu\text{m}$ ) were given. (B) The quantification (septic: N = 9; aseptic: N = 9) of the red fluorescence of the tissue area was presented as a scatter dot plot and was given as mean  $\pm$  SEM. The septic cohort was presented in black (0.48 %  $\pm$  0.98 %), and the aseptic cohort was presented in light grey (0.08 %  $\pm$  0.14 %). The statistical analysis using the Mann-Whitney-U-Test showed a significant difference between the groups ( $p = 0.0315$ ). (C) To analyse the predictive value of C3 as a biomarker for PJI using immunohistological staining in periprosthetic tissue, the percent of red fluorescence in the septic tissue (sensitivity) was plotted against the percent of red fluorescence in the aseptic tissue (100%-specificity). Using the respective fluorescent area values for each sample, the ROC curve calculated an AUC of 0.80. Using the Youden's criteria, the best ratio of sensitivity to specificity was selected (red dashed line). The sensitivity was 56 % (95 % of CI: 26.67 % to 81.12 %) while the specificity was at 100 % (95 % of CI: 70.09 % to 100 %). (D) Representative immunohistochemical staining of C5 with a magnification of 100x (above, scale bar: 100  $\mu\text{m}$ ) and 630x (below; scale bar: 2  $\mu\text{m}$ ) were given. (E) The quantification (septic: N = 9; aseptic: N = 9) of the red fluorescence of the tissue area was presented as a scatter dot plot and was given as mean  $\pm$  SEM. The septic cohort was presented in black (0.24%  $\pm$  0.08%), and the aseptic cohort was presented in light grey (0.04%  $\pm$  0.07%). The statistical analysis using the Mann-Whitney-U-Test showed a significant difference between the groups ( $p = 0.0056$ ). (F) To analyse the predictive value of C5 as a biomarker for PJI using immunohistological staining in periprosthetic tissue, the percent of red fluorescence in the septic tissue (sensitivity) was plotted against the percent of red fluorescence in the aseptic tissue (100%-specificity). Using the respective fluorescent area values for each sample, the ROC curve calculated an AUC of 0.88. Using the Youden's criteria, the best ratio of sensitivity to specificity was selected (red dashed line). The sensitivity was 67 % (95 % of CI: 35.42 % to 87.94 %) while the specificity was at 89 % (95 % of CI: 56.50% to 99.43 %). (G) Representative immunohistochemically staining of C9 with a magnification of 100x (above, scale bar: 100  $\mu\text{m}$ ) and 630x (below; scale bar: 2  $\mu\text{m}$ ) were given. (H) The quantification (septic: N = 9; aseptic: N = 9) of the red fluorescence of the tissue area was presented as a scatter dot plot and was given as mean  $\pm$  SEM. The septic cohort was presented in black (0.68 %  $\pm$  0.16 %), and the aseptic cohort was presented in light grey (0.09 %  $\pm$  0.07 %). The statistical analysis using the Mann-Whitney-U-Test showed a significant difference between the groups ( $p = 0.0008$ ). To analyse the predictive value of C9 as a biomarker for PJI using immunohistological staining in periprosthetic tissue, the percent of red fluorescence in the septic tissue (sensitivity) was plotted against the percent of red fluorescence in the aseptic tissue (100%-specificity). Using the respective fluorescent area values for each sample, the ROC curve calculated an AUC of 0.94. Using the Youden's criteria, the best ratio of sensitivity to specificity was selected (red dashed line). The sensitivity was 100 % (95 % of CI: 70.09 % to 100 %) while the specificity was at 89 % (95 % of CI: 56.50 % to 99.43 %).

In this part of my thesis, I investigated that  $\alpha$ -defensin and CD68 showed no significant difference between the aseptic and septic cohort. Using CD66b, C3, C5, and C9, a significant difference between the septic and aseptic cohort could be shown. However, the detection of C9 with a sensitivity of 100% and a specificity of 88.89% was shown to be a very reliable indicator for infection.

### 3.4 Validation of C9 as possible Biomarker for the improved diagnosis of PJI

As the immunohistological staining of C9 showed the best predictive value for the PJI detection in periprosthetic tissue (seen in 3.3) compared to the other investigated terminal complement factors, I decided to validate this observation in another cohort of PJI. For this validation, 98 samples from patients undergoing TKA and THA revision operations were used (see 3.1). Again, the cohorts were divided into aseptic (40/98) and septic (58/98) according to the identification of the microbiological diagnostic.

Both cohorts (septic and aseptic) were assessed for the presence of C9 using immunohistological stainings. For the detection of C9, the periprosthetic tissue was stained with anti-C9 (red) while the cell nuclei were stained with Dapi (blue) (fig. 16A). Representative immunohistochemical stainings of C9 with a magnification of 400x were taken. On the left side, a sample of the septic cohort was presented. The first picture showed the Dapi staining; the second picture showed the

staining of anti-C9. The last picture showed a merged picture with both stainings. On the right side, representative immunohistochemical staining of C9 in the aseptic cohort can be seen. Again, the first picture showed the Dapi staining, the second the staining of C9, and the last a merged version of both stainings. The red fluorescence was detectable in the septic slide, whereas the aseptic slide showed no red fluorescence. Only in a few slides, the red fluorescence staining observed partially in the aseptic tissue. For quantifying the staining (septic: N = 58; aseptic: N = 40), the red fluorescence of the tissue was presented as a scatter dot plot (fig. 16B). Using the statistical examination of the Mann-Whitney-U-Test, the difference between both cohorts were analyzed. The septic cohort (black) (mean ± SEM: 2.7% ± 0.65%) was significantly ( $p < 0.0001$ ) increased compared to the aseptic cohort (mean ± SEM: 0.34% ± 0.22%). To investigate the predictive value of C9 as a biomarker for PJI, I plotted the percent of red fluorescence in the septic tissue (sensitivity) against the percent of red fluorescence in the aseptic tissue (100 %-specificity) (fig. 16C). The respective fluorescent area values for each sample showed a ROC curve with an AUC value of 0.84. Using the Youden’s criteria, the threshold for the sensitivity and specificity (red dashed line) was estimated. The sensitivity was at 89% (95% of CI: 78.83 % to 96.11 %) while the specificity was at 75% (95% of CI: 58.80% to 87.31%). Using the classification of biomarkers (fig.4) [146], C9 can be described as an excellent biomarker for immunohistochemical detection of PJI in periprosthetic tissue.

Since C9 was not detected in all tissue samples using the septic cohort, the following paragraph discusses which factors could influence the C9 detection in more detail.

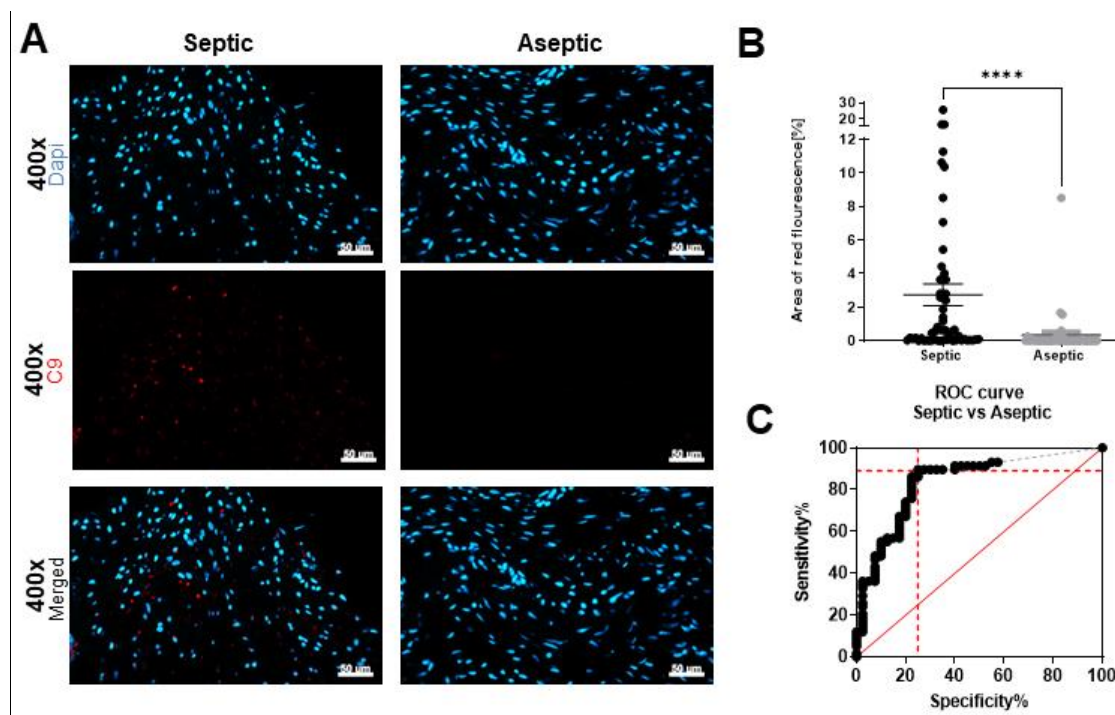
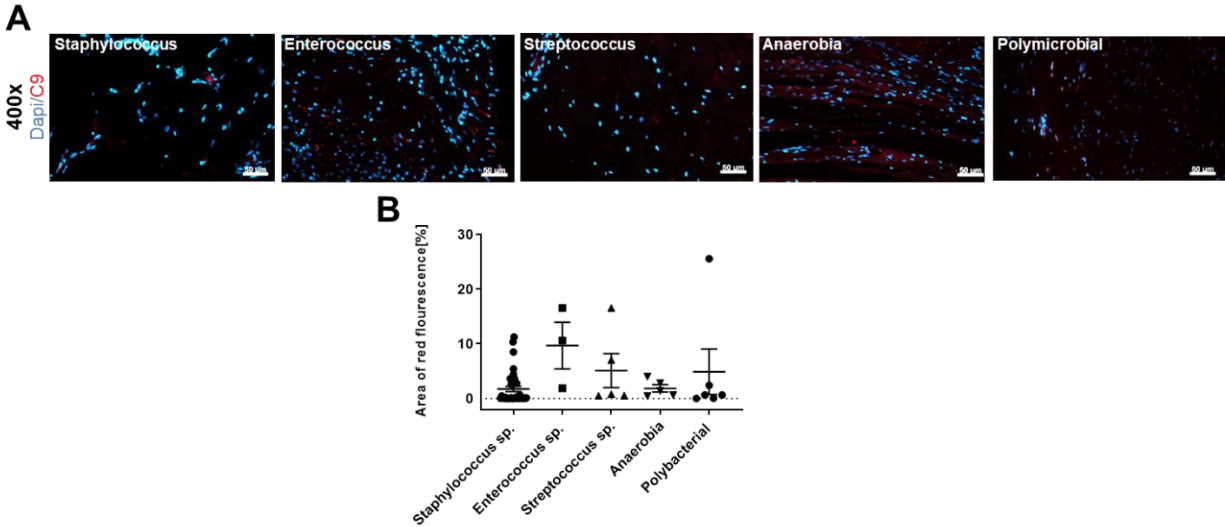


Figure 16 Significant increase of C9-antibody in septic periprosthetic tissue

(A) For the detection of C9 in THA and TKA samples from septic (right) and aseptic (left) samples, periprosthetic tissue was immunohistologically stained (right side) with anti-C9 (red), and the cell nuclei were stained with Dapi (blue). Representative immunohistochemically staining of C9 with a magnification of 400x (scale bar: 50  $\mu$ m) was given. The quantification (left side) (septic: N = 58; aseptic: N = 40) of the red fluorescence of the tissue area was presented as a scatter dot plot and was given as mean  $\pm$  SEM. The septic cohort was presented in black (2.7%  $\pm$  0.65%), and the aseptic cohort was presented in light grey (0.34%  $\pm$  0.22%). The statistical analysis using the Mann-Whitney-U-Test showed a significant difference between the groups ( $p < 0.0001$ ). (B) To analyse the predictive value of C9 as a biomarker for PJI using immunohistological staining in periprosthetic tissue, the percent of red fluorescence in the septic tissue (sensitivity) was plotted against the percent of red fluorescence in the aseptic tissue (100%-specificity). Using the respective fluorescent area values for each sample, the ROC curve calculated an AUC of 0.84. Using the Youden's criteria, the best ratio of sensitivity to specificity was selected (red dashed line). The sensitivity was 89% (95% of CI: 78.83% to 96.11%) while the specificity was at 75% (95% of CI: 58.80% to 87.31%).

Next, I investigated if the detection of C9 may be pathogen dependent and certain pathogens increase the detection level of C9 (fig. 17). Five bacteria that are most common in orthopedics; are *Staphylococcus* spp. [72], *Streptococcus* spp., *Enterococcus* spp. [72] and *Anaerobia* [23, 80]. Therefore, the tissue of the septic cohort from THA and TKA samples were divided into the following bacteria families: *Staphylococcus* spp. (N = 37), *Enterococcus* spp. (N = 3), *Streptococcus* spp. (N = 5), *Anaerobia* (N = 5) and Polymicrobial infections (N = 6). Representative immunohistological stainings were presented with a magnification of 400x (fig. 17A). C9 was stained by anti-C9 (red), while the cell nuclei were stained blue with Dapi. In all various pathogen stainings, red fluorescence was observed. In some cases, more fluorescence was suspected; therefore, a quantitative analysis was performed. For the quantitative analysis of the various pathogen groups, the red fluorescence of the tissue was presented as a scatter dot plot and was given as mean  $\pm$  SEM (fig. 17B). Between *Staphylococcus* spp. (1.75%  $\pm$  0.49%), *Enterococcus* spp. (9.69%  $\pm$  4.27%), *Streptococcus* spp. (5.1%  $\pm$  3.13%), *Anaerobia* (1.86%  $\pm$  0.68%) and Polymicrobial infections (4.9%  $\pm$  4.15%) were not significantly different measured, calculated by a One-Way-ANOVA using Tukey's multiple comparisons test as post-hoc.

The quantification of the C9 immunostaining showed no pathogen-dependent difference for C9. Therefore, this indicated that the C9 detection in periprosthetic tissue by immunohistological staining could be performed pathogen independently. These also suggested that other factors may influence the detection of C9 in tissue.



**Figure 17 No pathogen-dependent C9 detection was analyzed**

(A) For the detection of C9 in THA and TKA samples from various bacteria samples (Staphylococcus, Enterococcus, Streptococcus, Anaerobia, Polymicrobial) of the periprosthetic tissue was immunohistological stained (above) with anti-C9 (red), and the cell nuclei were stained with Dapi (blue). Representative immunohistochemical staining of C9 with a magnification of 400x (scale bar: 50  $\mu$ m) was given. (B) The quantification (*Staphylococcus* spp.: N = 37, *Streptococcus* spp.: N = 5, *Enterococcus* spp.: N = 3, Anaerobia: N = 5 and Polymicrobial infections: N = 6) of the red fluorescence of the tissue area was presented as a scatter dot plot and was given as mean  $\pm$  SEM for *Staphylococcus* spp. (1.75 %  $\pm$  0.49 %), *Enterococcus* spp. (9.69 %  $\pm$  4.27 %), *Streptococcus* spp. (5.1 %  $\pm$  3.13 %), Anaerobia (1.86 %  $\pm$  0.68 %) and Polymicrobial infections (4.9 %  $\pm$  4.15 %). The statistical analysis using the Mann-Whitney-U-Test showed no significant difference between the groups.

As the CRP is involved in the activation of the complement cascade (40), I tested whether the CRP value of each patient in the septic cohort would correlate with the amount of red fluorescence of the C9 staining from the septic cohort. (fig. 18A). The respective values were plotted and analyzed using a linear regression (Spearman  $r = 0.01315$ ; 95% CI = -0.008875 to 0.02146,  $p = 0.4090$ ; N = 54). I observed that non-significant correlation between both parameters was apparent. As the complement pathway is reactivated upon an infection very early, I wanted to investigate the correlation between the implantation time and C9 (fig. 18B). Again, a linear regression (Spearman  $r = 0.011332$ ; 95% CI = -0.02274 to 0.02270,  $p = 0.09985$ ; N = 53) was done and showed no significant correlation between these two groups.

As bacterial infection can be defined as (early, delayed- and late-onset infection), I wanted to investigate if the type of infection influences of the amount of C9 present in the tissue. For the quantification, the samples shown in fig. 18C were subdivided into early (>3 months after implantation, N = 12), delayed (3 – 12 months after implantation, N = 14) and late (<12 months after implantation, N = 27) infection. The red fluorescence of the tissue area was presented as a scatter dot plot and was given as mean  $\pm$  SEM; for better visualization, the samples were plotted logarithmically. Using a One-Way-ANOVA, the statistical difference was calculated. No significant

difference (Early vs Delayed: 0.5372; Early vs. Late: 0.2632; Delayed vs. Late: 0.9206) was observed between early (0.97 %  $\pm$  0.41%; N = 12), delayed (3.11 %  $\pm$  1.06 %, N = 14) and late (3.76 %  $\pm$  1.24 %, N = 27) infections.

After carefully testing the C9 detection in the periprosthetic tissue of the septic cohort, the test results showed that C9 was detectable independently from the pathogen family, the CRP value, implantation time, and infection classification.

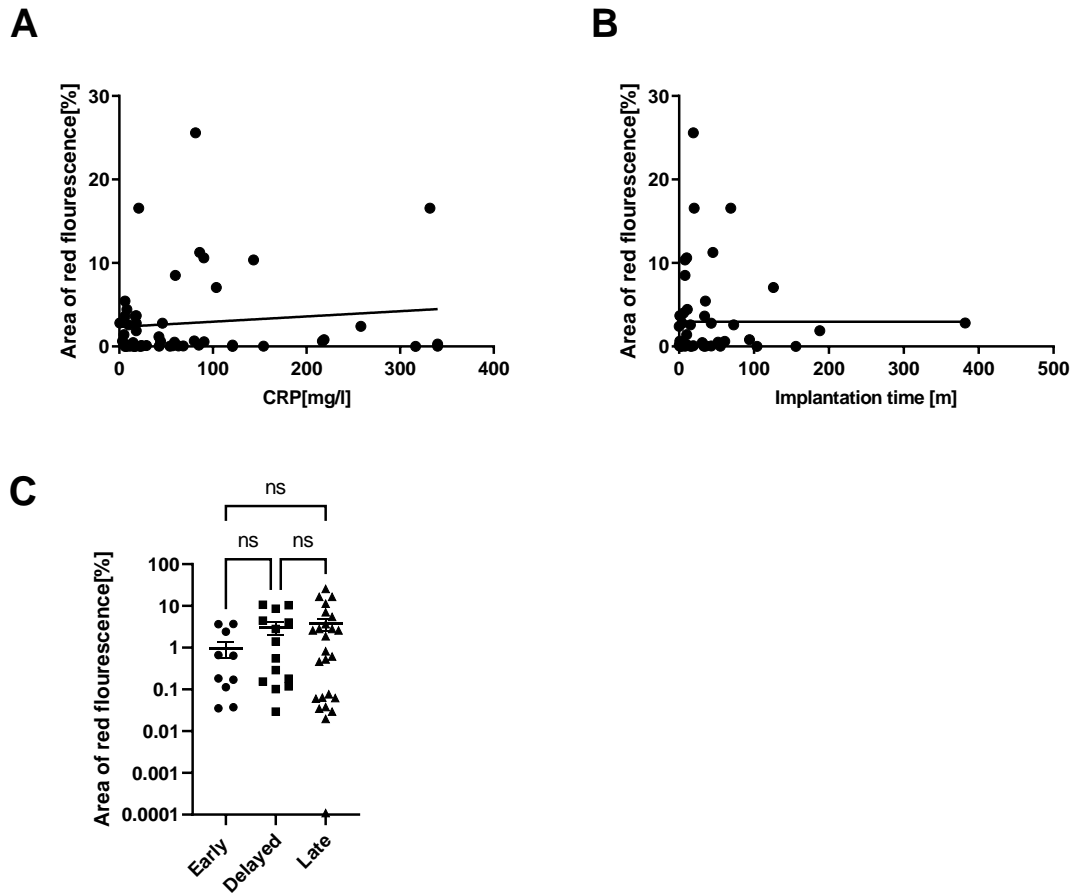


**Figure 18 No correlation between the amount of red fluorescence of C9 between the CRP value, implantation time and infection classification**

(A) In order to test the relation between C9 and the CRP value the respective values were plotted against each other. The groups did not correlate with each other (Spearman  $r = 0.01315$ ; 95% CI = -0.008875 to 0.02146,  $p = 0.9016$ ; N = 54). (B) In order to test the relation between C9 and the implantation time the respective values were plotted against each other. The groups did not correlate with each other (Spearman  $r = 0.011332$ ; 95% CI = -0.02274 to 0.02270,  $p = 0.09985$ ; N = 53). (C) To investigate if the type of infection (early: <3 months after implantation; N = 12, delayed: 3 – 12 months after implantation, N = 14; late: <12 months after implantation, N = 27) have an influence of the detection of C9 immunostaining in periprosthetic tissue. A scatter dot plot was used for quantification and was given as mean  $\pm$  SEM (early: 0.97 %  $\pm$  0.41%; N = 12, delayed: 3.11 %  $\pm$  1.06 %, N = 14, late: 3.76 %  $\pm$  1.24 %, N = 27), for better visibility the samples were plotted logarithmically. The statistical analysis using a One-Way Anova showed no significant difference between the groups (Early vs Delayed: 0.5372; Early vs. Late: 0.2632; Delayed vs. Late: 0.9206).

As  $\alpha$ -defensin is described to show cross reactivity in the presence of metallosis [159] and crystallopathies [160], I analyzed whether C9 can be detected in periprosthetic tissue of these conditions.

For this investigation, I analysed 110 patients undergoing primary knee and hip implantation. Except for the septic group, these patients were not used from the previously listed cohort (see. 3.1). I included four groups subdivided according to their inflammatory joint conditions in septic (58), Chondrocalzinosis (CC: N = 19), Rheumatoid Arthritis (RA: N = 17), and abrasive wear particles (N = 16) (table 17). According to the clinical diagnosis, 36 males and 22 females with an average age of  $72 \pm 9$  were included in the septic cohort. In the CC cohort, 15 males and 4 females with an average age of  $67 \pm 11$  were analysed. Two males and 15 females with an average age of  $66 \pm 18$  were included in the RA cohort. In the cohort with abrasive wear particles, 5 males and 11 females with an average age of  $70 \pm 13$  were included.

As shown in the analysis before (fig. 15 and 16) there was no difference in the C9 detection depending on the infected joint. Therefore, the periprosthetic tissue was collected from either shoulder, knee, or hip surgeries. 22 TKA and 36 THA were included in the septic cohort, while the CC cohort contained 19 TKA. In the RA group, 6 samples were collected from TKA, 5 from THA, 2 from TSA, and 2 from TTA, while in the wear particles cohort, 4 TKA and 12 THA samples were obtained.

Table 17 Biometric characteristics of the study population

Cohort	Number	Sex	Age [yr]	Location
<b>Septic</b>	58	♂ 36 ♀ 22	$72 \pm 9$	TKA: 22 THA: 36
<b>CC</b>	19	♂ 15 ♀ 4	$67 \pm 11$	TKA: 19 THA 0
<b>RA</b>	17	♂ 2 ♀ 15	$66 \pm 18$	TKA: 6 THA: 5 TTK: 2 TSA: 2
<b>Wear particles</b>	16	♂ 5 ♀ 11	$70 \pm 13$	TKA:4 THA:12

The four cohorts (septic, CC, RA, and wear particles) were assessed for the presence of C9 using immunohistological staining. For the detection of C9, the periprosthetic tissue was stained with an anti-C9 antibody (red), while the cell nuclei were stained blue using Dapi (fig. 19A). Representative immunohistochemical staining of C9 with a magnification of 400x can be seen in fig. 19A. The staining of the septic samples (left above) showed more red fluorescence compared to the CC (right above) and RA (left below) samples. In the tissue containing wear particles (right below), some C9 staining was detected. For the quantification of this observation, the C9 staining of the septic (N = 58), CC (N = 19), RA (N = 17), and wear particle-containing tissues (N = 16) are

depicted as a scatter dot blot (mean  $\pm$  SEM) (fig. 19B). The septic cohort is shown as black circle while the other inflammatory joint conditions are shown in light grey (CC  $\blacksquare$ : 0.25 %  $\pm$  0.16 %; RA  $\blacktriangle$ : 0.09 %  $\pm$  0.04 %; wear particles  $\blacktriangledown$ : 0.51 %  $\pm$  0.22 %). A One-Way-ANOVA with Dunn's post-hoc was performed for the statistical analysis, comparing the various inflammatory joint conditions with the septic (2.74 %  $\pm$  0.65 %) cohort. The septic cohort showed a significant ( $p = 0.0004$ ) increase in C9 staining compared to the CC cohort. The detection of C9 in RA tissue was significantly lower than in the septic cohort ( $p = 0.0009$ ). The detection of C9 in the periprosthetic tissue containing metallic wear particles showed no significant ( $p = 0.2224$ ) difference to the septic cohort.

To analyse the predictive value of C9 as a biomarker for PJI, I plotted the percentage of red fluorescence in the septic tissue (sensitivity) against the percent of red fluorescence in the CC tissue (100%-specificity) (fig. 19C). The ROC curve showed an AUC of 0.78 for the distinction between CC and PJI. Youden's index was used to calculate the sensitivity and the specificity (red dashed line). The sensitivity was 94 % (95 % of CI: 73.97 % to 99.87 %) while the specificity was at 57 % (95 % of CI: 43.23 % to 69.84 %).

The same analyses were carried out for the comparison between C9 staining in septic tissue (sensitivity) and RA tissue (100%-specificity) (fig. 19D). The ROC curve showed an AUC of 0.77. Again the sensitivity and the specificity were considered using the Youden's index (red dashed line); the sensitivity was 76 % (50.10 % to 93.19 %) while the specificity was at 76 % (95 % of CI: 62.83 % to 86.13 %).

The same analyses were performed for C9 staining in the septic tissue (sensitivity) compared to the C9 staining tissue containing abrasive wear (100%-specificity) (fig. 19E). Using the respective fluorescent area values for each sample, the ROC curve calculated an AUC of 0.62. Using the Youden's criteria the best ratio of sensitivity to specificity was selected (red dashed line). The sensitivity was 81 % (95 % of CI: 54.35 % to 95.95 %) while the specificity was 52 % (95 % of CI: 38.22 % to 65.05%).

After carefully testing possible cross-reactions for the detection of C9 using other inflammatory joint conditions (e.g., CC, RA, and abrasive wear) in comparison to the PJI cohort, it was shown that the C9 immunohistological staining could help to give a more detailed diagnosis to detect an infection. Patients with CC and RA would not need to be excluded as they do not show cross-reactivity with the staining. Due to the high sensitivity of 89% and specificity of 75% shown in this thesis, C9 could work as a Biomarker to identify Infections.

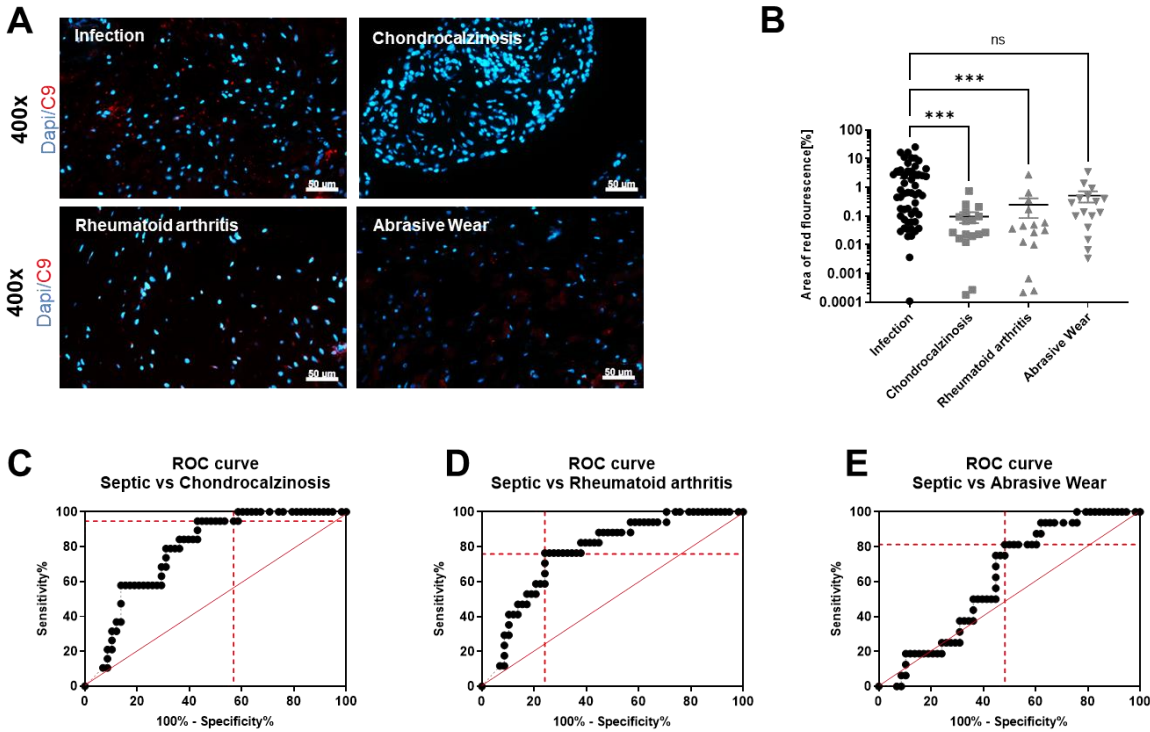


**Figure 19 Significant increase of the detection of C9 in periprosthetic tissue with infection compared to tissue with rheumatoid arthritis and chondrocalcinosis**

(A) For the detection of C9 in THA and TKA samples from septic (left above), chondrocalcinosis (CC) (left above), rheumatoid arthritis (right below), and abrasive wear (right below), periprosthetic tissue were immunohistochemically stained with anti-C9 (red), and the cell nuclei were stained with Dapi (blue). Representative immunohistochemical staining of C9 with a magnification of 400x (scale bar: 50  $\mu$ m) are given. (B) The quantification (infection  $\bullet$ : N = 58; CC  $\blacksquare$  N = 19; RA  $\blacktriangle$  N = 17; abrasive wear  $\blacktriangledown$  N = 16) of the red fluorescence of the tissue area was presented as bar chart and was given as mean  $\pm$  SEM. The septic cohort was presented in black (2.74 %  $\pm$  0.65 %), CC was presented in light grey (0.25 %  $\pm$  0.16 %), as well as RA (0.09 %  $\pm$  0.04 %) and abrasive wear (0.51 %  $\pm$  0.22 %). The statistical analysis using a One-way-Anova with Dunn's post-hoc showed a significant difference between septic and CC ( $p = 0.0004$ ), septic and RA ( $p = 0.0009$ ), and no significant difference between septic and abrasive wear ( $p = 0.8601$ ). (C) To analyse the predictive value of C9 as a biomarker for PJI using immunohistological staining in periprosthetic tissue, the percent of red fluorescence in the septic tissue (sensitivity) was plotted against the percent of red fluorescence in the CC tissue (100%-specificity). Using the respective fluorescent area values for each sample, the ROC curve calculated an AUC of 0.78. Using the Youden's criteria the best ratio of sensitivity to specificity was selected (red dashed line). The sensitivity was 94 % (95 % of CI: 73.97 % to 99.87 %) while the specificity was 57 % (95 % of CI: 43.23 % to 69.84 %). (D) The same was carried out for the percent of red fluorescence in the septic tissue (sensitivity) plotted against the percent of red fluorescence in the RA tissue (100%-specificity) Using the respective fluorescent area values for each sample, the ROC curve calculated an AUC of 0.77. Using the Youden's criteria the best ratio of sensitivity to specificity was selected (red dashed line). The sensitivity was 76 % (50.10 % to 93.19 %) while the specificity was 76 % (95 % of CI: 62.83 % to 86.13 %). (E) The same was carried out for the percent of red fluorescence in the septic tissue (sensitivity) plotted against the percent of red fluorescence in the abrasive wear tissue (100%-specificity) Using the respective fluorescent area values for each sample, the ROC curve calculated an AUC of 0.62. Using the Youden's criteria the best ratio of sensitivity to specificity was selected (red dashed line). The sensitivity was 81 % (95 % of CI: 54.35 % to 95.95 %) while the specificity was 52 % (95 % of CI: 38.22 % to 65.05 %).

## 4. Discussion

Culture-negative periprosthetic joint infections (CN-PJIs) are occurring with an incidence of 7% [68]. Typical inflammatory factors characterize them, but no bacteria can be detected in microbiological cultures. This could be due to the pre-administration of antibiotics or the presence of biofilms. Therefore, the screening process of std. microbiological diagnostic is disturbed in these cases [69]. However, there are also cases in which no clinical signs of inflammation could be detected and the std. microbiological diagnostic could not identify pathogens while an infection is present. These CN-PJIs are classified as false-negative and usually assumed to be aseptic loosening cases [69, 70]. The problem is that the typically applied screening method of tissue culturing [71] is in some cases not sensitive enough. Therefore, there is a need for biomarkers to secure the diagnosis in unclear cases. One of the most promising biomarkers for detecting infections is  $\alpha$ -defensin [147, 148] and is already part of the MSIS criteria for PJI diagnostics [27] (fig. 2). However, the ELISA-based detection of  $\alpha$ -defensin in synovial fluid of patients does not work in the presence of metallosis or crystallopathies, which makes this biomarker less reliable under these conditions [159] [160]. Therefore, the need for alternative biomarkers to support the detection of PJI is essential. The main goal of this thesis was to investigate an alternative biomarker for the detection of PJI.

### 4.1 The demographic data of the cohorts

In the first part of this thesis, the demographic data of the cohorts were described (table 13). I considered different factors, e.g., age, site of infection, and sex, which might influence the occurrence of PJI. In this thesis, 178 patients were hospitalized for revision surgery on the hip (THA), knee (TKA), and shoulders (TSA) and were included in the cohort. The reasons for revision were due to septic (95/178) or aseptic (81/178) conditions; therefore, the samples were divided into these two cohorts. The average age in the septic cohort was  $73 \pm 9$  years, while the average age of the aseptic cohort was  $70 \pm 12$  years. Using the Gaussian distribution (fig. 7A), I observed that more septic and aseptic revision were done within an age range of 70 to 75 years. The literature described that patients aged 65 to 75 years have a 3.36-fold higher risk of getting a PJI than those aged 45 to 65 [190]. Concerning this, in my cohort, this observation was confirmed. It has been discussed that elderly patients tend to have a high risk of infection due to their weakened immune system and their poor diet [190].

Furthermore, the literature describes that males have an increased risk of getting a PJI than women [20, 21]. In the septic cohort, there were 57 males, and 38 females, the distribution in the aseptic cohort was more homogeneous with 42 males and 39 females (fig. 7B). More males

contract a PJI due to the gender-specific difference in the immune system, as women generate stronger immune responses [191]. Other studies have shown that women are less susceptible to viral infections [192, 193] and bacterial infections due to their increased immune reactivity [194]. In contrast, men have a higher prevalence of bacterial and parasitic infectious diseases [195]. This observation was also confirmed in my cohort, where more males had an infection than women. Many different factors influence the risk of infection, but regardless of gender and age, the implant region also seems to influence the infection rate. It has been described that THA are less frequently infected (incidence: 1%) compared to TSA and TKA (incidence: 2%) [16]. This observation, however, could not be confirmed in the present cohort. The septic cohort, with a total of 95 patients, was divided into 42 % (40/95) THA, 39 % (37/95) TKA, and 19 % (18/95) TSA. In comparison, the aseptic cohort was divided into 36 % (29/81) THA, 41 % (33/81) TKA, and 23 % (19/81) TSA (table 13). The number of THA and TKA in this study was similar, but septic TSA were observed about half frequently. Another study showed that the infection rate between THA and TKA endoprostheses hardly differed about 2 - 2.24 % [196]. In some cases, it is described that THA infections were observed more frequently when they were performed in a direct anterior surgical approach [197]. This could be attributed to the surgical technique used, as the implantation technique is critical for the incidence of infection [198].

Comorbidities, including diabetes, renal disease, and cardiac insufficiency, have also been associated with an increased risk for PJI [18] (table 14). In my septic cohort, I observed a higher number of patients suffering from renal and cardiac insufficiency compared with the aseptic cohort. In contrast, the number of diabetes in the septic and aseptic cohort was similar. Other comorbidities were found less frequently in both cohorts. However, it was shown in another study that diabetic patients with chronic kidney disease (CKD) have a higher risk of developing PJI than the patients without CKD [199]. In addition, an *in vitro* study showed that biofilm formation was enhanced in the presence of elevated glucose concentration, such as in diabetes patients [24]. This suggests that the interaction of diabetes together with other diseases increases the chance of getting a PJI. This fact was also observed in this thesis, as 65 patients suffered from more than one comorbidity. However, the clinic is a tertiary referral center, particularly severe patient cases being treated here. Therefore, the number of comorbidities was exceptionally high in both cohorts. Furthermore, the population of Saxony-Anhalt, with an average age of 47.9 years, has the oldest population in Germany [200], with high numbers of diabetes mellitus, obesity, and hypertension [201]. Furthermore, this study also did not use a consecutive cohort but rather a case-control study. This could also have implications for the incidence of comorbidities.

The literature describes that PJIs occur more frequently after the first 3 months following joint implantation than PJIs that occur after 12 months following joint implantation [60, 202]. Based on

the classification of the PJI shown in the introduction (see 1.1.2), more early PJIs occurs than late PJIs [60, 202]. In this cohort, late PJIs (>12 months after implantation) were observed in 58 % (48/83) of all cases. In comparison, 24 % (20/83) were delayed infections (3 – 12 months after implantation), and early infections (<3 months after implantation) were about 18 % of all cases (fig. 7C). Early and delayed infections are more likely to be caused by intraoperatively acquired bacteria [23]. Therefore, prophylactic antibiotics are often administered to reduce the risk of infections [203]. Because late infections are often acquired later on by hematogenous pathways, the antibiotics administered directly during or after the surgery have no effect [204]. The combination of optimized sterile working conditions during the surgery [205, 206] and antibiotic treatment pre-operatively [207, 208] should reduce the risk of contamination; therefore, early and delayed infections should occur less frequently [209]. Whether this also applies to my cohort is speculation. However, it can be assumed that the surgical guidelines performed in this clinic reduce the risk of contamination through hygiene regulations and disinfection [210]. However, as the Department of Orthopaedic Surgery of the university hospital Magdeburg is a tertiary referral center, my cohort consists mostly of patients with more complicated cases. Most likely, more revision cases are operated in the department. Contrary to the literature, this could explain my cohort's many observed late infections [61]. Patients may be referred from other clinics because of non-specific pain of the joint, which is typical for late infections [65], has not been diagnosed as infection and was identified in my department during pre-operative biopsy cultures.

Since an increased number of late infections occurred in my cohort, it was expected that the pathogen spectrum consisted of a higher number of anaerobic bacteria [65] [62, 63]. As described, anaerobic bacteria are slow-growing and are often identified in late infections [211]. Nevertheless, in this cohort, most PJIs were caused by *Staphylococcus* spp. (58%) and polymicrobial infections (16%). Anaerobias (11%) were found a bit more frequently than *Streptococcus* spp. (8%), and were more prevalent than *Enterococcus* spp. (5%) (fig. 8A). My cohort's high incidence of *Staphylococcus* spp. aligns with the literature, as it is one of the most common pathogens found in a PJI [72]. Bacteria such as *Streptococcus* spp. or *Enterococcus* spp. have been described to occur less frequently in PJIs [72], which is in line with the observations in my cohort. Anaerobias can also cause a PJI, but they are less familiar with approximately 3 – 6 % of PJIs [23, 80], which were slightly increased in my cohort with 11%. In comparison, polymicrobial infections have been identified to cause up to 6% to 37% of all PJIs [83-85]. Similar to the literature, I also observed 16% of cases of polymicrobial infections. Furthermore, the pathogen spectrum was subdivided according to the site of implants, such as THA (fig. 8B), TKA (fig. 8C), and TSA (fig. 8D). Again, for each implantation site *Staphylococcus* spp. was the most frequently found pathogen. Interestingly, TSA had the slightest variation in the pathogen spectrum but an increased number

of anaerobia in comparison to the THA and TKA groups. Especially *C. acnes*, a typical anaerobia in PJI, has been described as highly frequently associated with shoulder PJIs [212]. That may be because of the high concentration of sebaceous follicles in this area [81, 213, 214], which is one of the most frequent sites of occurrence for *C. acnes* [212]. More polymicrobial (15%) infections in my cohort were detected in THA than TKA (5%). This finding has been observed in a previous publication showing that anaerobic and polymicrobial infections occurred more frequently in THA than in TKA [215].

#### 4.2 Serum inflammatory markers are not indicative of the presence of PJI

To identify a PJI, the Musculoskeletal Infection Society (MSIS) [27] described diagnostic criteria, which combine clinical and laboratory parameters (fig. 2).

Typical serum markers for the detection of PJI included the white blood cell (WBC) count and C-reactive protein (CRP), which are classified as minor factors (fig. 2) [36]. The WBC count is less than 10 Gpt/l in a healthy person, while the CRP value in a healthy patient is less than 5 mg/l [42]. In this thesis, the WBC count of the septic cohort and the aseptic cohort were compared. These results (fig. 9A) revealed no significant difference between both cohorts. It was expected that in the septic cohort, more patients had a WBC above the threshold of 10 Gpt/l, but only 30 % (27/91) of the patients had an elevated WBC while the remaining 70 % (64/91) had a decreased WBC count. Recent literature described that the WBC is not an objective criterion for identifying a PJI [216]. Thus, the WBC has a sensitivity of only 20 % and a specificity of 96 % [217]. The sensitivity increases to only 79.2 % during acute postoperative infection, and the specificity decreases to 46.3 % [218]. In contrast to Zmistowski et al., who suggested that the WBC count is a good indicator of PJI and is elevated in septic problems [219], I observed that the WBC could not be indicated whether there was infection PJI present or not.

Therefore, the CRP levels of the septic and aseptic cohorts were compared with each other. CRP is a very sensitive marker for PJI, which, however, has low specificity, as it can be influenced by other inflammatory diseases [220, 221]. The cohort studied in this thesis confirmed this observation. 58% of the aseptic cases showed an elevated CRP value (fig. 9B). In addition, 7% of the patients in the septic cohort had a CRP value below the pathologic threshold of 5 mg/l.

If there is a clinical suspicion of PJI that the MSIS criteria can confirm, it is not difficult to identify a PJI and initiate the correct treatment. The problem is when the clinical suspicion suggests a PJI, but it cannot be confirmed by the MSIS criteria [222]. The false-negative diagnosis of CN-PJI occurs in up to 7% of all PJI cases [68]. Therefore, how accurate the standard (std.) microbiological

diagnostic could identify a pathogen in periprosthetic tissue cultures and whether other techniques come to the same result.

### **4.3 Dithiothreitol and Next Generation Sequencing showed Similar Diagnostic Security as Periprosthetic Tissue Cultures to Diagnose a PJI**

Microbiological diagnosis is often considered insufficient for a reliable diagnosis of PJI, as several factors can influence the sensitivity and specificity of the analysis [118, 223-225]. These factors include contamination of fluids or tissue biopsies, a biofilm that could complicate the screening method, and even antibiotic pre-treatment can confound the results [226-228]. Dithiothreitol (DTT) could be used to destabilize the extracellular matrix of biofilms on orthopedic implants by reducing the disulfide bonds between polysaccharides and proteins [122]. A specially designed device (NCS Lab Srl, Carpi, Italy) was used to store the implant under sterile conditions after the explantation directly. After the explantation of the potentially infected implant, the prosthesis gets stored in the sterile bag and rinsed with the DTT solution. This treatment is thought to dissolve the adherent biofilm. Part of the DTT solution was subsequently used for microbiological diagnostics in bacterial cultivation from this fluid. Since NGS is also becoming important in diagnosing PJI [103, 104], the other syringe containing the DTT solution was used for DNA isolation and NGS (fig. 6).

Since microbiological standard periprosthetic tissue cultivation was performed for the routine diagnosis according to the MSIS criteria [27], these results were used as a reference. The DTT solution for culturing and for NGS analysis was compared with the results obtained from microbiological diagnostics.

This thesis, investigated 66 patients undergoing septic (28) and aseptic (38) hip and knee revisions. In the first part, I compared the std. diagnostic using tissue culturing versus (vs) the DTT culturing method (table 15). The results from the septic cohort showed that tissue culturing might be superior to DTT culturing. 25% of the cases were not detected as septic by DTT culturing. This confirms the results from Randau et al. 2021, where he proposed that the pathogen detection based on DTT cultures was less sensitive than bacterial cultures from intraoperative tissue biopsies [124]. However, DTT cultivation was able to identify pathogens in three (#48, #94, #53) of the aseptic cases (fig. 10B), but these findings were not confirmed using tissue cultures. Patient #48 showed a positive culture of *S. aureus*, while *S. agalactiae* was found in patient #94. In patient #53 *C. avidium*, an anaerobia was identified using DTT cultures. As anaerobia are more difficult to culture, there could be a low-grade infection that was not detected by the std. microbiology using tissue cultures. The use of DTT may have destabilized the biofilm [121],

leading to a release of the bacteria on the implant. In patient #48 and #53 the CRP value was also slightly increased with 10.1 mg/l (#48) and with 23.9 mg/l (#53). In patient #94, no pre-operative CRP was examined, which is why no statement can be made in this regard. However, the patient had a relatively short implantation time of 6 months. Since *S. agalactiae* is primarily responsible for early and delayed PJIs [229], a possible CN-PJI could also be identified here. Furthermore, patient #94 was the only one in whom the detection of bacteria was positive in both DTT cultivation and NGS. In 67% (20/30) of the samples, the same pathogen was identified by both techniques. The literature describes that CN-PJI can occur in up to 7% of cases [68]. In this thesis, the number of CN-PJI would be 8% (3/38) and would, therefore, be consistent with the literature. To analyse the predictive value of DTT culturing as a diagnostic method for PJI, I calculated the sensitivity (DTT culturing) against the 100%-specificity (tissue culturing). The comparison revealed a sensitivity of 75% and a specificity of 92% for the microDTTect device while using DTT cultures and the results from tissue culture as a control. In other studies, it was already shown that bacterial biofilms can be destabilized by DTT and were subsequently cultivable [121]. In the study from Drago et al., DTT was compared with sonication and displayed equivalent results; another study also described [123]. Through my thesis, it was again shown that DTT cultivation could detect possible CN-PJIs. Whether these were actual CN-PJIs is ultimately difficult to validate. Further studies should be performed to improve the diagnosis of PJIs, which would further reduce the number of CN-PJIs.

As NGS is described as a proper alternative technique in diagnosing PJI [116, 230], I compared the tissue culturing method from the std. microbiological diagnostic, with the DNA that was isolated from microDTTect solution and analyzed with NGS. The results showed (table 16) that bacterial DNA could not be detected in 29% of the samples from the septic cohort. These results indicate that tissue culture might be superior to NGS-based pathogen detection. In contrast, bacterial DNA was detected in 21% of the aseptic cases. Only in one case (#94) could a pathogen be detected using DTT cultivation but not with the tissue cultivation technique, which indicated a possible CN-PJI. In the other seven cases, no cultivation method could identify a pathogen. Furthermore, only one case (#13) showed an elevated CRP of 10 mg/l. I, therefore, propose that these samples were contaminated during the isolation process. Due to the high sensitivity of NGS, it is susceptible for contamination and false-positive results [231, 232]. In addition, a meta-analysis showed that the sensitivity and specificity of NGS are lower than previously reported [233]. To analyze the sensitivity and specificity of NGS from DTT solution, I calculated the sensitivity (NGS) against the 100%- specificity (tissue culturing), using the std. diagnostic microbiology tissue culturing as reference. The comparison showed a sensitivity of 71% and a specificity of 79% for NGS from the DTT solution. This was lower than the sensitivity and specificity of the DTT-based

bacteria cultures. However, NGS can detect bacteria that are difficult to culture, the pathogen spectrum identified in std. microbiology using tissue cultures and NGS from DTT solution was similar in 30% (11/37) for the septic cases. Interestingly, NGS was able to detect more polymicrobial infections compared to the other cultivation techniques. Furthermore, the characterization of polymicrobial infections might be easier and more precise [104, 234]. As in polymicrobial cultures, faster-growing bacteria can overgrow slower-growing bacteria [235], only one bacteria can be identified.

It is possible that other factors could have influenced and limited the results of these experiments. First of all, only a low number of polymicrobial and anaerobic infections were included according to the std. microbiological diagnostic using tissue cultures. This concludes the possible superiority of NGS compared to the routine microbiological diagnostic difficult. Furthermore, the NGS-based detection method did not include the examination of RNA. NGS for DNA only detects the presence of pathogens [236-238]. RNA would indicate the activity of a pathogen. However, using the microDTTect device, it was impossible to isolate RNA from the samples, as it is processed at RT for 1h after the explantation of the implant, possible RNA components may be destroyed.

These results highlighted the importance of the std. microbiological diagnostic using tissue culture, as it is a well-established method to diagnose a PJI. So far, microDTTect analysis by DTT cultivation and NGS showed promising results, but they were not superior to the std. microbiological diagnostic using tissue cultures for the identification of bacteria. Comparing the DTT culturing with the tissue culturing, a few samples showed different results, which might indicate CN-PJI in 8% (3/38) of the aseptic cohort. Therefore, establishing a new and more reliable methodology to facilitate the detection of PJIs is essential. Using a specific indicator for a more secure PJI analysis could help to improve the treatment of PJI patients. Therefore, a biomarker for PJI identification would be helpful in questionable cases.

#### **4.4 Parts of the terminal complement pathway can be used as a biomarker for the diagnosis of PJI**

The identification of a PJI is based on the MSIS criteria (fig. 2) [27]. Here, the patient had at least one of the major criteria or a score over six from the minor criteria when classified as septic for my study. The interaction of serum markers, histology, microbiology, and anamneses already achieves good results for diagnosing a PJI. Especially the std. microbiological diagnostic using tissue cultures work very accurately, as shown in this thesis (see 4.3). Nevertheless, this thesis also shows that the typical serum markers like WBC and CRP were vulnerable as a biomarker for PJI. These markers can be easily influenced by other factors [147]. Another biomarker proposed

to improve the identification of a PJI and is also part of the minor MSIS criteria is  $\alpha$ -defensin [27].  $\alpha$ -defensin is one of the most promising published biomarkers for PJI so far [147, 148]. The detection of  $\alpha$ -defensin in synovial fluid of potential PJI patients by an ELISA showed a sensitivity of 100% and a specificity of 95% [29, 152-154]. Unfortunately,  $\alpha$ -defensin was also detected in the presence of metallosis and crystallopathies in the synovial fluid [160] [33, 159]. A study from 2020 announced the use of the  $\alpha$ -defensin test in the routine analysis of a PJI to test cases in which PJI was not diagnosed directly [31]. It was suggested that the  $\alpha$ -defensin biomarker should only be used as a supplementary method [108] in unclear cases [31]. The need for alternative biomarkers to support the detection of PJI or other identification is still needed. In cancer diagnosis, identifying a specific protein to classify a tumor is performed mainly by immunohistochemistry in the tissue and is the gold standard in this field [239]. Using immunohistochemistry, proteins can be visualized in tissue by specific fluorescent antibodies [240, 241]. In oncology, the immunohistochemistry technique is already being used for precise analysis and a substitute for other methods, as it is faster and less expensive. [242]. This led to the second aim of this thesis, as I wanted to detect different proteins by immunohistological staining as an alternative biomarker for PJI.

For this purpose, the periprosthetic tissue of patients from the septic and aseptic PJI was stained immunohistologically with fluorescence antibodies against different proteins. As  $\alpha$ -defensin has been described to be the most promising biomarker for synovial fluid-based diagnosis so far [147, 148], the periprosthetic tissue was first stained with an antibody against  $\alpha$ -defensin. I found  $\alpha$ -defensin in the septic as well as the aseptic tissue. Using quantitative analysis of tissue staining, I observed no statistical difference between both cohorts. As mentioned before,  $\alpha$ -defensin detection was not specific in cases of metallosis, where false-positive results were described [159]. The abrasive wear particles in the aseptic tissue might have interfered with the detection of  $\alpha$ -defensin in my cohort. It cannot be ruled out that the metal particles have an auto-fluorescence, as this was already described for plastic particles [243, 244]. The auto-fluorescence would lead to false-positive results.

The analysis of a predictive value of  $\alpha$ -defensin as a biomarker for PJI showed an AUC at 0.68 (fig. 12C). According to the classification of biomarkers [146] (fig. 4), the immunohistological staining for  $\alpha$ -defensin would be classified to be a fair biomarker for the identification of infections in periprosthetic tissue. In this thesis, I calculated a sensitivity of 55.56 % and a specificity of 88.89 % for immunohistological  $\alpha$ -defensin staining. The tissue staining showed less sensitivity (100%) and specificity (95%) than the ELISA from synovial fluid for the detection of  $\alpha$ -defensin [29, 152-154]. As  $\alpha$ -defensin was also only rarely detectable in the septic tissue and seen in the

aseptic tissue, I propose that  $\alpha$ -defensin staining as a biomarker for PJI exhibits a low predictive value.

During the histopathological diagnostic for identifying a PJI, macrophages and neutrophils are used as a marker for inflammation and as an indicator for potential infection [49, 50]. During the cellular host defense, the recruitment of macrophages to the infected area is an essential process in the defense against bacteria [50]. In routine histopathology, CD68 is used as a marker to detect macrophages [135]. CD68 expression in macrophages is triggered upon an inflammatory response induced by ,e.g., bacterial lipopolysaccharide (LPS) or the inflammatory cytokine interferon- $\gamma$  (IFN- $\gamma$ ) [136]. To date, CD68 has been used as a biomarker to identify tumor-associated macrophages (TAMs) [245, 246]. As a biomarker for the detection of PJI, it was only rarely described to date [33]. Therefore, septic and aseptic tissue were stained with an antibody for CD68. I was able to detect CD68 in septic as well as in aseptic tissue. The statistical significance showed no difference between both cohorts (fig. 13B). It is assumed that macrophages are recruited into the tissue with abrasion particles in cases of aseptic implant loosening [133]. Macrophages phagocytose the abrasion particles, which leads to the secretion of pro-inflammatory cytokines in the respective tissue [247, 248]. Due to this, macrophages are predominant cells in particle-induced osteolysis [54, 55]. In septic tissue, macrophages are part of the first line of defense against bacteria, as they remove the pathogens by phagocytosis and recruit other immune cells to the infected area. Therefore, they have been suggested as an indicator of septic complications [186]. The ROC curve showed an AUC of 0.73 (fig. 13C), based on the biomarker classification [146] (fig. 4); this corresponds to an acceptable biomarker. The sensitivity of CD68 was 100%, while the specificity was 66%. This indicated a low predictive value of CD68 staining as a biomarker for PJI.

On the one hand, neutrophils are found in increased amounts under inflammatory pathological conditions. They are involved in processes such as eliminating bacteria; on the other hand, they are essential in repairing tissue [49, 50]. CD66b is a marker for neutrophils and is located in granules. It is expressed by granulocytes and helps in the aggregation of neutrophils [140, 141]. Therefore, I investigated if CD66b was detectable using a specific antibody for immunohistological staining of septic and aseptic periprosthetic tissue. I found CD66b in septic and in aseptic periprosthetic tissue; a statistical significance between both cohorts could be observed (fig. 14B). This confirms previous reports in the literature, where it was described that CD66b was mainly detected in septic tissue of infected patients [139]. Unfortunately, CD66b was also detectable in aseptic periprosthetic tissue. The literature describes that nanoparticles generated by wear from implants materials can recruit neutrophils to immigration into the tissue. One study showed that a sterile inflammatory response to implant wear debris in mice resulted in the recruitment of active

neutrophils into the tissue [56]. Likewise, neutrophils bind to sterile implant surfaces after implantation and release extracellular DNA, called NETosis (neutrophil extracellular traps) [57]. Neutrophils can generate extracellular fibers to enhance their antimicrobial properties by releasing NETs, killing bacteria extracellularly [249]. Therefore, my observations need to be interpreted with care, and further research on the presence of CD66b in tissue from aseptic loosening patients should be performed. For the analysis of the predictive value of CD66b as a biomarker for PJI, the ROC curve showed an AUC of 0.65 (fig. 14C), based on the biomarker classification [146] (fig. 4) this corresponds to a fair biomarker. The sensitivity of CD66b was 63%, while the specificity was 72%.

The complement pathway is an important defense mechanism of the human body against bacteria. An essential function of the complement pathway is the labeling of pathogens for phagocytosis (opsonization), the formation of pro-inflammatory mediators (anaphylatoxin), and the lysis of pathogens by the membrane attack complex (MAC), activated by the terminal complement pathway [161]. There are three different activation ways of the complement pathway, all leading to the activation of the C3 convertase, with the subsequent cleavage of C5 [165, 166]. The terminal complement pathway gets initiated by the cleavage of C5 [162] and forms the MAC through the combination of C6 to C9 [167]. Therefore, the periprosthetic tissue of septic and aseptic periprosthetic tissue samples were immunohistochemically stained with antibodies against C3 (fig. 15A), C5 (fig. 15D), and C9 (fig. 15G). I detected the proteins C3, C5, and C9 in the periprosthetic tissue of PJI samples. In comparison, there was significantly less staining for C3, C5, and C9 in the aseptic tissue (fig. 15B, 15E, 15H). The statistical significance for distinguishing between septic and aseptic tissue became stronger the further down the protein was detected in the terminal complement cascade. After the invasion of a pathogen in the human body, the complement pathway gets activated. C3 was cleaved into two fragments, the C3b and the C3a [250]. The C3b is essential for activating macrophages and neutrophils [251], while it also initiates the terminal complement pathway, resulting in the cleavage of C5 [250]. The literature describes that C3 is increased in the presence of insulin resistance and chronic inflammation [252], and C5 is suggested as a biomarker for detecting subclinical atherosclerosis [253]. Both were shown to be detectable in serum levels of patients by using ELISA and Western Blots [253]. In my thesis, C3 and C5 showed no interaction in the tissue, despite comorbidities. The ROC curve showed an AUC value of the C3 with 0.8 and C5 with 0.88 indicated an excellent biomarker using the biomarker classification [146] (fig. 4). Furthermore, C9 showed, with an AUC of 0.94, to be an outstanding biomarker [146]. The sensitivity of C9 was 100%, while the specificity was 89%. C9 was described with the MAC complex as a possible serum biomarker for head injuries [254]. C9 has not yet been investigated as a biomarker for the detection of PJI.

The bacteria are killed by forming pores in the bacterial membrane built up by the MAC complex. The MAC complex consists of multiple C9 proteins [167]. The high number of C9 in the MAC complex might facilitate the detection of immunohistological staining and, therefore, might be superior to C5 and C3.

In this part of my thesis, I screened periprosthetic tissue of septic and aseptic revision cases for possible new biomarkers to detect PJI. My results provide evidence that the detection of C9 with immunohistological staining can allow discriminating a PJI from aseptic failure, suggesting a potential biomarker for the detection of PJI.

#### 4.5 Validation of C9 as a novel biomarker for the identification of PJIs

A biomarker is an essential analytical tool for evaluating biological parameters and can be used to detect and quantify specific indicators that are increased during, e.g., an infection [142]. Using a Biomarker as a diagnostic tool has to go through four main phases defined by the FDA [145]. The first phase consists of the discovery of a potential biomarker. With the previously described chapter, this work demonstrated that C9 proved to be a potential biomarker candidate detecting a PJI. The second phase developing a biomarker as a diagnostic tool is the analytical validation [145]. To use C9 as a biomarker for the detection of PJI by immunohistochemical staining, a larger cohort of 98 samples was examined. The samples were divided into aseptic and septic failure according to the MSIS criteria [27].

Both cohorts (septic and aseptic) were assessed for the presence of C9 in the periprosthetic tissue using immunohistological staining (fig. 16). I detected significantly increased amounts of C9 in the septic tissue compared to the aseptic tissue. This confirms my previous observation of C9 protein being increased in PJI of the TSA cohort (see 4.4). According to the classification of biomarkers [146] (fig. 4), the immunohistological staining for C9 (AUC: 0.84) is an excellent biomarker for the identification of infections in periprosthetic tissue (fig. 16C). While the sensitivity was at 89 % and the specificity was at 75% for C9. Comparing these with the sensitivity (100 %) and specificity (95 %) of the detection of  $\alpha$ -defensin using an ELISA for synovial fluid [29, 152-154], C9 is not as sensitive and specific by identifying a PJI. However, the  $\alpha$ -defensin test is costly [31, 147] as it costs about US\$524.79 per application [31]. Comparatively, the immunohistochemistry technique is already being used for precise analysis in cases of cancer identification, as it is fast and, compared with the ELISA technique, less expensive [242]. On an economic basis, this could support the utility of C9 as a biomarker.

To investigate if other factors could influence the C9 detection I first investigated if the detection, of C9 may be pathogen dependent. For that, I chose five of the most common bacteria during a

PJI (*Staphylococcus* spp. [72], *Streptococcus* spp., *Enterococcus* spp. [72], and *Anaerobia*) [23, 80] (fig. 17). These pathogens can occur during a PJI, either monomicrobial or polymicrobial [255]; therefore, polymicrobial infection samples were also investigated. The septic cohort was subdivided according to these criteria and was assessed for the presence of C9 (fig. 17). I found C9 present in all PJI tissues independent from the pathogen family, and no significant difference was analyzed. The literature describes that gram-negative bacteria can resist lysis induced by the MAC complex. As the transmembrane region of a MAC pore is only <10 nm in size [256, 257], the thick cell wall in comparison to the gram-positive bacteria could protect from MAC-induced cell lysis [258]. Because of that, maybe C9 would be less detectable in the presence of gram-negative bacteria as it is part of the MAC complex. Whether this applies as a speculation, as in my cohort, only two patients suffered from a PJI caused by gram-negative bacteria, therefore this cannot be verified. Future work should compare the detection of C9 in periprosthetic tissue from patients that suffer from PJI caused by gram-negative and gram-positive bacteria. In summary, the quantification of the C9 immunostaining showed no pathogen-dependent difference for C9. Therefore, my results indicate that the C9 detection in periprosthetic tissue by immunohistological staining can be performed by pathogen independently with reliable results.

As CRP activates the complement cascade (40), I assumed that the CRP value would correlate with the amount of C9 staining in the periprosthetic tissue. Therefore, the measurement of red fluorescence indicating C9 was plotted against the respective CRP values (fig. 18A). The statistical analysis showed no correlation between these two factors. Suggesting that the serum CRP level does not predict the amount of C9 in the tissue, and therefore, might not be a direct regulator of C9 protein expression at the site of infection. This observation also suggests that high-grade infections with high CRP levels might show similar amounts of C9 as low-grade infections, indicating a good probability to facilitate the problematic diagnose of low-grade infections.

Furthermore, I wanted to investigate if the implantation time-correlated with the amount of C9 in the tissue (fig. 18 B+C). Again, the values for the red fluorescence in the septic tissues were plotted against the implantation time for each patient using linear regression. Again, no significant correlation was observed between both parameters. This observation indicates that generated wear debris and early or late PJIs do not influence on the detection of C9 in the tissue.

It is proposed that autoantibodies such as in rheumatoid arthritis (RA) can activate the complement system [259-261]. Other Biomarkers showed a cross-reactivity in wear particles [159] and crystallopathies [160]. Therefore, I investigated possible cross-reactivity with typical inflammatory joint conditions such as chondrocalcinosis (CC), RA, and wear particles (fig. 19A) by staining the periprosthetic tissue for C9. I analyzed a statistical difference between the PJI cohort and CC, as well as against RA. I proved that the detection of C9 in the presence of CC and RA could well

distinguish septic from aseptic tissue. The AUC of CC was 0.78, and RA had an AUC of 0.77. Using the biomarker classification [146] (fig. 4), C9 would still be an acceptable biomarker in the presence of these joint diseases.

No significant difference was calculated between the septic and the abrasive wear using the aseptic periprosthetic tissue with abrasive wear. Similar to the  $\alpha$ -defensin test, C9 also showed cross-reactivity in the presence of abrasion material [33, 159]. As mentioned before, the reason could be that the human immune system perceives the implant itself as a foreign body. A previous study demonstrated activation of the complement system after primary hip implants [171]. Also, in other cases, it could be shown that abrasion particles can trigger typical inflammatory signals like infiltration of macrophages and neutrophils to the site of inflammation [54, 55] [56, 57]. Therefore, it cannot be excluded that abrasion particles may also influence parts of the complement system and, therefore, the detection of C9. Furthermore, it cannot be ruled out that the particles have an auto-fluorescence, as this was already described before (seen 4.4). Calculating the AUC of 0.62 a C9 would be a fair biomarker [146] in the presence of abrasive wear.

Other biomarkers, e.g.,  $\alpha$ -defensin, are suggested as a supplementary method [108] is unclear cases [31]. I would also propose that the C9 biomarker should not be used as a stand-alone technique but could be used in histopathology as a supplementary method to decrease the number of CN-PJIs.

I am aware that my research may have some limitations. The tissue was not collected standardized. The problem with this collection method performed in this clinic is that the samples were not collected after either quality control or quality assurance. This may impact the quality of the specimens, which affects the diagnosis [262, 263]. Another problem could be that the location of the collected periprosthetic tissue was not clearly defined. If the inflammation was localized to specific sites around the prosthesis, the detection of C9 might not be meaningful because the tissue was not collected at the correct site. Another limitation is that only a few gram-negative bacteria were tested. It would also be helpful to test a higher number of different bacterial families and investigate a possible difference between gram-positive and gram-negative bacteria for the detection of C9. Another limitation of my thesis is that possible CN-PJIs in the aseptic cohort cannot be excluded entirely. This could lead to the detection of C9 in aseptic classified tissue, leading to false-positive results for the detection of C9 in the aseptic cohort. Further experiments will be needed to validate the possible use of C9 immunostaining for more reliable detection of CN-PJIs and low-grade infections.

In this thesis, I provided the basis for the developing a novel biomarker for a possible more accurate detection of PJI to decrease the number of CN-PJIs. Due to the high AUC value and the

high sensitivity and specificity of C9 immunostaining, I propose using this biomarker in the unclear diagnosis of PJI to secure the treatment suggestion.

## 5. Conclusion and Future work

My research aims were separated into two parts; the first part aimed to compare the diagnostic results of the commercially available microDTTect (DTT) device with routine PJI diagnostics and next-generation sequencing (NGS) from DTT-treated samples. The purpose of the second part was to analyze a potential novel biomarker for the identification of PJI.

A combination of clinical and laboratory findings was used for the diagnosis of PJI. The MSIS criteria were applied to diagnose the PJI and served as the reference for the research applications. Several factors can influence the sensitivity and specificity of the diagnosis using the MSIS criteria. Therefore, I investigated whether using the microDTTect device would lead to an increase in diagnostic security. DTT is thought to destabilize the bacterial biofilm on implants, allowing a higher efficacy of bacteria isolation and, therefore, a more detailed analysis of the pathogen spectrum. I compared the results of the DTT cultures and the NGS from DTT-treated samples with the results to the std. microbiological diagnostic using tissue cultures. The DTT pretreated bacteria cultivation and the NGS from DTT treated explants were not superior to the std. microbiological diagnostic using tissue cultures for the identification of a pathogen. However, using the microDTTect device, I detected possible CN-PJIs in 8% of the aseptic samples. Whether this 8% of aseptic samples were indeed CN-PJI is difficult to validate in the end, but further research should be performed to improve the diagnosis of PJI and reduce the number of CN-PJIs. This fact further highlights the necessity of a biomarker to identify questionable PJI cases to facilitate a secure diagnosis.

In the second part of my thesis, I focused on analyzing possible new biomarker candidates to facilitate the identification of a PJI. The literature had proposed  $\alpha$ -defensin detection by ELISA in synovial fluid of PJI patients as one of the most promising biomarkers for PJI identification. However, due to the cross-reactivity of  $\alpha$ -defensin in immunostaining with wear debris and crystallopathies in my cohort. The use of  $\alpha$ -defensin as a potential biomarker for PJI was not advisable. Furthermore, due to the high cost of the  $\alpha$ -defensin ELISA test, an alternative biomarker is needed. In tumor research, the use of fluorescent antibodies to detect specific proteins is the gold standard. Thus, immunohistochemical staining was used to analyze the periprosthetic tissue for specific proteins that could help an easier detection of PJI. The aseptic and septic endoprosthetic implant revision cohort detected the proteins CD68, CD66b, C3, C5, and C9. Using quantitative analysis, I demonstrated that C9 was the most promising biomarker candidate due to its high sensitivity and specificity for identifying PJI patients. By using a larger cohort, the analytical validation of the biomarker was performed. The biomarker classification proved that C9 was an excellent biomarker for PJI identification using immunohistological staining of periprosthetic tissue.

The detection capacity was not influenced by pathogen type, CRP value, and implantation time. Most importantly, I demonstrated that C9 could be used as a biomarker to detect PJI in the presence of chondrocalcinosis and rheumatoid arthritis, indicating that other inflammatory joint conditions do not influence the sensitivity and specificity of C9.

To use C9 as a biomarker for clinical identification of PJI and giving treatment advice, further research is needed. No distinction between low-grade and high-grade PJIs was made in this work. It would be interesting to investigate whether the detection of C9 is more efficient in high-grade than in low-grade infections. I investigated only the presence of C9 in periprosthetic tissue samples. Furthermore, the activity of C9 was not detected. It would be interesting for further research if the activity of C9 differs in the aseptic and septic periprosthetic tissue.

The identification of PJIs is already very well-identified by the MSIS criteria. In this thesis, it could be shown that std. microbiological diagnosis by tissue culture is a very secure method to diagnose a PJI. Nevertheless, possible CN-PJIs were detected using the microDTTect device. The C9 biomarker has the potential to reduce the number of CN-PJIs. The high sensitivity and specificity of the C9 immunohistological staining showed that C9 is an excellent biomarker candidate for identifying a PJI. C9 should not be used as a stand-alone technique, but it should be used in unclear PJI cases to secure the treatment suggestions.

## 6. Supplement

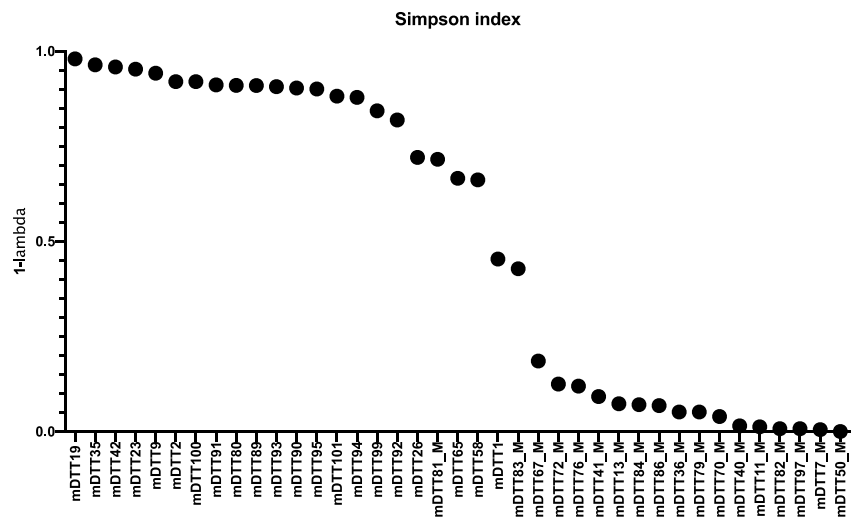


**Figure 20 Diversity of microbial communities in DTT samples as indicated by the Simpson index**  
 Using the Simpson diversity index (fig. 6) the samples were classified as monomicrobial infection (<0.25) or polymicrobial infection (<0.8) (fig. 6). Cases that had a Simpson index of 0.41 – 0.73 had one dominated pathogen but also high but high amounts of other bacterial DNA were also found.

## Abbreviations

°C	Degree Celcius
μ	Mikro
AF	Alexa Fluor
Ag	Silver
Aqua dest	water
AUC	Area under the curve
BHI	Brain Heart Infusion Broth
BIM	biofilm-related implantat malfunctions
bp	base pairs
BSA	Bovine serum albumin
C. avidium	Cutibacterium avidium
cDNA	Complementary deoxyribonucleic acid
CFU	colony forming units
CN-PJI	cultur-negativ periprosthetic joint infection
CoNS	Coagulase-negative
CXCL	CXC-chemokine ligand
DAPI	4',6-Diamidino-2-phenylindole dihydrochloride
DH2O	distilled water
DMSO	Dimethylsulfoxid
DNA	deoxiribonucleic acid
dNTP	Deoxynucleotide
DTT	Dithiothreitol
E coli	Escherichia coli
E. faecalis	Enterococcus faecalis
ELISA	enzyme-linked immunosorbent assay
FCS	Fetal calf serum
GFP	Green Fluorescent protein
GFP	Gravity
h	hours
HG-PJI	high-grade periprosthetic joint infection
kb	kilo bases
LB	Lysic Broth

LB	Liter
LG-PJI	low-grade periprosthetic joint infection
m	Milli
M	Molar
MAC	Membran Attack complex
min	Minutes
mRNA	messenger RNA
MRSA	Methicillin-resistant <i>Staphylococcus aureus</i>
MSSA	Methicillin-susceptible <i>Staphylococcus aureus</i>
NET	Neutrophil extracellular Traps
NGS	Next-Generation Sequencing
NGS	Nano
OA	Osteoarthritis
OD	optical density
<i>P. aeruginosa</i>	<i>Propionibacterium aeruginosa</i>
PCR	Polymerase Chain Reaction
PE	Polyethylen
PET	Polyethylenerephthalat
PFA	Paraformaldehyde
PJI	periprosthetic joint infection
PMEDM	power mixed electrical discharge machining
QS	quorum sensing
RIPA	Radioimmunoprecipitation Assay Puffer
RNA	ribonucleic acid
ROC	receiver operating characteristics
ROS	reactive oxygen species
rpm	revolutions per minute
RT	Room Temperatur
RT-PCR	Reverse Transcriptase PCR
s	seconds
<i>S. aureus</i>	<i>Staphylococcus aureus</i>
<i>S. epidermidis</i>	<i>Staphylococcus epidermidis</i>
SEM	Scanning electron microscopy
TEP	Totalendoprosthesis

Ti	Titan
TLR	toll-like receptor
TNF	tumor necrosis factor
TSP	Tryptic Soy Broth
UV	Ultraviolet
WAIOT	World Association against Infection in Orthopedics and Trauma

## List of Figures

<b>Figure 1 Structure of a hip and knee endoprosthesis</b> .....	10
<b>Figure 2 The updated 2018 definition for PJI from the Musculoskeletal Infection Society (MSIS)</b> . ...	13
<b>Figure 3 The five steps leading to the biofilm formation</b> .....	17
<b>Figure 4 Biomarker classification based on the AUC value</b> .....	21
<b>Figure 5 A scheme of the complement system</b> .....	23
<b>Figure 6 The analytical process in a flow-chart</b> .....	37
<b>Figure 7 Demographic data of the patients in the septic and aseptic revision cohort</b> .....	45
<b>Figure 8 Pathogen spectrum of the patients from the septic cohort</b> .....	46
<b>Figure 9 WBC- und CRP-values of the patients in the septic and aseptic revision cohort</b> .....	48
<b>Figure 10 The correlation between the three used methods were in some results distinct</b> .....	51
<b>Figure 11 Pathogens identified from microDTTect samples are typically also identified by routine diagnostic</b> .....	53
<b>Figure 12 Immunohistological staining of <math>\alpha</math>-defensin in periprosthetic tissue shows no significant difference between the septic and the aseptic cohort</b> .....	55
<b>Figure 13 Immunohistological staining of CD68 in periprosthetic tissue shows no significant difference between the septic and the aseptic cohort</b> .....	57
<b>Figure 14 Immunohistological staining of CD66b in periprosthetic tissue shows a significant difference between the septic and the aseptic cohort</b> .....	59
<b>Figure 15 Immunohistological staining of the terminal complement pathway (C3, C5, C9) in periprosthetic tissue shows a significant difference between the septic and the aseptic cohort</b> ...	61
<b>Figure 16 Significant increase of C9-antibody in septic periprosthetic tissue</b> .....	63
<b>Figure 17 No pathogen-dependent C9 detection was analyzed</b> .....	65
<b>Figure 18 No correlation between the amount of red fluorescence of C9 between the CRP value, implantation time and infection classification</b> .....	66
<b>Figure 19 Significant increase of the detection of C9 in periprosthetic tissue with infection compared to tissue with rheumatoid arthritis and chondrocalcinosis</b> .....	69
<b>Figure 20 Diversity of microbial communities in DTT samples as indicated by the Simpson index</b>	86

## List of Tables

<i>Table 1: Biochemical and chemical reagents</i> .....	26
<i>Table 2: Consumables</i> .....	27
<i>Table 3: Equipment</i> .....	28
<i>Table 4: Primer for the first and second nested PCR</i> .....	30
<i>Table 5 Primer for the Illumina-Next-Generation Sequencing</i> .....	30
<i>Table 6: Antibodies</i> .....	34
<i>Table 7: IgG Control</i> .....	34
<i>Table 8: Secondary Fluorescence Antibodies</i> .....	35
<i>Table 9: Buffer and media</i> .....	35
<i>Table 10: Reagents for the first and second reaction mix of the nested PCR</i> .....	38
<i>Table 11: Protocol first and second reverse transcription using Takara</i> .....	39
<i>Table 12: Reaction mix for the third amplification</i> .....	39
<i>Table 13 Demographic data</i> .....	44
<i>Table 14 Comorbidities</i> .....	44
<i>Table 15 Concordance of standard microbiology diagnostic vs. DTT culturing based identification of infection</i> .....	49
<i>Table 16: Concordance of standard microbiology diagnostic vs. NGS from DTT solution</i> .....	50
<i>Table 17 Biometric characteristics of the study population</i> .....	67

## 7. References

1. Kurtz, S., et al., *Projections of primary and revision hip and knee arthroplasty in the United States from 2005 to 2030*. J Bone Joint Surg Am, 2007. **89**(4): p. 780-5.
2. Cram, P., et al., *Total knee arthroplasty volume, utilization, and outcomes among Medicare beneficiaries, 1991-2010*. Jama, 2012. **308**(12): p. 1227-36.
3. Kurtz, S.M., et al., *Future young patient demand for primary and revision joint replacement national projections from 2010 to 2030*. Clin Orthop Relat Res, 2009. **467**(10): p. 2606-12.
4. Deutschland, E.E., *The German Arthroplasty Registry*. 2021.
5. Jin, W. and P.K. Chu, *Orthopedic Implants*. 2019: p. 425-439.
6. Fisher, J. and D. Dowson, *Tribology of total artificial joints*. Proc Inst Mech Eng H, 1991. **205**(2): p. 73-9.
7. Sutula, L.C., et al., *The Otto Aufranc Award. Impact of gamma sterilization on clinical performance of polyethylene in the hip*. Clin Orthop Relat Res, 1995(319): p. 28-40.
8. Malhotra, R., et al., *A Comparison of Bacterial Adhesion and Biofilm Formation on Commonly Used Orthopaedic Metal Implant Materials: An In vitro Study*. Indian journal of orthopaedics, 2019. **53**(1): p. 148-153.
9. Nuss, K.M.R. and B. von Rechenberg, *Biocompatibility issues with modern implants in bone - a review for clinical orthopedics*. The open orthopaedics journal, 2008. **2**: p. 66-78.
10. Morehead, J.M. and G.R. Holt, *Soft-tissue response to synthetic biomaterials*. Otolaryngol Clin North Am, 1994. **27**(1): p. 195-201.
11. Boss, J.H., et al., *The relativity of biocompatibility. A critique of the concept of biocompatibility*. Isr J Med Sci, 1995. **31**(4): p. 203-9.
12. Sanchez-Sotelo, J., *Total shoulder arthroplasty*. Open Orthop J, 2011. **5**: p. 106-14.
13. Hallab, N.J. and J.J. Jacobs, *Biologic effects of implant debris*. Bull NYU Hosp Jt Dis, 2009. **67**(2): p. 182-8.
14. Sousa, A., et al., *Economic Impact of Prosthetic Joint Infection - an Evaluation Within the Portuguese National Health System*. J Bone Jt Infect, 2018. **3**(4): p. 197-202.
15. Ulrich, S.D., et al., *Total hip arthroplasties: what are the reasons for revision?* International orthopaedics, 2008. **32**(5): p. 597-604.
16. Zimmerli, A.T.a.W., *Diagnosis and Treatment of Implant-Associated Septic Arthritis and Osteomyelitis*. Current Infectious Disease Reports, 2008. **10**: p. 394-403.
17. Fehring, T.K., et al., *Articulating versus static spacers in revision total knee arthroplasty for sepsis. The Ranawat Award*. Clin Orthop Relat Res, 2000(380): p. 9-16.

18. Bozic, K.J., et al., *Patient-related risk factors for postoperative mortality and periprosthetic joint infection in medicare patients undergoing TKA*. Clin Orthop Relat Res, 2012. **470**(1): p. 130-7.
19. Baek, S.-H., *Identification and preoperative optimization of risk factors to prevent periprosthetic joint infection*. World journal of orthopedics, 2014. **5**(3): p. 362-367.
20. Kurtz, S.M., et al., *Prosthetic joint infection risk after TKA in the Medicare population*. Clin Orthop Relat Res, 2010. **468**(1): p. 52-6.
21. Dowsey, M.M. and P.F. Choong, *Obese diabetic patients are at substantial risk for deep infection after primary TKA*. Clin Orthop Relat Res, 2009. **467**(6): p. 1577-81.
22. Liabaud, B., D.A. Patrick, Jr., and J.A. Geller, *Higher body mass index leads to longer operative time in total knee arthroplasty*. J Arthroplasty, 2013. **28**(4): p. 563-5.
23. Tande, A.J. and R. Patel, *Prosthetic joint infection*. Clin Microbiol Rev, 2014. **27**(2): p. 302-45.
24. Seneviratne, C.J., et al., *Effect of culture media and nutrients on biofilm growth kinetics of laboratory and clinical strains of Enterococcus faecalis*. Arch Oral Biol, 2013. **58**(10): p. 1327-34.
25. Bongartz, T., et al., *Incidence and risk factors of prosthetic joint infection after total hip or knee replacement in patients with rheumatoid arthritis*. Arthritis Rheum, 2008. **59**(12): p. 1713-20.
26. Poss, R., et al., *Factors influencing the incidence and outcome of infection following total joint arthroplasty*. Clin Orthop Relat Res, 1984(182): p. 117-26.
27. Parvizi, J., et al., *The 2018 definition of periprosthetic hip and knee infection: an evidence-based and validated criteria*. The Journal of arthroplasty, 2018. **33**(5): p. 1309-1314. e2.
28. Bingham, J., et al., *The alpha defensin-1 biomarker assay can be used to evaluate the potentially infected total joint arthroplasty*. Clin Orthop Relat Res, 2014. **472**(12): p. 4006-9.
29. Deirmengian, C., et al., *Combined measurement of synovial fluid  $\alpha$ -Defensin and C-reactive protein levels: highly accurate for diagnosing periprosthetic joint infection*. J Bone Joint Surg Am, 2014. **96**(17): p. 1439-45.
30. Sigmund, I.K., et al., *Qualitative  $\alpha$ -defensin test (Synovasure) for the diagnosis of periprosthetic infection in revision total joint arthroplasty*. Bone Joint J, 2017. **99-b**(1): p. 66-72.
31. Amanatullah, D.F., et al., *The routine use of synovial alpha-defensin is not necessary*. The Bone & Joint Journal, 2020. **102-B**(5): p. 593-599.

32. Parvizi, J. and T. Gehrke, *Definition of Periprosthetic Joint Infection*. The Journal of Arthroplasty, 2014. **29**(7): p. 1331.
33. Meinshausen, A.K., et al., *The terminal complement pathway is activated in septic but not in aseptic shoulder revision arthroplasties*. J Shoulder Elbow Surg, 2018. **27**(10): p. 1837-1844.
34. Kamme, C. and L. Lindberg, *Aerobic and anaerobic bacteria in deep infections after total hip arthroplasty: differential diagnosis between infectious and non-infectious loosening*. Clin Orthop Relat Res, 1981(154): p. 201-7.
35. Watts, J.C. and F.W. Chandler, *The Surgical Pathologist's Role in the Diagnosis of Infectious Diseases*. Journal of Histotechnology, 1995. **18**(3): p. 191-193.
36. Osmon, D.R., et al., *Diagnosis and Management of Prosthetic Joint Infection: Clinical Practice Guidelines by the Infectious Diseases Society of America*. Clinical Infectious Diseases, 2012. **56**(1): p. e1-e25.
37. Saleh, A., et al., *Serum biomarkers in periprosthetic joint infections*. Bone & Joint Research, 2018. **7**(1): p. 85-93.
38. Prucha, M., G. Bellingan, and R. Zazula, *Sepsis biomarkers*. Clinica chimica acta, 2015. **440**: p. 97-103.
39. Ansar, W. and S. Ghosh, *C-reactive protein and the biology of disease*. Immunologic Research, 2013. **56**(1): p. 131-142.
40. Mold, C., H. Gewurz, and T.W. Du Clos, *Regulation of complement activation by C-reactive protein*. Immunopharmacology, 1999. **42**(1-3): p. 23-30.
41. Pepys, M.B. and G.M. Hirschfield, *C-reactive protein: a critical update*. J Clin Invest, 2003. **111**(12): p. 1805-12.
42. Bereza, P.L., et al., *Identification of silent prosthetic joint infection: preliminary report of a prospective controlled study*. Int Orthop, 2013. **37**(10): p. 2037-43.
43. Zappe, B., et al., *Propionibacterium spp. in prosthetic joint infections: a diagnostic challenge*. Archives of Orthopaedic and Trauma Surgery, 2008. **128**(10): p. 1039-1046.
44. Lamagni, T., *Epidemiology and burden of prosthetic joint infections*. Journal of Antimicrobial Chemotherapy, 2014. **69**(suppl\_1): p. i5-i10.
45. T.N. Peel, K.L.B.a.P.F.C., *Diagnosis and management of prosthetic joint infection*. Curr Opin Infect Dis, 2012. **25**: p. 670-676.
46. Renshaw, A.A., *The relative sensitivity of special stains and culture in open lung biopsies*. Am J Clin Pathol, 1994. **102**(6): p. 736-40.
47. Gupta, E., et al., *HISTOPATHOLOGY FOR THE DIAGNOSIS OF INFECTIOUS DISEASES*. Indian Journal of Medical Microbiology, 2009. **27**(2): p. 100-106.

48. Woods, G.L. and D.H. Walker, *Detection of infection or infectious agents by use of cytologic and histologic stains*. Clin Microbiol Rev, 1996. **9**(3): p. 382-404.
49. Chaplin, D.D., *Overview of the immune response*. J Allergy Clin Immunol, 2010. **125**(2 Suppl 2): p. S3-23.
50. A Murphy, K.M., *Janeway's Immunobiology*. Taylor & Francis Group, 2011. **9**(Taylor & Francis Group): p. 1 - 888.
51. Musso, A.D., K. Mohanty, and R. Spencer-Jones, *Role of frozen section histology in diagnosis of infection during revision arthroplasty*. Postgrad Med J, 2003. **79**(936): p. 590-3.
52. Chalifour, A., et al., *Direct bacterial protein PAMP recognition by human NK cells involves TLRs and triggers  $\alpha$ -defensin production*. Blood, 2004. **104**(6): p. 1778-1783.
53. Ganz, T., et al., *Defensins. Natural peptide antibiotics of human neutrophils*. J Clin Invest, 1985. **76**(4): p. 1427-35.
54. Trindade, M.C., et al., *In vitro reaction to orthopaedic biomaterials by macrophages and lymphocytes isolated from patients undergoing revision surgery*. 2001. **22**(3): p. 253-259.
55. Tuan, R.S., et al., *What are the local and systemic biologic reactions and mediators to wear debris, and what host factors determine or modulate the biologic response to wear particles?* J Am Acad Orthop Surg, 2008. **16 Suppl 1**(Suppl 1): p. S42-8.
56. Jhunjunwala, S., et al., *Neutrophil Responses to Sterile Implant Materials*. PLoS One, 2015. **10**(9): p. e0137550.
57. Vitkov, L., et al., *The initial inflammatory response to bioactive implants is characterized by NETosis*. PLoS One, 2015. **10**(3): p. e0121359.
58. Kanthawang, T., et al., *Diagnostic value of fluoroscopy-guided hip aspiration for periprosthetic joint infection*. Skeletal Radiology, 2021.
59. Punchard, N.A., C.J. Whelan, and I. Adcock, *The Journal of Inflammation*. Journal of Inflammation, 2004. **1**(1): p. 1.
60. Zimmerli, W., A. Trampuz, and P.E. Ochsner, *Prosthetic-joint infections*. N Engl J Med, 2004. **351**(16): p. 1645-54.
61. Baumbach, S.F., et al., *Significant increase of pathogen detection rate by dry arthroscopic biopsies at suspected low-grade infection following total knee arthroplasty: a prospective observational study*. Arch Orthop Trauma Surg, 2018. **138**(11): p. 1583-1590.
62. Trampuz, A. and W. Zimmerli, *Prosthetic joint infections: update in diagnosis and treatment*. Swiss Med Wkly, 2005. **135**(17-18): p. 243-51.
63. Li, C., N. Renz, and A. Trampuz, *Management of Periprosthetic Joint Infection*. Hip Pelvis, 2018. **30**(3): p. 138-146.

64. Del Pozo, J.L. and R. Patel, *Clinical practice. Infection associated with prosthetic joints*. N Engl J Med, 2009. **361**(8): p. 787-94.
65. Romanò, C.L., et al., *The W.A.I.O.T. Definition of High-Grade and Low-Grade Peri-Prosthetic Joint Infection*. J Clin Med, 2019. **8**(5).
66. Bozhkova, S., et al., *The W.A.I.O.T. Definition of Peri-Prosthetic Joint Infection: A Multi-center, Retrospective Validation Study*. J Clin Med, 2020. **9**(6).
67. Beswick, A.D., et al., *What proportion of patients report long-term pain after total hip or knee replacement for osteoarthritis? A systematic review of prospective studies in unselected patients*. BMJ Open, 2012. **2**(1): p. e000435.
68. Berbari, E.F., et al., *Culture-Negative Prosthetic Joint Infection*. Clinical Infectious Diseases, 2007. **45**(9): p. 1113-1119.
69. Ehrlich, G.D., et al., *Culture negative orthopedic biofilm infections*. Vol. 7. 2012: Springer Science & Business Media.
70. Jacovides, C.L., et al., *Successful identification of pathogens by polymerase chain reaction (PCR)-based electron spray ionization time-of-flight mass spectrometry (ESI-TOF-MS) in culture-negative periprosthetic joint infection*. J Bone Joint Surg Am, 2012. **94**(24): p. 2247-54.
71. Portillo, M.E., et al., *Prosthesis failure within 2 years of implantation is highly predictive of infection*. Clinical orthopaedics and related research, 2013. **471**(11): p. 3672-3678.
72. Nair, P., V. Bhat, and M.S. Vaz. *Prosthetic joint infections-a clinico-microbiological perspective: Review article*. 2014.
73. Jensen, A.G., et al., *Risk factors for hospital-acquired Staphylococcus aureus bacteremia*. Arch Intern Med, 1999. **159**(13): p. 1437-44.
74. Jacobsson, G., et al., *The epidemiology of and risk factors for invasive Staphylococcus aureus infections in western Sweden*. Scand J Infect Dis, 2007. **39**(1): p. 6-13.
75. Fey, P.D. and M.E. Olson, *Current concepts in biofilm formation of Staphylococcus epidermidis*. Future Microbiol, 2010. **5**(6): p. 917-33.
76. Vuong, C., et al., *Regulated expression of pathogen-associated molecular pattern molecules in Staphylococcus epidermidis: quorum-sensing determines pro-inflammatory capacity and production of phenol-soluble modulins*. Cell Microbiol, 2004. **6**(8): p. 753-9.
77. Marculescu, C.E. and J.R. Cantey, *Polymicrobial Prosthetic Joint Infections: Risk Factors and Outcome*. Clinical Orthopaedics and Related Research, 2008. **466**(6): p. 1397.
78. Cobo, J., et al., *Early prosthetic joint infection: outcomes with debridement and implant retention followed by antibiotic therapy*. Clin Microbiol Infect, 2011. **17**(11): p. 1632-7.

79. Peel, T.N., et al., *Early onset prosthetic hip and knee joint infection: treatment and outcomes in Victoria, Australia*. J Hosp Infect, 2012. **82**(4): p. 248-53.
80. Shah, N.B., et al., *Anaerobic prosthetic joint infection*. Anaerobe, 2015. **36**: p. 1-8.
81. Piper, K.E., et al., *Microbiologic diagnosis of prosthetic shoulder infection by use of implant sonication*. Journal of clinical microbiology, 2009. **47**(6): p. 1878-1884.
82. Zeller, V., et al., *Propionibacterium acnes: An agent of prosthetic joint infection and colonization*. Journal of Infection, 2007. **55**(2): p. 119-124.
83. Pulido, L., et al., *Periprosthetic Joint Infection: The Incidence, Timing, and Predisposing Factors*. Clinical Orthopaedics and Related Research, 2008. **466**(7): p. 1710-1715.
84. Moran, E., et al., *Guiding empirical antibiotic therapy in orthopaedics: The microbiology of prosthetic joint infection managed by debridement, irrigation and prosthesis retention*. J Infect, 2007. **55**(1): p. 1-7.
85. Peel, T.N., et al., *Microbiological aetiology, epidemiology, and clinical profile of prosthetic joint infections: are current antibiotic prophylaxis guidelines effective?* Antimicrob Agents Chemother, 2012. **56**(5): p. 2386-91.
86. Zmistowski, B., et al., *Prosthetic joint infection caused by gram-negative organisms*. J Arthroplasty, 2011. **26**(6 Suppl): p. 104-8.
87. Römling, U. and C. Balsalobre, *Biofilm infections, their resilience to therapy and innovative treatment strategies*. J Intern Med, 2012. **272**(6): p. 541-61.
88. Murray, J.L., et al., *Mechanisms of synergy in polymicrobial infections*. J Microbiol, 2014. **52**(3): p. 188-99.
89. Hansen, M.C., R.J. Palmer, and D.C. White, *Flowcell culture of Porphyromonas gingivalis biofilms under anaerobic conditions*. J Microbiol Methods, 2000. **40**(3): p. 233-9.
90. Hawser, S.P. and L.J. Douglas, *Biofilm formation by Candida species on the surface of catheter materials in vitro*. Infect Immun, 1994. **62**(3): p. 915-21.
91. Vasudevan, R., *Biofilms: Microbial Cities of Scientific Significance*. Journal of Microbiology & Experimentation, 2014. **1**(3).
92. Donlan, R.M., *Biofilm Formation: A Clinically Relevant Microbiological Process*. Clinical Infectious Diseases, 2001. **33**(8): p. 1387-1392.
93. Donlan, R.M., *Biofilms: microbial life on surfaces*. Emerg Infect Dis, 2002. **8**(9): p. 881-90.
94. Garibaldi, R.A., et al., *Meatal colonization and catheter-associated bacteriuria*. N Engl J Med, 1980. **303**(6): p. 316-8.
95. Boháčová, M., et al., *Quantitative evaluation of biofilm extracellular DNA by fluorescence-based techniques*. Folia Microbiologica, 2019. **64**(4): p. 567-577.

96. Flemming, H.-C. and J. Wingender, *The biofilm matrix*. Nature Reviews Microbiology, 2010. **8**(9): p. 623-633.
  97. Rabin, N., et al., *Biofilm formation mechanisms and targets for developing antibiofilm agents*. Future Med Chem, 2015. **7**(4): p. 493-512.
  98. Hausner, M. and S. Wuertz, *High rates of conjugation in bacterial biofilms as determined by quantitative in situ analysis*. Appl Environ Microbiol, 1999. **65**(8): p. 3710-3.
  99. Fletcher, M. and G.I. Loeb, *Influence of substratum characteristics on the attachment of a marine pseudomonad to solid surfaces*. Appl Environ Microbiol, 1979. **37**(1): p. 67-72.
  100. Pringle, J.H. and M. Fletcher, *Influence of substratum wettability on attachment of freshwater bacteria to solid surfaces*. Appl Environ Microbiol, 1983. **45**(3): p. 811-7.
  101. de Kievit, T., *1.41 - Biofilms*, in *Comprehensive Biotechnology (Second Edition)*, M. Moo-Young, Editor. 2011, Academic Press: Burlington. p. 547-558.
  102. Gbejude, H.O., A.M. Lovering, and J.C. Webb, *The role of microbial biofilms in prosthetic joint infections*. Acta Orthop, 2015. **86**(2): p. 147-58.
  103. *Applications of Clinical Microbial Next-Generation Sequencing: Report on an American Academy of Microbiology Colloquium held in Washington, DC, in April 2015*, in *Applications of Clinical Microbial Next-Generation Sequencing: Report on an American Academy of Microbiology Colloquium held in Washington, DC, in April 2015*. 2016, American Society for Microbiology
- Copyright 2017 American Academy of Microbiology.: Washington (DC).
104. Tarabichi, M., et al., *Diagnosis of Periprosthetic Joint Infection: The Potential of Next-Generation Sequencing*. J Bone Joint Surg Am, 2018. **100**(2): p. 147-154.
  105. Monsen, T., et al., *In vitro effect of ultrasound on bacteria and suggested protocol for sonication and diagnosis of prosthetic infections*. Journal of clinical microbiology, 2009. **47**(8): p. 2496-2501.
  106. Pinto, A.M., et al., *Bacteriophages for Chronic Wound Treatment: from Traditional to Novel Delivery Systems*. Viruses, 2020. **12**(2).
  107. Dunne, W.M., Jr., L.F. Westblade, and B. Ford, *Next-generation and whole-genome sequencing in the diagnostic clinical microbiology laboratory*. Eur J Clin Microbiol Infect Dis, 2012. **31**(8): p. 1719-26.
  108. Goswami, K., J. Parvizi, and P. Maxwell Courtney, *Current Recommendations for the Diagnosis of Acute and Chronic PJI for Hip and Knee-Cell Counts, Alpha-Defensin, Leukocyte Esterase, Next-generation Sequencing*. Current reviews in musculoskeletal medicine, 2018. **11**(3): p. 428-438.

109. Qin, J., et al., *A human gut microbial gene catalogue established by metagenomic sequencing*. Nature, 2010. **464**(7285): p. 59-65.
110. Sanschagrín, S. and E. Yergeau, *Next-generation sequencing of 16S ribosomal RNA gene amplicons*. J Vis Exp, 2014(90).
111. Patel, J.B., *16S rRNA gene sequencing for bacterial pathogen identification in the clinical laboratory*. Mol Diagn, 2001. **6**(4): p. 313-21.
112. Kozich, J.J., et al., *Development of a dual-index sequencing strategy and curation pipeline for analyzing amplicon sequence data on the MiSeq Illumina sequencing platform*. Appl Environ Microbiol, 2013. **79**(17): p. 5112-20.
113. Konstantinidis, K.T. and J.M. Tiedje, *Prokaryotic taxonomy and phylogeny in the genomic era: advancements and challenges ahead*. Curr Opin Microbiol, 2007. **10**(5): p. 504-9.
114. Poretsky, R., et al., *Strengths and limitations of 16S rRNA gene amplicon sequencing in revealing temporal microbial community dynamics*. PLoS One, 2014. **9**(4): p. e93827.
115. Luo, C., R.L. Rodriguez, and K.T. Konstantinidis, *A user's guide to quantitative and comparative analysis of metagenomic datasets*. Methods Enzymol, 2013. **531**: p. 525-47.
116. Swearingen, M.C., et al., *16S rRNA analysis provides evidence of biofilms on all components of three infected periprosthetic knees including permanent braided suture*. Pathog Dis, 2016. **74**(7).
117. Bogut, A., et al., *Characterization of Staphylococcus epidermidis and Staphylococcus warneri small-colony variants associated with prosthetic-joint infections*. J Med Microbiol, 2014. **63**(Pt 2): p. 176-185.
118. Trampuz, A., et al., *Sonication of explanted prosthetic components in bags for diagnosis of prosthetic joint infection is associated with risk of contamination*. J Clin Microbiol, 2006. **44**(2): p. 628-31.
119. Piyasena, P., E. Mohareb, and R.C. McKellar, *Inactivation of microbes using ultrasound: a review*. International Journal of Food Microbiology, 2003. **87**(3): p. 207-216.
120. Stanley KD, G.D., Williams RC and Weiss J, *Inactivation of Escherichia coli O157:H7 by High-Intensity Ultrasonication in the Presence of Salts*. Foodborne Pathogens and Disease, 2004. **1**(4): p. 267 - 280.
121. Drago, L., et al., *Use of dithiothreitol to improve the diagnosis of prosthetic joint infections*. J Orthop Res, 2013. **31**(11): p. 1694-9.
122. Wu, X., Y. Wang, and L. Tao, *Sulfhydryl compounds reduce Staphylococcus aureus biofilm formation by inhibiting PIA biosynthesis*. FEMS Microbiol Lett, 2011. **316**(1): p. 44-50.
123. Sambri, A., et al., *Is Treatment With Dithiothreitol More Effective Than Sonication for the Diagnosis of Prosthetic Joint Infection?* Clin Orthop Relat Res, 2018. **476**(1): p. 137-145.

124. Randau, T.M., et al., *The Performance of a Dithiothreitol-Based Diagnostic System in Diagnosing Periprosthetic Joint Infection Compared to Sonication Fluid Cultures and Tissue Biopsies*. Z Orthop Unfall, 2021. **159**(4): p. 447-453.
125. Lewis, K., *Persister cells and the riddle of biofilm survival*. Biochemistry (Mosc), 2005. **70**(2): p. 267-74.
126. Keren, I., et al., *Specialized persister cells and the mechanism of multidrug tolerance in Escherichia coli*. J Bacteriol, 2004. **186**(24): p. 8172-80.
127. Wagner, C., U. Obst, and G.M. Hänsch, *Implant-associated posttraumatic osteomyelitis: collateral damage by local host defense?* Int J Artif Organs, 2005. **28**(11): p. 1172-80.
128. Prat, C., et al., *A new staphylococcal anti-inflammatory protein that antagonizes the formyl peptide receptor-like 1*. J Immunol, 2006. **177**(11): p. 8017-26.
129. Sun, J., *Pathogenic Bacterial Proteins and their Anti-Inflammatory Effects in the Eukaryotic Host*. Anti-inflammatory & anti-allergy agents in medicinal chemistry, 2009. **8**(3): p. 214-227.
130. Pajarinen, J., et al., *Innate immune reactions in septic and aseptic osteolysis around hip implants*. J Long Term Eff Med Implants, 2014. **24**(4): p. 283-96.
131. Gallo, J., et al., *Particle disease: biologic mechanisms of periprosthetic osteolysis in total hip arthroplasty*. Innate Immun, 2013. **19**(2): p. 213-24.
132. Purdue, P.E., et al., *The cellular and molecular biology of periprosthetic osteolysis*. Clin Orthop Relat Res, 2007. **454**: p. 251-61.
133. Nich, C. and S.B. Goodman, *Role of macrophages in the biological reaction to wear debris from joint replacements*. J Long Term Eff Med Implants, 2014. **24**(4): p. 259-65.
134. Nich, C., et al., *Macrophages-Key cells in the response to wear debris from joint replacements*. J Biomed Mater Res A, 2013. **101**(10): p. 3033-45.
135. Ferenbach, D. and J.J.K.i. Hughes, *Macrophages and dendritic cells: what is the difference?* 2008. **74**(1): p. 5-7.
136. Papageorgiou, I.E., et al., *TLR4-activated microglia require IFN- $\gamma$  to induce severe neuronal dysfunction and death in situ*. Proc Natl Acad Sci U S A, 2016. **113**(1): p. 212-7.
137. Amanzada, A., et al., *Identification of CD68(+) neutrophil granulocytes in in vitro model of acute inflammation and inflammatory bowel disease*. Int J Clin Exp Pathol, 2013. **6**(4): p. 561-70.
138. Rittirsch, D., M.A. Flierl, and P.A. Ward, *Harmful molecular mechanisms in sepsis*. Nat Rev Immunol, 2008. **8**(10): p. 776-87.
139. Martins, P.S., et al., *Expression of cell surface receptors and oxidative metabolism modulation in the clinical continuum of sepsis*. Crit Care, 2008. **12**(1): p. R25.

140. Nakae, H., et al., *Changes in adhesion molecule levels in sepsis*. Res Commun Mol Pathol Pharmacol, 1996. **91**(3): p. 329-38.
141. Ahmed, N.A., et al., *Mechanisms for the diminished neutrophil exudation to secondary inflammatory sites in infected patients with a systemic inflammatory response (sepsis)*. 1999. **27**(11): p. 2459-2468.
142. *Biomarkers and surrogate endpoints: preferred definitions and conceptual framework*. Clin Pharmacol Ther, 2001. **69**(3): p. 89-95.
143. Califf, R.M., *Biomarker definitions and their applications*. Exp Biol Med (Maywood), 2018. **243**(3): p. 213-221.
144. Terms, N.C.I.D.o.C., <https://www.cancer.gov/publications/dictionaries/cancer-terms>. cited 24.08.2021, 2021.
145. Kraus, V.B., *Biomarkers as drug development tools: discovery, validation, qualification and use*. Nat Rev Rheumatol, 2018. **14**(6): p. 354-362.
146. Turabieh, H., M. Mafarja, and X. Li, *Iterated feature selection algorithms with layered recurrent neural network for software fault prediction*. Expert Systems with Applications, 2019. **122**: p. 27-42.
147. Arvieux, C. and H. Common, *New diagnostic tools for prosthetic joint infection*. Orthop Traumatol Surg Res, 2019. **105**(1s): p. S23-s30.
148. Pupaibool, J., et al., *Alpha-defensin-novel synovial fluid biomarker for the diagnosis of periprosthetic joint infection*. Int Orthop, 2016. **40**(12): p. 2447-2452.
149. White, S.H., W.C. Wimley, and M.E. Selsted, *Structure, function, and membrane integration of defensins*. Current Opinion in Structural Biology, 1995. **5**(4): p. 521-527.
150. Lehrer, R.I., *Microbicidal Mechanisms, Oxygen-Independent*, in *Encyclopedia of Immunology (Second Edition)*, P.J. Delves, Editor. 1998, Elsevier: Oxford. p. 1719-1725.
151. Satchell, D.P., et al., *Interactions of mouse Paneth cell alpha-defensins and alpha-defensin precursors with membranes. Prosegment inhibition of peptide association with biomimetic membranes*. J Biol Chem, 2003. **278**(16): p. 13838-46.
152. Deirmengian, C., et al., *Synovial fluid biomarkers for periprosthetic infection*. Clin Orthop Relat Res, 2010. **468**(8): p. 2017-23.
153. Deirmengian, C., et al., *The alpha-defensin test for periprosthetic joint infection outperforms the leukocyte esterase test strip*. Clin Orthop Relat Res, 2015. **473**(1): p. 198-203.
154. Deirmengian, C., et al., *Diagnosing periprosthetic joint infection: has the era of the biomarker arrived?* Clin Orthop Relat Res, 2014. **472**(11): p. 3254-62.

155. Deirmengian, C., et al., *The Alpha-defensin Test for Periprosthetic Joint Infection Responds to a Wide Spectrum of Organisms*. Clin Orthop Relat Res, 2015. **473**(7): p. 2229-35.
156. Kasperek, M.F., et al., *Intraoperative Diagnosis of Periprosthetic Joint Infection Using a Novel Alpha-Defensin Lateral Flow Assay*. The Journal of Arthroplasty, 2016. **31**(12): p. 2871-2874.
157. Gehrke, T., et al., *The Accuracy of the Alpha Defensin Lateral Flow Device for Diagnosis of Periprosthetic Joint Infection: Comparison with a Gold Standard*. J Bone Joint Surg Am, 2018. **100**(1): p. 42-48.
158. Renz, N., et al., *Alpha Defensin Lateral Flow Test for Diagnosis of Periprosthetic Joint Infection: Not a Screening but a Confirmatory Test*. J Bone Joint Surg Am, 2018. **100**(9): p. 742-750.
159. Bonanzinga, T., et al., *How Reliable Is the Alpha-defensin Immunoassay Test for Diagnosing Periprosthetic Joint Infection? A Prospective Study*. Clin Orthop Relat Res, 2017. **475**(2): p. 408-415.
160. Plate, A., et al., *Inflammatory disorders mimicking periprosthetic joint infections may result in false-positive  $\alpha$ -defensin*. Clinical Microbiology and Infection, 2018. **24**(11): p. 1212.e1-1212.e6.
161. Janeway CA Jr, T.P., Walport M, et al., *Immunobiology: The Immune System in Health and Disease. 5th edition*. New York: Garland Science, 2001.
162. Dunkelberger, J.R. and W.C. Song, *Complement and its role in innate and adaptive immune responses*. Cell Res, 2010. **20**(1): p. 34-50.
163. Walport, M.J., *Complement. First of two parts*. N Engl J Med, 2001. **344**(14): p. 1058-66.
164. Walport, M.J., *Complement. Second of two parts*. N Engl J Med, 2001. **344**(15): p. 1140-4.
165. Gros, P., F.J. Milder, and B.J.C. Janssen, *Complement driven by conformational changes*. Nature Reviews Immunology, 2008. **8**(1): p. 48-58.
166. Janssen, B.J., et al., *Structures of complement component C3 provide insights into the function and evolution of immunity*. Nature, 2005. **437**(7058): p. 505-11.
167. Taylor, P.W., *Complement-mediated killing of susceptible gram-negative bacteria: an elusive mechanism*. Exp Clin Immunogenet, 1992. **9**(1): p. 48-56.
168. Berends, E.T., et al., *Contribution of the complement Membrane Attack Complex to the bactericidal activity of human serum*. Mol Immunol, 2015. **65**(2): p. 328-35.
169. Struglics, A., et al., *The complement system is activated in synovial fluid from subjects with knee injury and from patients with osteoarthritis*. Arthritis Res Ther, 2016. **18**(1): p. 223.

170. Sena, L., et al., *C3 Gene Functional Polymorphisms and C3 Serum Levels in Patients with Rheumatoid Arthritis*. Immunol Invest, 2020: p. 1-15.
171. Thordardottir, S., et al., *Activation of Complement Following Total Hip Replacement*. Scand J Immunol, 2016. **83**(3): p. 219-24.
172. Barretto, J.M., et al., *Evaluation of serum levels of C-reactive protein after total knee arthroplasty*. Rev Bras Ortop, 2017. **52**(2): p. 176-181.
173. Fröschen, F.S., et al., *Synovial Complement Factors in Patients with Periprosthetic Joint Infection after Undergoing Revision Arthroplasty of the Hip or Knee Joint*. Diagnostics, 2021. **11**(3): p. 434.
174. Lee, J.H., et al., *Proteomic analysis of human synovial fluid reveals potential diagnostic biomarkers for ankylosing spondylitis*. Clin Proteomics, 2020. **17**: p. 20.
175. Voytas, D., *Agarose gel electrophoresis*. Curr Protoc Immunol, 2001. **Chapter 10**: p. Unit 10.4.
176. Chen, Z., et al., *Impact of Preservation Method and 16S rRNA Hypervariable Region on Gut Microbiota Profiling*. 2019. **4**(1): p. e00271-18.
177. Rath, S., et al., *Uncovering the trimethylamine-producing bacteria of the human gut microbiota*. Microbiome, 2017. **5**(1): p. 54.
178. Camarinha-Silva, A., et al., *Comparing the anterior nares bacterial community of two discrete human populations using Illumina amplicon sequencing*. Environ Microbiol, 2014. **16**(9): p. 2939-52.
179. Cole, J.R., et al., *Ribosomal Database Project: data and tools for high throughput rRNA analysis*. Nucleic Acids Res, 2014. **42**(Database issue): p. D633-42.
180. Shannon, P., et al., *Cytoscape: a software environment for integrated models of biomolecular interaction networks*. Genome Res, 2003. **13**(11): p. 2498-504.
181. Kulakov, L.A., et al., *Analysis of bacteria contaminating ultrapure water in industrial systems*. Appl Environ Microbiol, 2002. **68**(4): p. 1548-55.
182. Salter, S.J., et al., *Reagent and laboratory contamination can critically impact sequence-based microbiome analyses*. BMC Biology, 2014. **12**(1): p. 87.
183. Million, M., et al., *Culture-negative prosthetic joint arthritis related to Coxiella burnetii*. Am J Med, 2014. **127**(8): p. 786 e7-786 e10.
184. Parikh, M.S. and S. Antony, *A comprehensive review of the diagnosis and management of prosthetic joint infections in the absence of positive cultures*. J Infect Public Health, 2016. **9**(5): p. 545-56.
185. Young, G., et al., *Bacterial DNA persists for extended periods after cell death*. J Endod, 2007. **33**(12): p. 1417-20.

186. Parwaresch, M.R., et al., *Monocyte/macrophage-reactive monoclonal antibody Ki-M6 recognizes an intracytoplasmic antigen*. American Journal of Pathology, 1986. **125**(1): p. 141-151.
187. Saito, N., et al., *Ultrastructural localization of the CD68 macrophage-associated antigen in human blood neutrophils and monocytes*. American Journal of Pathology, 1991. **139**(5): p. 1053-1059.
188. Torsteinsdóttir, I., et al., *Enhanced expression of integrins and CD66b on peripheral blood neutrophils and eosinophils in patients with rheumatoid arthritis, and the effect of glucocorticoids*. Scand J Immunol, 1999. **50**(4): p. 433-9.
189. Zhao, L., et al., *An enzyme-linked immunosorbent assay for human carcinoembryonic antigen-related cell adhesion molecule 8, a biological marker of granulocyte activities in vivo*. J Immunol Methods, 2004. **293**(1-2): p. 207-14.
190. Wu, C., et al., *Risk factors for periprosthetic joint infection after total hip arthroplasty and total knee arthroplasty in Chinese patients*. PLoS One, 2014. **9**(4): p. e95300.
191. Klein, S.L., A. Jedlicka, and A. Pekosz, *The Xs and Y of immune responses to viral vaccines*. Lancet Infect Dis, 2010. **10**(5): p. 338-49.
192. Ngo, S.T., F.J. Steyn, and P.A.J.F.i.n. McCombe, *Gender differences in autoimmune disease*. 2014. **35**(3): p. 347-369.
193. Mangalam, A.K., V. Taneja, and C.S.J.T.J.o.I. David, *HLA class II molecules influence susceptibility versus protection in inflammatory diseases by determining the cytokine profile*. 2013. **190**(2): p. 513-519.
194. Bouman, A., M.J. Heineman, and M.M. Faas, *Sex hormones and the immune response in humans*. Hum Reprod Update, 2005. **11**(4): p. 411-23.
195. Roberts, C.W., W. Walker, and J. Alexander, *Sex-associated hormones and immunity to protozoan parasites*. Clin Microbiol Rev, 2001. **14**(3): p. 476-88.
196. Kurtz, S.M., et al., *Economic burden of periprosthetic joint infection in the United States*. J Arthroplasty, 2012. **27**(8 Suppl): p. 61-5.e1.
197. Aggarwal, V.K., et al., *2019 Frank Stinchfield Award: A comparison of prosthetic joint infection rates between direct anterior and non-anterior approach total hip arthroplasty*. Bone Joint J, 2019. **101-b**(6\_Supple\_B): p. 2-8.
198. Schlegel, U. and S.M. Perren, *Surgical aspects of infection involving osteosynthesis implants: implant design and resistance to local infection*. Injury, 2006. **37** Suppl 2: p. S67-73.

199. Kuo, L.T., et al., *Chronic kidney disease is associated with a risk of higher mortality following total knee arthroplasty in diabetic patients: a nationwide population-based study*. *Oncotarget*, 2017. **8**(59): p. 100288-100295.
200. Länder, D.P.B.-. *Altersstruktur der Bevölkerung in Sachsen-Anhalt*. 2019; Available from: <https://www.demografie-portal.de/DE/Fakten/bevoelkerung-altersstruktur-sachsen-anhalt.html#:~:text=Mit%20einem%20Durchschnittsalter%20von%2047,2019%20die%20bundesweit%20%C3%A4lteste%20Bev%C3%B6lkerung>.
201. Gesundheitsberichterstattung des Landes Sachsen-Anhalt. *Gesundheitsberichterstattung des Landes Sachsen-Anhalt* 2015, December 31; 2015:[Available from: <https://lavst.azurewebsites.net/gbenet/tabellen/them03/0301900152015.pdf>.
202. Sendi, P., et al., *Clinical comparison between exogenous and haematogenous periprosthetic joint infections caused by Staphylococcus aureus*. *Clinical Microbiology and Infection*, 2011. **17**(7): p. 1098-1100.
203. Pollard, J.P., et al., *Antibiotic prophylaxis in total hip replacement*. *British Medical Journal*, 1979. **1**(6165): p. 707-709.
204. Stinchfield, F.E., et al., *Late hematogenous infection of total joint replacement*. *J Bone Joint Surg Am*, 1980. **62**(8): p. 1345-50.
205. Mangram, A.J., et al., *Guideline for Prevention of Surgical Site Infection, 1999*. *Centers for Disease Control and Prevention (CDC) Hospital Infection Control Practices Advisory Committee*. *Am J Infect Control*, 1999. **27**(2): p. 97-132; quiz 133-4; discussion 96.
206. Shahi, A. and J. Parvizi, *Prevention of Periprosthetic Joint Infection*. *Arch Bone Jt Surg*, 2015. **3**(2): p. 72-81.
207. Pavel, A., et al., *Prophylactic antibiotics in clean orthopaedic surgery*. *J Bone Joint Surg Am*, 1974. **56**(4): p. 777-82.
208. Meehan, J., A.A. Jamali, and H. Nguyen, *Prophylactic antibiotics in hip and knee arthroplasty*. *J Bone Joint Surg Am*, 2009. **91**(10): p. 2480-90.
209. Forse, R., et al., *Antibiotic prophylaxis for surgery in morbidly obese patients*. 1989. **106**(4): p. 750-757.
210. AWMF online das Portal der wissenschaftlichen Medizin. *Deutsche Gesellschaft für Orthopädie und Orthopädische Chirurgie e.V. (DGOOC) Aktuelle Leitlinien*. 2021; Available from: <https://www.awmf.org/leitlinien/aktuelle-leitlinien/ll-liste/deutsche-gesellschaft-fuer-orthopaedie-und-orthopaedische-chirurgie-e-v.html>.
211. Kwok, Y.Y., et al., *Disk susceptibility testing of slow-growing anaerobic bacteria*. *Antimicrobial agents and chemotherapy*, 1975. **7**(1): p. 1-7.

212. Grice, E.A. and J.A.J.N.r.m. Segre, *The skin microbiome*. 2011. **9**(4): p. 244-253.
213. Sampedro, M.F., et al., *A biofilm approach to detect bacteria on removed spinal implants*. *Spine (Phila Pa 1976)*, 2010. **35**(12): p. 1218-24.
214. Portillo, M.E., et al., *Propionibacterium acnes: an underestimated pathogen in implant-associated infections*. *Biomed Res Int*, 2013. **2013**: p. 804391.
215. Tsai, Y., et al., *Different microbiological profiles between hip and knee prosthetic joint infections*. *Journal of Orthopaedic Surgery*, 2019. **27**(2): p. 2309499019847768.
216. Zmistowski, B., et al., *Periprosthetic joint infection diagnosis: a complete understanding of white blood cell count and differential*. *J Arthroplasty*, 2012. **27**(9): p. 1589-93.
217. Spangehl, M.J., et al., *Prospective analysis of preoperative and intraoperative investigations for the diagnosis of infection at the sites of two hundred and two revision total hip arthroplasties*. *J Bone Joint Surg Am*, 1999. **81**(5): p. 672-83.
218. Deirmengian, G.K., et al., *Leukocytosis is common after total hip and knee arthroplasty*. 2011. **469**(11): p. 3031-3036.
219. Zmistowski, B., et al., *Diagnosis of periprosthetic joint infection*. *J Orthop Res*, 2014. **32 Suppl 1**: p. S98-107.
220. Ghanem, E., et al., *The use of receiver operating characteristics analysis in determining erythrocyte sedimentation rate and C-reactive protein levels in diagnosing periprosthetic infection prior to revision total hip arthroplasty*. *Int J Infect Dis*, 2009. **13**(6): p. e444-9.
221. Berbari, E., et al., *Inflammatory blood laboratory levels as markers of prosthetic joint infection: a systematic review and meta-analysis*. *J Bone Joint Surg Am*, 2010. **92**(11): p. 2102-9.
222. Kim, S.G., et al., *Diagnostic Value of Synovial White Blood Cell Count and Serum C-Reactive Protein for Acute Periprosthetic Joint Infection After Knee Arthroplasty*. *J Arthroplasty*, 2017. **32**(12): p. 3724-3728.
223. Holinka, J., et al., *Sonication cultures of explanted components as an add-on test to routinely conducted microbiological diagnostics improve pathogen detection*. *J Orthop Res*, 2011. **29**(4): p. 617-22.
224. Trampuz, A., et al., *Molecular and antibiofilm approaches to prosthetic joint infection*. *Clin Orthop Relat Res*, 2003(414): p. 69-88.
225. Cremniter, J., et al., *Decreased susceptibility to teicoplanin and vancomycin in coagulase-negative Staphylococci isolated from orthopedic-device-associated infections*. *J Clin Microbiol*, 2010. **48**(4): p. 1428-31.
226. Zmistowski, B., et al., *Periprosthetic joint infection increases the risk of one-year mortality*. *J Bone Joint Surg Am*, 2013. **95**(24): p. 2177-84.

227. TP, W.J.a.S., *Limited Role of Direct Exchange Arthroplasty in the Treatment of Infected Total Hip Replacements*. Clinical Orthopaedics and related Research, 2000. **381**: p. 101-105.
228. Wimmer, M.D., et al., *Polymicrobial infections reduce the cure rate in prosthetic joint infections: outcome analysis with two-stage exchange and follow-up  $\geq$ two years*. International orthopaedics, 2016. **40**(7): p. 1367-1373.
229. Zimmerli, W., *Clinical presentation and treatment of orthopaedic implant-associated infection*. J Intern Med, 2014. **276**(2): p. 111-9.
230. Ivy, M.I., et al., *Direct Detection and Identification of Prosthetic Joint Infection Pathogens in Synovial Fluid by Metagenomic Shotgun Sequencing*. J Clin Microbiol, 2018. **56**(9).
231. Portillo, M.E., et al., *Multiplex PCR of sonication fluid accurately differentiates between prosthetic joint infection and aseptic failure*. J Infect, 2012. **65**(6): p. 541-8.
232. Hartley, J.C. and K.A. Harris, *Molecular techniques for diagnosing prosthetic joint infections*. Journal of Antimicrobial Chemotherapy, 2014. **69**(suppl\_1): p. i21-i24.
233. Y, J. and J. L., *Diagnosis of Periprosthetic Joint Infection Using Polymerase Chain Reaction: An Updated Systematic Review and Meta-Analysis*. Surgical Infections, 2018. **19**(6): p. 555-565.
234. Thoendel, M.J., et al., *Identification of Prosthetic Joint Infection Pathogens Using a Shotgun Metagenomics Approach*. Clinical infectious diseases : an official publication of the Infectious Diseases Society of America, 2018. **67**(9): p. 1333-1338.
235. Abayasekara, L.M., et al., *Detection of bacterial pathogens from clinical specimens using conventional microbial culture and 16S metagenomics: a comparative study*. BMC Infect Dis, 2017. **17**(1): p. 631.
236. Skvarc, M., et al., *Non-culture-based methods to diagnose bloodstream infection: does it work?* 2013. **3**(2): p. 97-104.
237. Gosiewski, T., et al., *Comparison of nested, multiplex, qPCR; FISH; SeptiFast and blood culture methods in detection and identification of bacteria and fungi in blood of patients with sepsis*. 2014. **14**(1): p. 1-8.
238. Gosiewski, T., et al., *Comprehensive detection and identification of bacterial DNA in the blood of patients with sepsis and healthy volunteers using next-generation sequencing method - the observation of DNAemia*. Eur J Clin Microbiol Infect Dis, 2017. **36**(2): p. 329-336.
239. Dunstan, R.W., et al., *The use of immunohistochemistry for biomarker assessment--can it compete with other technologies?* Toxicol Pathol, 2011. **39**(6): p. 988-1002.

240. Brandtzaeg, P., *The increasing power of immunohistochemistry and immunocytochemistry*. J Immunol Methods, 1998. **216**(1-2): p. 49-67.
241. Haines, D.M. and K.H. West, *Immunohistochemistry: forging the links between immunology and pathology*. Vet Immunol Immunopathol, 2005. **108**(1-2): p. 151-6.
242. Yu, J., et al., *Mutation-specific antibodies for the detection of EGFR mutations in non-small-cell lung cancer*. Clin Cancer Res, 2009. **15**(9): p. 3023-8.
243. Hawkins, K.R. and P. Yager, *Nonlinear decrease of background fluorescence in polymer thin-films - a survey of materials and how they can complicate fluorescence detection in microTAS*. Lab Chip, 2003. **3**(4): p. 248-52.
244. Llopis, S.D., W. Stryjewski, and S.A. Soper, *Near-infrared time-resolved fluorescence lifetime determinations in poly(methylmethacrylate) microchip electrophoresis devices*. 2004. **25**(21-22): p. 3810-3819.
245. Steidl, C., et al., *Tumor-associated macrophages and survival in classic Hodgkin's lymphoma*. 2010. **362**(10): p. 875-885.
246. Greaves, P., et al., *Expression of FOXP3, CD68, and CD20 at diagnosis in the microenvironment of classical Hodgkin lymphoma is predictive of outcome*. 2013. **31**(2): p. 256.
247. Horowitz, S.M., et al., *Studies of the mechanism by which the mechanical failure of polymethylmethacrylate leads to bone resorption*. J Bone Joint Surg Am, 1993. **75**(6): p. 802-13.
248. Jiranek, W.A., et al., *Production of cytokines around loosened cemented acetabular components. Analysis with immunohistochemical techniques and in situ hybridization*. J Bone Joint Surg Am, 1993. **75**(6): p. 863-79.
249. Brinkmann, V., et al., *Neutrophil extracellular traps kill bacteria*. 2004. **303**(5663): p. 1532-1535.
250. Ricklin, D., et al., *Complement: a key system for immune surveillance and homeostasis*. Nat Immunol, 2010. **11**(9): p. 785-97.
251. Anderlueh, G. and R. Gilbert, *MACPF/CDC Proteins-Agents of Defence, Attack and Invasion*. Vol. 80. 2014: Springer.
252. Al Haj Ahmad, R.M. and H.A. Al-Domi, *Complement 3 serum levels as a pro-inflammatory biomarker for insulin resistance in obesity*. Diabetes Metab Syndr, 2017. **11 Suppl 1**: p. S229-s232.
253. Martínez-López, D., et al., *Complement C5 Protein as a Marker of Subclinical Atherosclerosis*. J Am Coll Cardiol, 2020. **75**(16): p. 1926-1941.

254. Parry, J., et al., *Soluble terminal complement activation fragment sC5b-9: a new serum biomarker for traumatic brain injury?* Eur J Trauma Emerg Surg, 2020.
255. Peel, T.N., et al., *Microbiological Aetiology, Epidemiology, and Clinical Profile of Prosthetic Joint Infections: Are Current Antibiotic Prophylaxis Guidelines Effective?* Antimicrobial Agents and Chemotherapy, 2012. **56**(5): p. 2386-2391.
256. Serna, M., et al., *Structural basis of complement membrane attack complex formation.* Nat Commun, 2016. **7**: p. 10587.
257. Sharp, M.E., et al., *Dopamine selectively remediates 'model-based' reward learning: a computational approach.* Brain : a journal of neurology, 2016. **139**(Pt 2): p. 355-364.
258. Silhavy, T.J., D. Kahne, and S. Walker, *The bacterial cell envelope.* Cold Spring Harb Perspect Biol, 2010. **2**(5): p. a000414.
259. Heinen, S., et al., *Monitoring and modeling treatment of atypical hemolytic uremic syndrome.* Molecular Immunology, 2013. **54**(1): p. 84-88.
260. Lintner, K.E., et al., *Early Components of the Complement Classical Activation Pathway in Human Systemic Autoimmune Diseases.* Frontiers in Immunology, 2016. **7**(36).
261. Thurman, J.M. and R. Yapa, *Complement Therapeutics in Autoimmune Disease.* Frontiers in Immunology, 2019. **10**(672).
262. Grizzle, W.E., K.H. Woodruff, and T.D. Trainer, *The pathologist's role in the use of human tissues in research--legal, ethical, and other issues.* Arch Pathol Lab Med, 1996. **120**(10): p. 909-12.
263. Grizzle, W.E., W.C. Bell, and K.C. Sexton, *Issues in collecting, processing and storing human tissues and associated information to support biomedical research.* Cancer Biomark, 2010. **9**(1-6): p. 531-49.

## Ehrenerklärung

Ich versichere hiermit, dass ich die vorliegende Arbeit ohne unzulässige Hilfe Dritter und ohne Benutzung anderer als der angegebenen Hilfsmittel angefertigt habe; verwendete fremde und eigene Quellen sind als solche kenntlich gemacht.

Ich habe insbesondere nicht wissentlich:

- Ergebnisse erfunden oder widersprüchlich Ergebnisse verschwiegen,
- statistische Verfahren absichtlich missbraucht, um Daten in ungerechtfertigter Weise zu interpretieren,
- fremde Ergebnisse oder Veröffentlichungen plagiiert,
- fremde Forschungsergebnisse verzerrt wiedergegeben.

Mir ist bekannt, dass Verstöße gegen das Urheberrecht Unterlassungs- und Schadensersatzansprüche des Urhebers sowie eine strafrechtliche Ahndung durch die Strafverfolgungsbehörden begründen kann.

Ich erkläre mich damit einverstanden, dass die Arbeit ggf. mit Mitteln der elektronischen Datenverarbeitung auf Plagiate überprüft werden kann.

Die Arbeit wurde bisher weder im Inland noch im Ausland in gleicher oder ähnlicher Form als Dissertation eingereicht und ist als Ganzes auch noch nicht veröffentlicht.

---

(Ort, Datum, Unterschrift)